UNCLASSIFIED

SECURITY CLASSIFICATION OF THIS PAGE *(When Data Entered)*

(14) **REPORT DOCUMENTATION PAGE**

READ INSTRUCTIONS BEFORE COMPLETING FORM

1. REPORT NUMBER: GE/EE/76-16
2. GOVT ACCESSION NO.
3. RECIPIENT'S CATALOG NUMBER

4. TITLE *(and Subtitle)* (6): PERFORMANCE OF THE HUMAN PERIPHERAL VISUAL SYSTEM UNDER VARIOUS LOADS.

5. TYPE OF REPORT & PERIOD COVERED: MS Thesis

6. PERFORMING ORG. REPORT NUMBER

7. AUTHOR(s) (10): Daniel R. Burchfield
Capt USAF

8. CONTRACT OR GRANT NUMBER(s) (9): Master's thesis,

9. PERFORMING ORGANIZATION NAME AND ADDRESS
Air Force Institute of Technology(AFIT-EN)
Wright-Patterson AFB, Ohio 45433

10. PROGRAM ELEMENT, PROJECT, TASK AREA & WORK UNIT NUMBERS

11. CONTROLLING OFFICE NAME AND ADDRESS
Aerospace Medical Research Laboratory
WPAFB, OH 45433

(11) 12. REPORT DATE: Dec 1976

13. NUMBER OF PAGES: 140 (12) 152p.

14. MONITORING AGENCY NAME & ADDRESS *(if different from Controlling Office)*

15. SECURITY CLASS. *(of this report)*: UNCLASSIFIED

15a. DECLASSIFICATION/DOWNGRADING SCHEDULE

16. DISTRIBUTION STATEMENT *(of this Report)*

Approved for public release; distribution unlimited

17. DISTRIBUTION STATEMENT *(of the abstract entered in Block 20, if different from Report)*

18. SUPPLEMENTARY NOTES

Approved for public release; IAW AFR 190-17

JERRAL F. GUESS, Captain, USAF
Director of Information

19. KEY WORDS *(Continue on reverse side if necessary and identify by block number)*

Human Factors Engineering and Vision
Pattern Recognition
Perception
Vision

20. ABSTRACT *(Continue on reverse side if necessary and identify by block number)*

This report measured the effects of single and multiple spatial presentations in various positions in the human peripheral visual field. Subjects fixated on a central point and attempted to accurately discern orientations of peripherally located stimuli. The peripheral tasks were sine-wave gratings generated on HP-1205A oscilloscopes. Stimuli were presented at various positions along the horizontal and vertical axes of the visual field. Stimulus presentation times were 20, 50, 100, and 500 msec.

DD FORM 1 JAN 73 1473 EDITION OF 1 NOV 65 IS OBSOLETE

012225

UNCLASSIFIED

SECURITY CLASSIFICATION OF THIS PAGE *(When Data Entered)*

20. (Continued)

Lateral differences in perception were noted with the data showing high statistical significance. The number of events processed also proved to be a significant variable. The dominance of the right cerebral hemisphere for processing spatial information was very evident. Such results have strong implications as to where spatial presentations should be located in the visual field to maximize visual performance.

GE/EE/76-16

(1)

PERFORMANCE OF THE HUMAN PERIPHERAL VISUAL SYSTEM UNDER VARIOUS LOADS

THESIS

GE/EE/76-16

Daniel R. Burchfield
Capt USAF

GE/EE/76-16

PERFORMANCE OF THE HUMAN PERIPHERAL VISUAL SYSTEM UNDER VARIOUS LOADS

THESIS

Presented to the Faculty of the School of Engineering
of the Air Force Institute of Technology
Air University
in Partial Fulfillment of the
Requirements for the Degree of
Master of Science

by

Daniel R. Burchfield, B.A.
Capt USAF
Graduate Electrical Engineering
December 1976

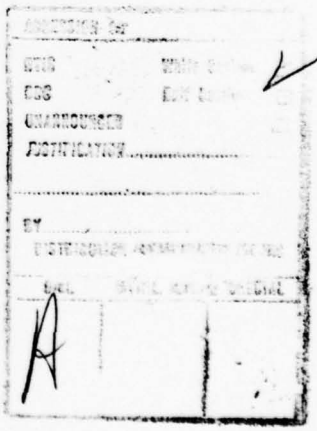

Approved for public release; distribution unlimited.

Preface

At this time, the USAF Institute of Technology (USAFIT) is conducting research measuring the performance of the human visual system under various visual tasks. This research is being done in conjunction with the Aerospace Medical Research Laboratory (AMRL). The purpose is to attempt to gain further insight into processing in the human visual system.

Previous USAFIT theses have dealt with foveal contrast sensitivity, peripheral contrast sensitivity, and expanded field of vision. This study was designed to evaluate the peripheral visual system under various loading conditions.

I would like to express my deepest appreciation to Dr. Matthew Kabrisky for his encouragement and assistance. His insight and advice contributed greatly to the completion of this thesis. In addition, no psychophysiological experiment can be completed without subjects, and my thanks go out to them for the many hours of time they gave:

Karena Burchfield
Cynthia Hopkins
Matthew Kabrisky
John Klose
Rachel Sims

Daniel R. Burchfield

Contents

List of Figures

List of Tables

Abstract

This report measured the effects of single and multiple spatial presentations in various positions in the human peripheral visual field. Subjects fixated on a central point and attempted to accurately discern orientations of peripherally located stimuli. The peripheral tasks were sine-wave gratings generated on HP-1205A oscilloscopes. Stimuli were presented at various positions along the horizontal and vertical axes of the visual field. Stimulus presentation times were 20, 50, 100, and 500 msec.

Lateral differences in perception were noted with the data showing high statistical significance. The number of events processed also proved to be a significant variable. The dominance of the right cerebral hemisphere for processing spatial information was very evident. Such results have strong implications as to where spatial presentations should be located in the visual field to maximize visual performance.

PERFORMANCE OF THE HUMAN PERIPHERAL VISUAL SYSTEM UNDER VARIOUS LOADS

I. Introduction

Purpose

The purpose of this thesis was to determine the effect of single and multiple spatial presentations in various positions in the human peripheral visual field. While the subject fixated on a central point, ability to discern accurately orientations of peripherally located stimuli was observed. Sine-wave gratings at two possible orientations were presented as the peripheral stimuli on Hewlett-Packard 1205A oscilloscopes. Testing was accomplished at various positions along the horizontal and vertical axes of the subject's visual field. Display exposure times to the subjects ranged from 500 msec to 20 msec.

The goal of the experiment was to determine if any detectable difference occurred in subject accuracy which would correlate with visual hemifield presentation and number of events to be processed. Previous study has shown that peripheral expansion of a field of attention along both the left and right horizontal axes does not effect foveal contrast sensitivity to any significant level. Also, the field of attention extends at least to

equal eccentricities from the foveal midpoint both left and right along the horizontal axis. In addition, processing of multiple events along the right horizontal axis seems highly more complex than single event processing (Ref 14:147-152). This experiment investigated the nature of single and multiple event processing at various eccentricities of the peripheral visual system in left, right, upper, and lower hemifields.

Background

The manner in which man perceives his surrounding environment is very complex. Perception in the human visual system is controlled by physiological and psychophysical factors as well as the optical factors of the eye. The optics of the eye are well-understood, but the other subjective factors have to be studied in many contexts to glean knowledge of the workings of the visual system.

A fundamental ability of the human visual system is the detection of changes in the spatial distribution of stimulus intensity in the visual field. The advent of Fourier analysis in optics has led to the usage of sine-wave gratings as visual stimuli. The angular spacing of the bars of the grating is expressed in cycles-per-degree of visual field (Ref 3:312-324). Fig. 1 illustrates the sine-wave grating contrast, which can ultimately be

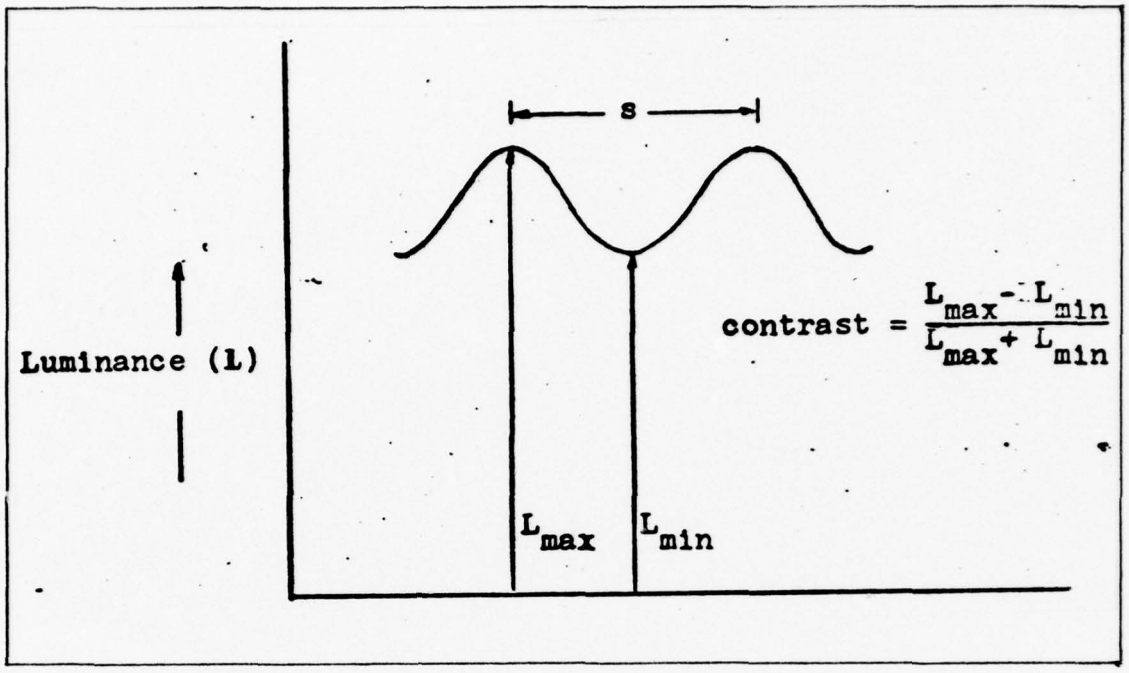

Fig. 1. Luminance Profile of a Sine-Wave Grating

defined in terms of the maximum and minimum luminance (L_{max} and L_{min} respectively) of the sinusoidal luminance variation by the equation

$$\text{Contrast} = \frac{L_{max} - L_{min}}{L_{max} + L_{min}} \qquad (1)$$

The reciprocal of the center-to-center separation (s) is the spatial frequency.

Many investigations have been concentrated on the imaging properties of the foveal portion of the human visual system. In comparison, very little work has been done with the imaging properties of the peripheral visual system.

The functioning cells of the retina are the receptor

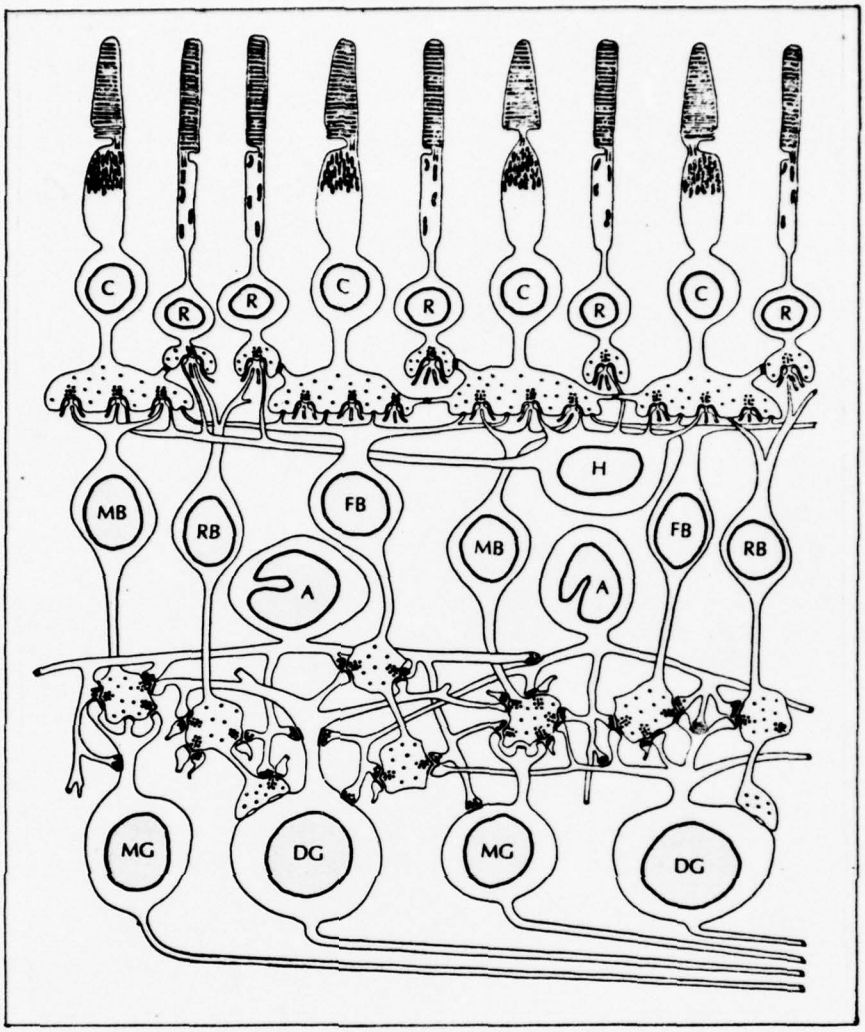

Fig. 2. Neural Elements in the Primate Retina (Ref 3:125).

cells, rods (R) and cones (C); the intermediary cells, bipolar (B) and horizontal (H); and the ganglion cells (G), whose axons make up the optic nerve. The bipolar cells consist of two major types, midget bipolar (MB) and diffuse bipolar (RB). The midget bipolar makes connection with only one receptor cell -- a cone; diffuse bipolars connect with as many as 50 rods and 7 cones. Likewise, ganglion cells are made up of midget ganglion (MG) and

diffuse ganglion (DG) types, with the midget making a connection with only one midget bipolar and the diffuse connecting with groups of bipolar cells. Fig. 2 is a schematic diagram of these connections.

As a result of the neural connections, large differences exist between the foveal region of the retina and the peripheral region of the retina. Only cones exist

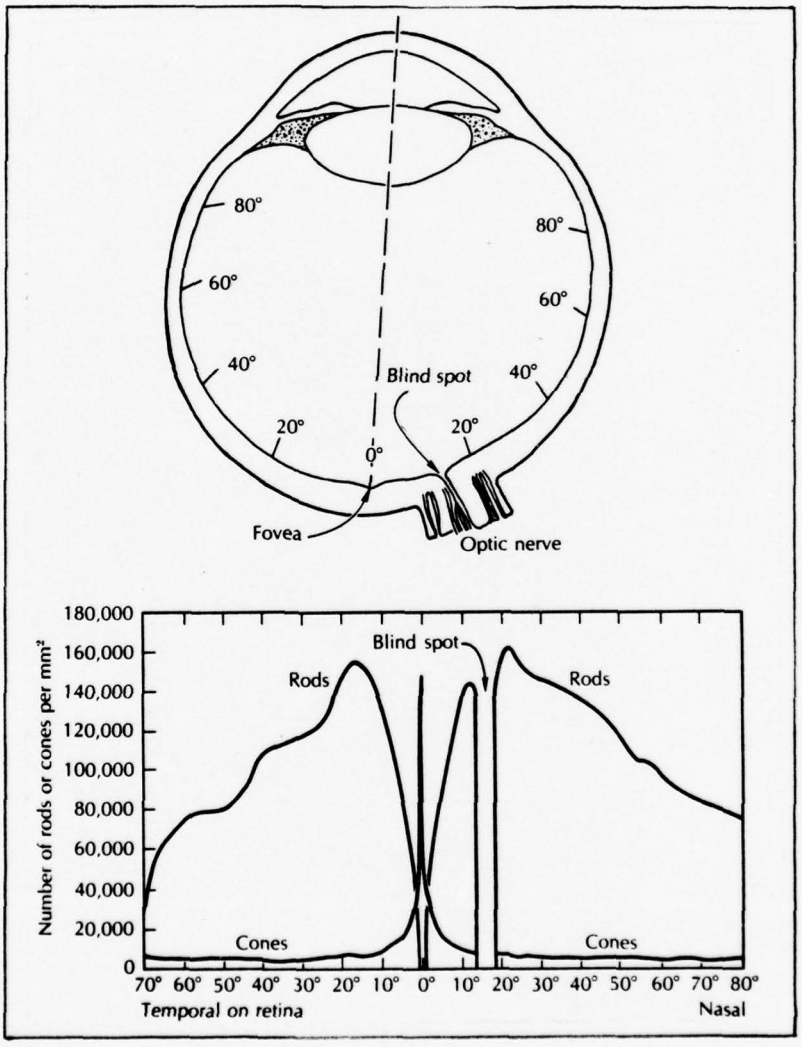

Fig. 3. Density of Rods and Cones Across the Retina (Ref 3:137)

in the fovea and a one-to-one relationship between cones and the underlying bipolar cells exists presumably enabling high spatial resolution information transmission. However, the predominant receptors in the peripheral region are the rods, yet both rods and cones converge at the bipolar cells in the process of transmission of information. This leads to higher acuity in the foveal region compared to the peripheral, but the high density of rods converging on single bipolar cells in the peripheral retina leads to higher sensitivity to light energy in the peripheral region.

Cowger (Ref 4) studied the acuity of the peripheral visual field to eccentricities up to 45 degrees. Contrast sensitivity decreased as eccentricity and spatial frequency increased. Cowger attributed this to the rods, which, as the predominant receptors in the peripheral region of the retina, would receive the largest proportion of peripheral incident light.

In attempting to explain the peripheral retina functional organization, Hilz and Cavonius (Ref 10:1333-1337) also reported that contrast sensitivity decreased with increases in eccentricity. They also found that the amount of decrease depended on the spatial frequency of the stimulus as shown in Fig. 4.

The limits of the visual field of the eye can be determined by the physical dimensions of the retina and

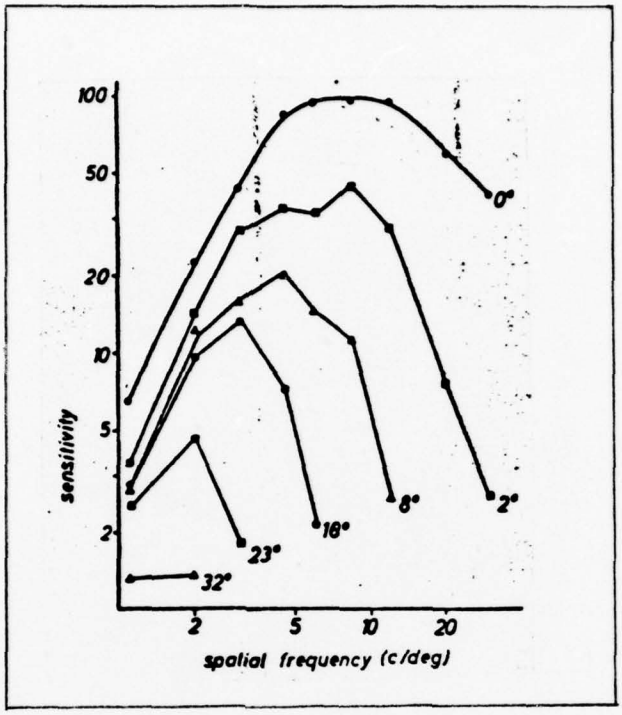

Fig. 4. *Contrast Sensitivity in the Temporal Retina for Various Eccentricities* (Ref 10:1334).

retinal sensitivity. Together, these factors determine the accessibility of light rays to the visual system. On the side of the eye nearest the nose (nasal field), the visual field is restricted to approximately 60 degrees from the middle of the field. The binocular field of vision is typically defined as the field common to both eyes; thus, the binocular field is approximately 60 degrees either side of the vertical meridian.

Asymmetry of the Cerebral Hemispheres

Many studies have dealt with the subject of cerebral

dominance in man. In most animals, the structure of the nervous system is basically symmetrical. However, in man the two cerebral hemispheres differ greatly in function. Before 1970, most information on the differing functions of the two cerebral hemispheres has come from the study of malfunctions in the brain caused by surgical procedures, disease, or accidental damage. One apparent division of function suggested by studies of patients whose cerebral hemispheres had been surgically disconnected is that of the processing of linguistic (verbal) information versus nonlinguistic (spatial) information. In both visual and auditory modes, linguistic processing appears to be located predominately in the left cerebral hemisphere; whereas, nonlinguistic processing appears to be localized in the right cerebral hemisphere. Right-handed subjects tend to show this dominance more predominantly than left-handed subjects (Ref 6, Ref 7).

The human nervous system provides information to each cerebral hemisphere primarily from the opposite half of the body. The human visual system is arranged such that vision to the left of a fixation point (left hemifield) is mediated by the right half of the brain (right hemisphere) and vice versa. In binocular vision, objects in the left hemifield are seen by the right half of the retina of each eye, and the neural channels from the right side of both retinas go to the visual cortex of the

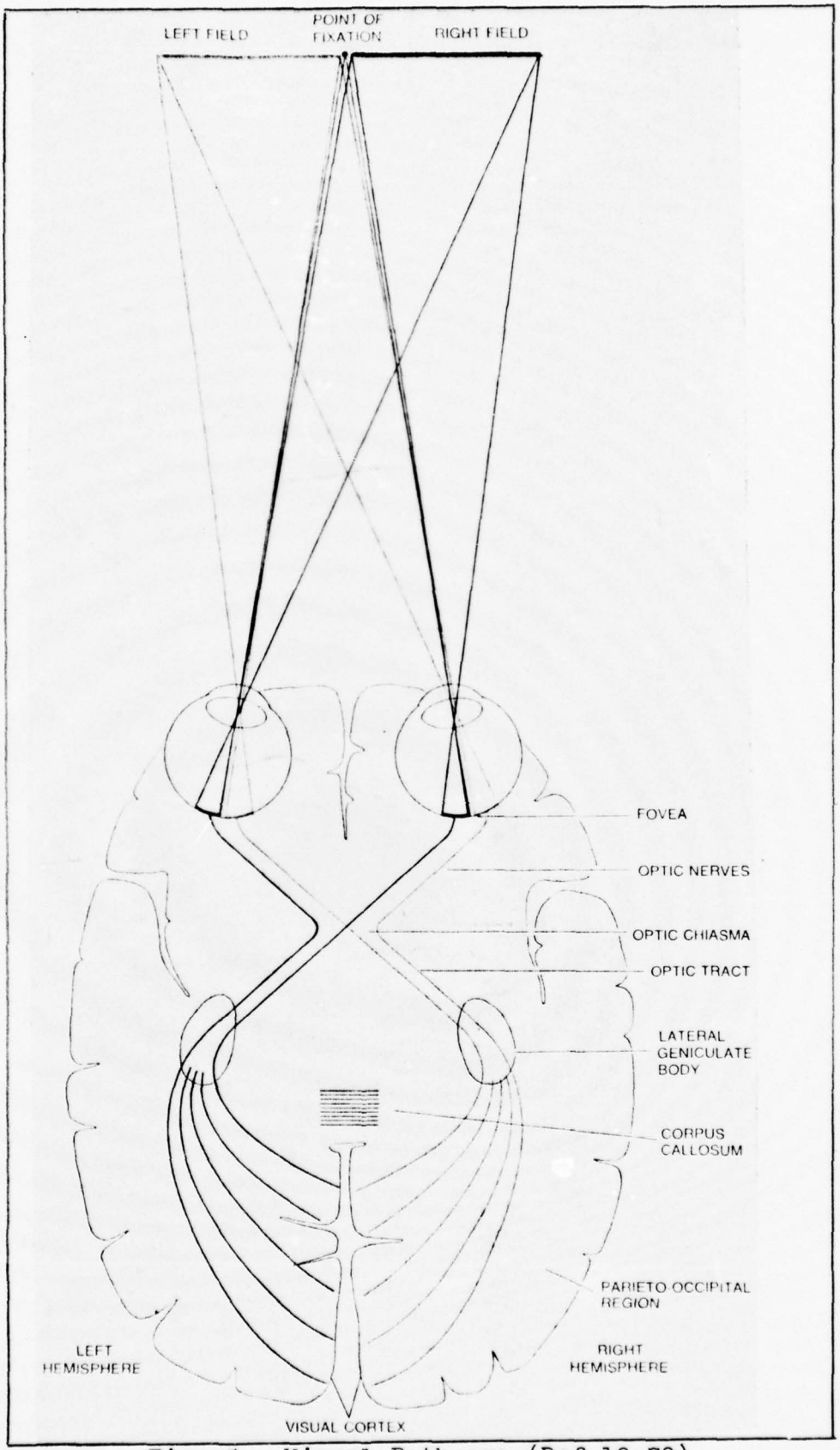

Fig. 5. Visual Pathways (Ref 12:73).

right hemisphere. Nerve pathways interconnect the two hemispheres to allow the visual field to be perceived as a single unit. The largest of these pathways is the interhemispheric commissure (the point of union between the two hemispheres). This pathway is commonly known as the corpus callosum, and it plays a key role in coordinating activities between the hemispheres.

During the 1970s, researchers have been involved in developing methods to study the asymmetry of hemispheric functions in normal people, since data from damaged brains is always open to question.

Kimura (Ref 12) has studied normal subjects by using a tachistoscope to present a visual stimulus to either the left or right of a fixation point thus stimulating only one cerebral hemisphere directly. Her studies involved determining the accuracy of locating dots in space and the slant of lines in space. Both of these tasks were performed by matching what had been seen to multiple-choice arrays on a sheet of paper. She found a clear right hemisphere dominance in analyzing this information and further found that specialization of the right hemisphere for spatial tasks is more noticeable in males than in females. In addition, her data showed no difference in the accuracy of detecting that a dot or slanted line was present from one hemifield to the other. Kimura felt that such simple tasks show primary process asymmetry and are a testing of

the regions near the striate cortex, not remote temporal readings.

Klatzky in 1970 (Ref 13), Gross in 1972 (Ref 8), Isseroff in 1974 (Ref 11), Cohen in 1975 (Ref 2), and others have used reaction time measures as possibly more sensitive to the dominance theory than accuracy reports. Also, reaction times have been used by these researchers to study the nature of the flow of information between the hemispheres. Any differences in reaction times could be related to information loss in transmission or corpus callosum crossing time. Stimuli in these experiments generally consisted of facial identification, dot patterns, letters, or words.

Evidence exists that shows a definite callosal crossing time. The primary positive wave of an excitation exclusively in one hemisphere takes approximately 10 msec to reach the opposite hemisphere. The secondary negative wave takes approximately 35 msec crossing time (Ref 16). Behavioral studies in cats have shown that stimuli projected by way of the corpus callosum was not identical to the same stimuli projected by way of the geniculocortical pathways (Ref 1). This brings out the possibility that the corpus callosum is a rather limited communications channel and does not encode weak signals effectively. Thus, inferior transmission performance would be most pronounced where stimulus information was already at a minimum. An example of this

would be when stimuli are presented at very short display times (Ref 5). Isseroff, Carmon, and Nachshon (Ref 11), as well as others, have shown that the corpus callosum crossing time error is small compared to differences directly attributable to visual field effects.

Typically, however, reaction time measures to study normal subjects is unstable and often produces very small statistical differences; that is, the difference quantities may vary considerably and may come or go at different stages of learning (Ref 2:367). This experiment, then, was an attempt to expand on, with a more statistically dominant method, some of the theories related to the human peripheral vision processing system.

II. Apparatus

The apparatus used to generate the peripheral stimulus was designed by Dr. Matthew Kabrisky, a professor at AFIT, and was the same basic arrangement used by Guidry (Ref 9) and Sakai (Ref 14). The viewing distance was arranged to maintain a two degree diameter test field presentation. The peripheral stimulus was designed in such a manner as to be challenging to the subject and yet simple to implement. Another aspect of the stimulus was that it was complete in itself; that is, results could be obtained from the answers to the stimulus and not through a matching scheme with other patterns.

A sine-wave grating with the capability of varying contrast and varying spatial frequency was chosen. Such a grating met the desired requirements and presented the visual system with a truly spatial, nonlinguistic input. A vertical sine-wave grating was generated on an HP-1205A oscilloscope. Fig. 6 shows the necessary inputs to the HP-1205A to generate the sine-wave grating.

A triangular wave from Wavetek I produced the required Y-axis deflection for the sine-wave grating. The X-axis signal was not synchronized with the Y-axis signal. A frequency of approximately 85 KHz was used on Wavetek I to prevent drifting of raster lines visible on the oscilloscope display because of this non-synchronization.

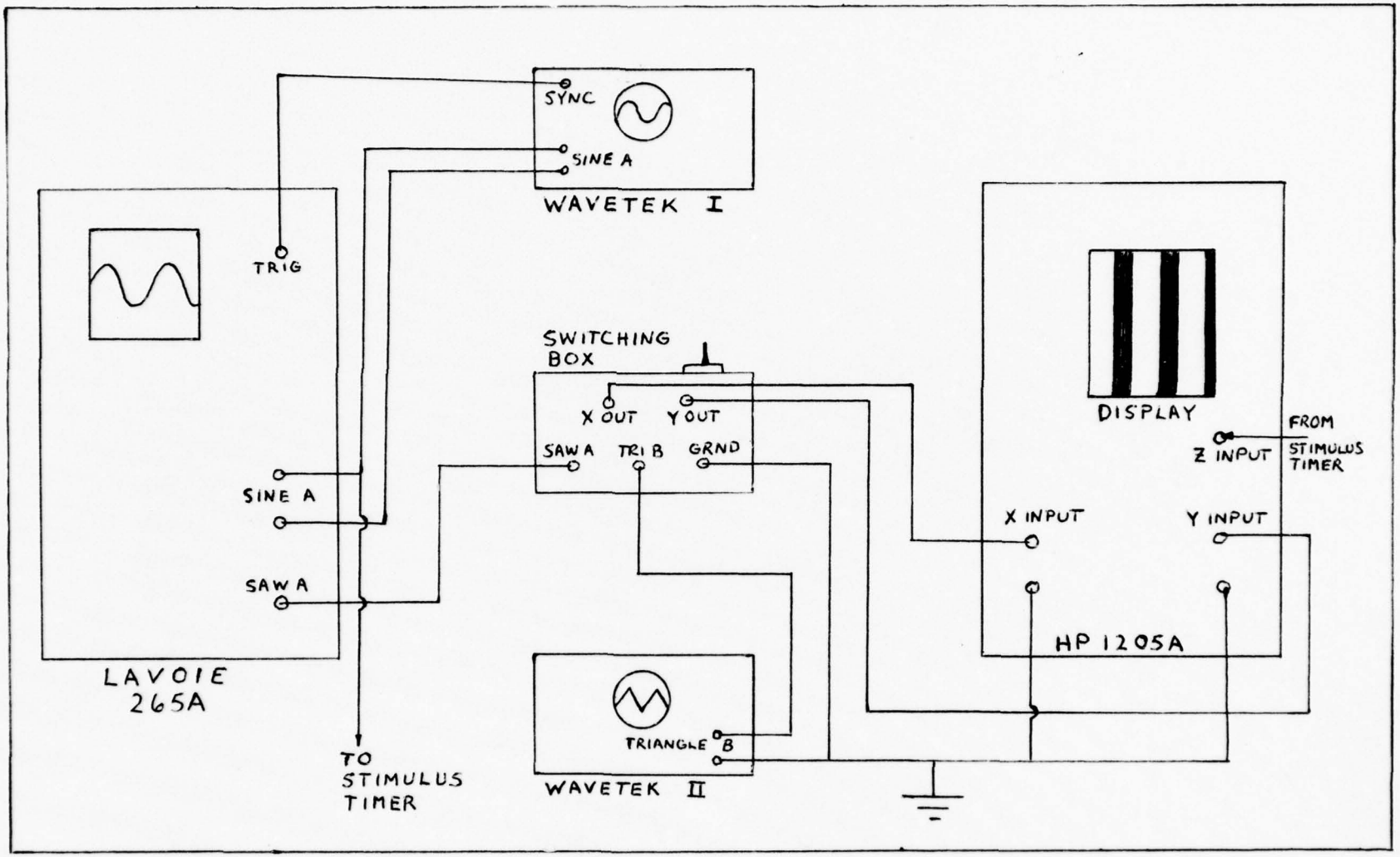

Fig. 6. Stimulus Pattern Generator.

The stimulus raster was, however, synchronized with the grating input frequency by externally synchronizing the sine-wave input from Wavetek II with the sawtooth output from the Lavoie 265A oscilloscope. With this external synchronization, the z-axis modulation signal from Wavetek II was synchronized with the X input to the stimulus display. The contrast of the sine-wave grating display was controlled by varying the z-axis output of Wavetek II, and the spatial frequency of the grating was controlled by the output frequency of Wavetek II. The spatial frequency was set to one cycle-per-degree throughout this experiment. The contrast was varied by changing the voltage input to the z-axis over a range of 6 volts to 0.05 volts.

An orthogonal display of the sine-wave grating was made possible by interchanging the X and Y inputs by means of a double-pole, double-throw switch (Fig. 7). This presented a horizontal sine-wave grating pattern. Cowger had shown a depressed orthogonal effect, the phenomenon whereby contrast sensitivity for the orientation orthogonal to the meridian on which the stimulus is viewed is approximately one-half the sensitivity to the orientation parallel to that meridian (Ref 4:24). Therefore, the HP-1205A oscilloscope was tilted 45 degrees off the vertical to avoid any problems in this area. This allowed display presentations of 45 degrees left of vertical and 45 degrees right of vertical (See Fig. 8).

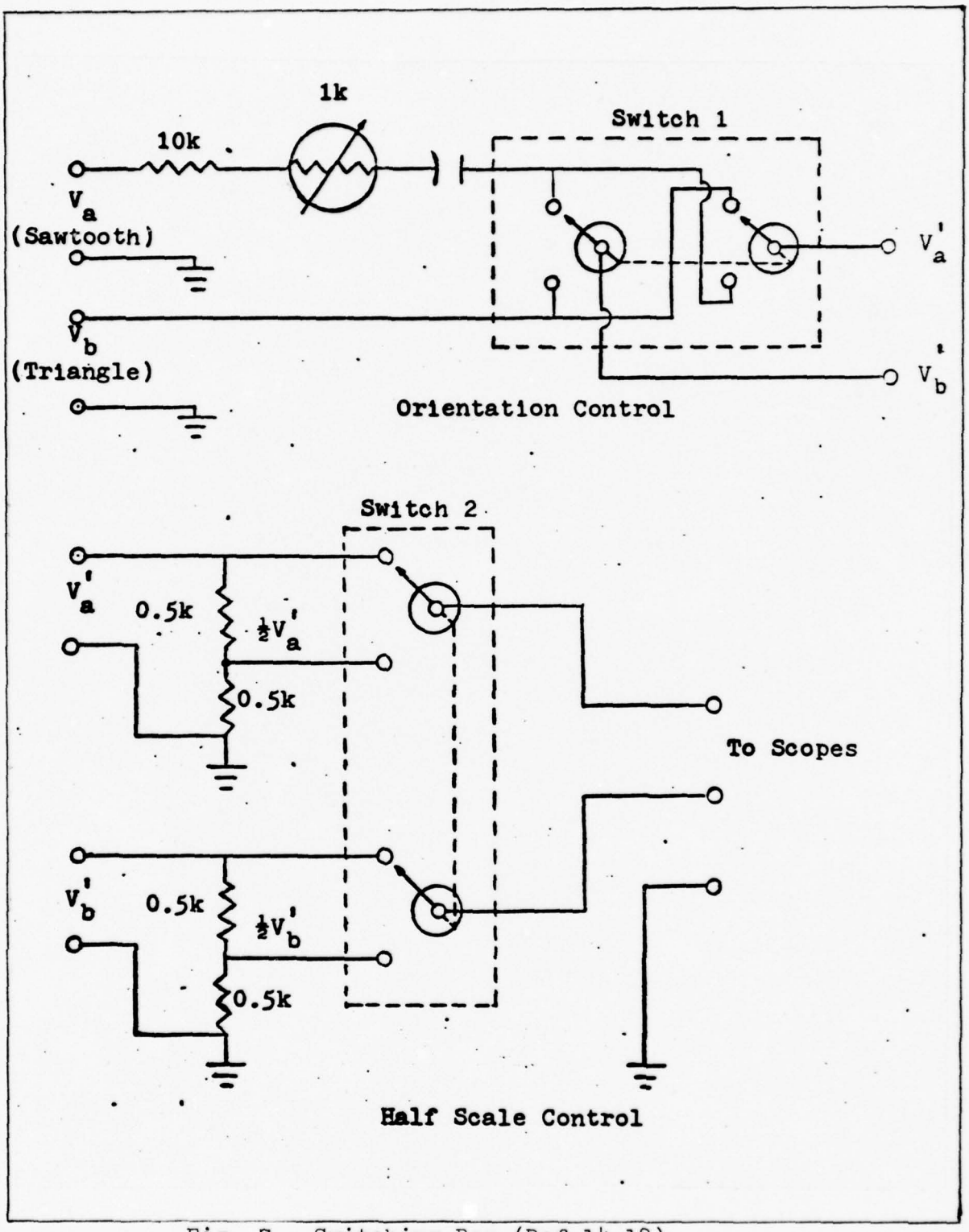

Fig. 7. Switching Box (Ref 14:18).

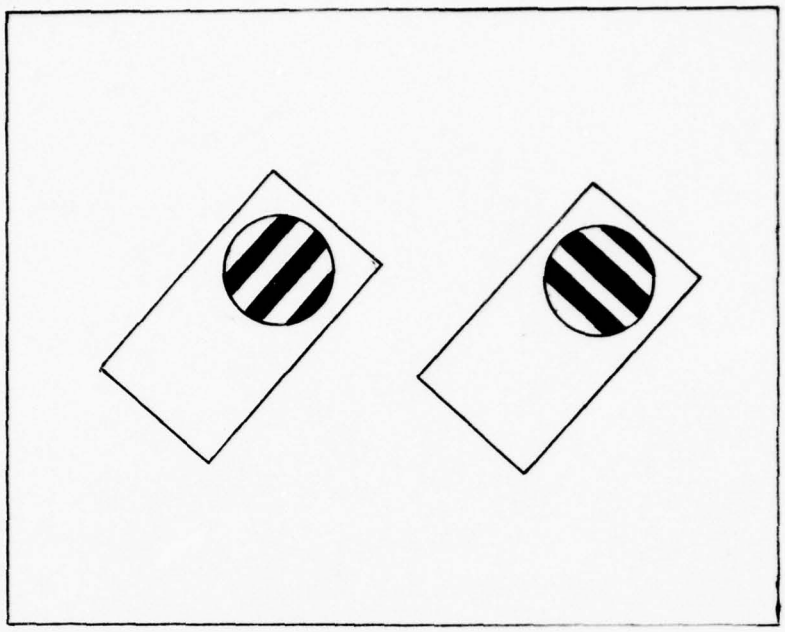

Fig. 8. Possible Presentations On HP-1205A Oscilloscope.

A second HP-1205A oscilloscope was connected in parallel with the first to provide the capability of additional loading of the peripheral visual system. All inputs were the same except the X - Y interchange was wired through a separate switch to allow same or opposite orientations of the second scope in relation to the first scope.

The timer that controlled the stimulus exposure time was adjustable to four different times: 500 msec, 100 msec, 50 msec, and 20 msec. The peripheral display scope showed no variation in contrast or any pattern until the subject depressed the button which remotely triggered the timer. When actuated, the timer circuit allowed the z-axis input,

which contributed the sine-wave grating pattern, to appear on the scope for the period of time selected from the four possible times. Then, the scope returned to the no variation in contrast, no pattern presentation.

III. Testing Procedure

Five subjects were tested in this experiment. One subject (MK) was highly experienced in psychophysiological testing and had participated as a subject in previous testing using similar test apparatus. The other four subjects (KB, JK, CH, and RS) had no previous training but were highly motivated as determined in the indoctrination sessions. The experiment was concerned with relative changes in accuracy of perceiving the test stimulus, so the experimenter was not concerned with visual problems as long as they were correctable with the use of glasses. In fact, only one subject (RS) required corrective lenses. Two subjects (MK and JK) were male and three subjects (KB, CH, and RS) were female. Three subjects (MK, KB, and JK) exhibited strong right-hand dominance, while the other two (CH and RS) showed strong left-hand dominance.

Table I
Subject Data

Subject	Male	Female	Left Handed	Right Handed
MK	X			X
KB		X		X
JK	X			X
CH		X	X	
RS		X	X	

Approach

Three subjects (KB, JK, and CH) were presented stimuli in six positions along the horizontal meridian. One subject (MK) participated in the testing of these six positions but also participated in an extension of the testing along the vertical meridian and quadrants of the visual field. Thus, MK was tested with stimuli in 22 positions. Subject RS was tested only at four positions due to time constraints on subject availability. The positions used with RS were chosen to add to existing data at those positions. Tests one through eight were concerned with stimuli along the horizontal meridian. Displays 9 through 14 tested along the vertical meridian, while tests 15 through 22 were concerned with the quadrants of the visual field. The positioning of the display scopes is graphically presented in Fig. 9. Presentations were either 10 degrees or 20 degrees from the fixation point or combinations at 10 degrees and 20 degrees.

The peripheral displays were "one-shot" stimuli, and, in the case of the two peripheral displays, both displays were presented simultaneously. The range of latencies of eye movements to peripheral stimuli is about 120 to 240 msec with the mean latency approximately 200 msec (Ref 17:482). Thus, the duration of the stimulus display covered a wide range of values (500 msec, 100 msec, 50 msec, and 20 msec). The shorter durations were long enough to perceive the

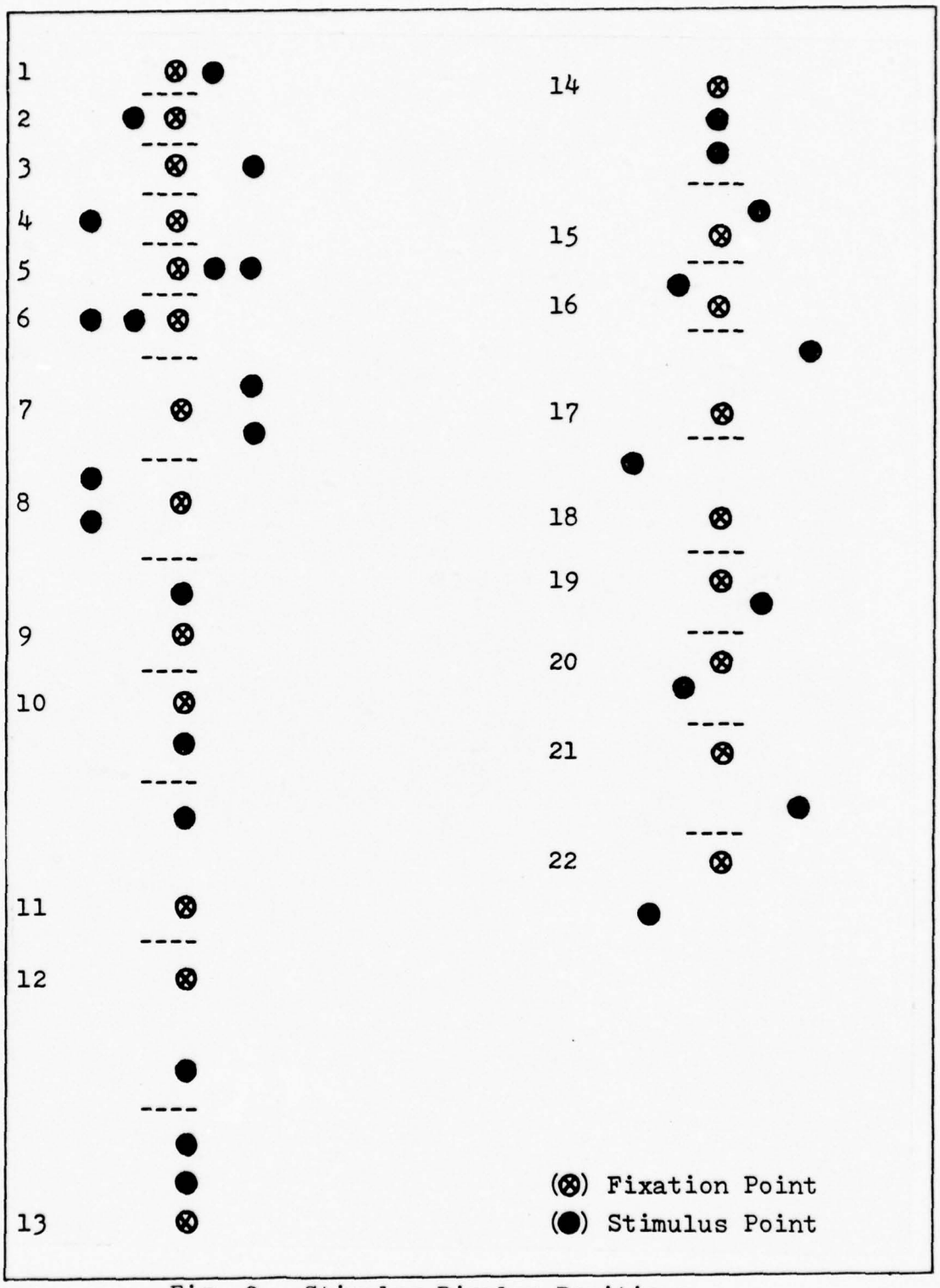

Fig. 9. Stimulus Display Positions.

peripheral display but short enough to prevent inadvertently shifting the foveal axis to the peripheral display. Various tests have shown that the eye axis does drift during attempts to fixate on a point source. This movement is irregular, but the image of the fixation point always remains inside the fovea while consciously attempting to fixate on a point. Thus, no eye fixing was used during subject testing other than by voluntary fixation on a point. Likewise, since small changes in viewing distance had little

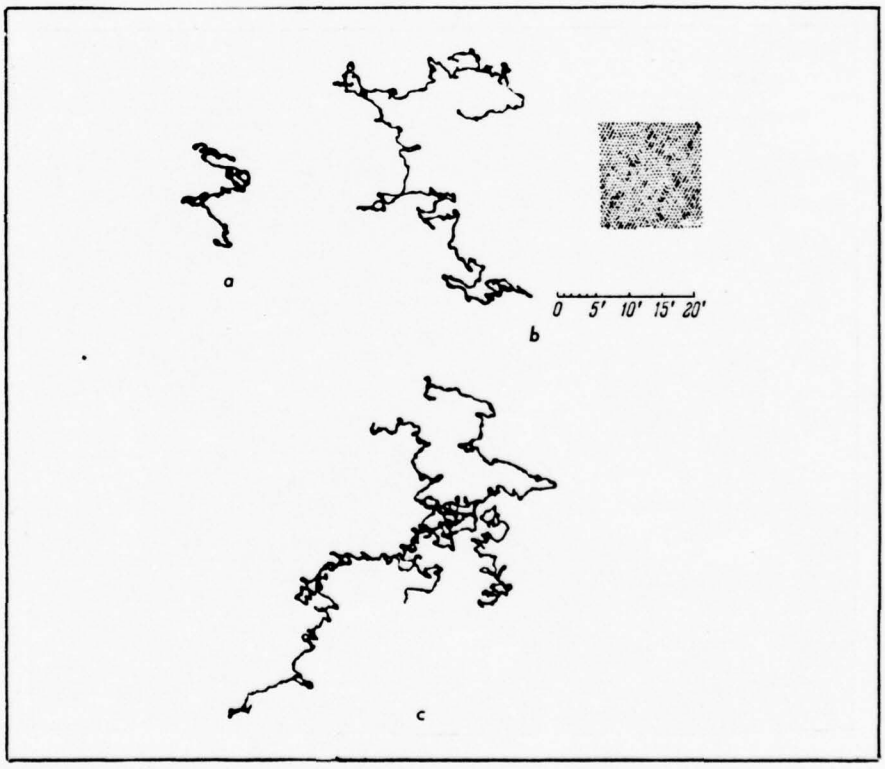

Fig. 10. Eye Movement During Fixation on a Stationary Point. a) Fixation for 10 Sec; b) Fixation for 30 Sec; c) Fixation for 60 Sec. Scale in Minutes of Angle (Ref 18:107).

effect on testing angles, a head restraint device was deemed unnecessary. Four subjects (MK, KB, JK, and CH) were tested at all four display durations. RS could not adjust to any display duration less than 100 msec.

Prior to recording data, each subject was made fully aware of the testing and scoring procedures as well as some of the problems of psychophysiological testing in general. Each subject was free to comment on procedures or feelings concerning the testing. The general purpose of the testing was explained to each subject along with the general workings of the apparatus.

Responses

Before testing began, the subject was adapted to the experimental lighting conditions for approximately ten minutes. Then, the various orientation combinations were presented to the subject several times without scoring accuracy. This allowed the subject to gain a mental picture of the stimuli prior to collecting data.

The subject was requested to give a response by illuminating the face of the peripheral display oscilloscope by means of the switching box in the control of the experimenter. The subject fixated on a central point, pressed the stimulus button, and observed the sine-wave grating in the peripheral hemifield. The grating did not appear until the z-axis signal was allowed to reach the

oscilloscope. This signal was available through the stimulus duration timer which was activated when the stimulus button was depressed.

The subject responded verbally with the orientation of the peripheral display. With one peripheral display, one of two orientations was called out. With two peripheral displays, the orientations of each display was required to be reported correctly. Fig. 11 shows the possible responses to the two display arrangement. Orientations were presented randomly by use of random units tables (Ref 15:628-632). The only requirement varying from total randomness was that each orientation was allotted the number of presentations found by dividing the total presentations to be displayed by the number of possible orientations (e.g., in the two-scope display, if 100

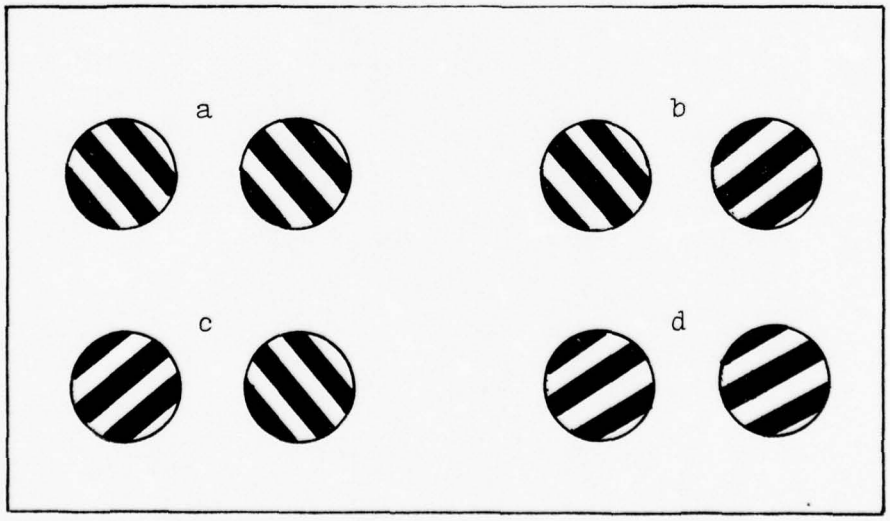

Fig. 11. Possible Displays With Two Peripheral Oscilloscopes.

presentations were to be made, each orientation would be presented 25 times). Responses and correctness of the responses were recorded by the experimenter.

Positions of the scopes, stimulus duration, and contrast levels did not follow any specific pattern from subject to subject. The total number of presentations at a particular contrast level varied but appeared statistically reliable throughout. This number varied from 60 presentations in some cases to 120 presentations in others. The determining factor was the ability of the individual subject to maintain a high degree of concentration. Fatigue produced drastic changes in results; however, both subject and experimenter found it relatively simple to determine when fatigue was setting in, and the experiment was adjusted to account for these subject differences.

IV. Results

Five subjects were tested using the experimental conditions described in the previous chapter. Four of the subjects (MK, KB, JK, and CH) were tested at all four stimulus durations. The fifth subject was tested in accordance with the constraints outlined previously. Appendices B through S are the results of the various subjects with percentage of accuracy of responses as a function of the contrast of the sine-wave grating pattern. The contrast is based on voltage input to the z-axis. Heading each appendix is a table of the values plotted within that appendix. Each appendix is restricted to testing accomplished with one subject at one stimulus duration. The peripheral scope positions are based on those depicted in Fig. 9.

This experiment attempted to investigate relative changes in accuracy as a function of position of the stimulus in the peripheral visual field. Percentage scores outlined with parentheses indicate values determined by interpolating from plots of experimental data.

Appendix T is a summary of the data collected from the five subjects using the mean scores. The trends are the same as the individual subjects and can be referred to for demonstration of the data. Similar graphic results are obtainable from individual subjects.

The subject data was analyzed using the ANOVA7 computer program, a FORTRAN program which computes analysis of variance. The program handles up to seven variables combined factorially. The combination of factors involved in this experiment were analyzed on a within-subject manipulation.

The results were analyzed using a six-way analysis of variance (sex, handedness, contrast, hemisphere, stimulus duration, and stimulus position within a hemifield). No significant variations occurred with males versus females ($F=6.3515$, p less than .2486). Similarly, no significance could be attributed to handedness ($F=1.1062$, p less than .4680). Stimuli presented in the left hemifield were significantly more visible than those presented in the right hemifield ($F=32.0636$, p less than .0095). As expected, decreasing contrast levels as well as decreasing stimulus display duration were significant variations ($F=442.9527$, p less than .0000 and $F=198.6328$, p less than .0000 respectively). Changing from positon 1 or 2 to 3 or 4 to 5 or 6 was a significant variable ($F=21.5892$, p less than .0025); however, the difference between one scope at 10 degrees and one scope at 20 degrees (position 5 or 6) versus two scopes at 20 degrees (position 7 or 8) was not significant ($F=1.1969$, p less than .4724).

Significant interaction effects were reached with all variables except sex related, handedness related, and

contrast variation versus hemifield results. Table II shows these significant interactions.

Table II
Interactions of Variables

Variable (*)	F	p
13	36.7637	.0000
14	16.8745	.0000
23	13.3054	.0069
24	3.0863	.0824
34	17.6569	.0000
123	3.3365	.0216
124	4.3207	.0017
134	11.0186	.0000
234	2.8147	.0409
1234	2.1267	.0170

* 1 Contrast Variation
2 Hemifield Presentation
3 Display Position
4 Display Duration

With subject MK, experiments along the vertical meridian and quadrants were accomplished. Although insufficient data exists to adequately perform significant analysis, the initial results appear to be hemifield oriented also, with the lower hemifield superior to the upper hemifield.

V. Conclusions

The apparatus used in this experiment was sufficient to show the dominance of the right cerebral hemisphere for processing spatial information. This dominance was demonstrated at a very significant statistical level. The apparatus was also adequate to provide preliminary data which shows that lower hemifield spatial presentations are similarly dominant. To carry this to the fullest extent, the quadrants of the visual field vary similarly. In this case, the ease of processing spatial information from maximum to minimum is left-lower, right-lower, left-upper, and right-upper. Such results have strong implications as to where spatial presentations should be located in the visual field for maximum perception. For example, in panel displays, secondary gauges or warning lights would be most easily seen in the left hemifield. If the preliminary data with subject MK is accurate, further arrangement of the panel with secondary gauges in the lower left quadrant would seem appropriate. This would allow the peripheral visual system to be used to the fullest capacity, while allowing the foveal region to concentrate on primary gauges. The quadrant breakdown warrants further investigation.

The results also showed a decrease in accuracy when the number of displays was increased. The significant interaction of this effect with the hemisphere dominance

effect could point to the type of processing involved in the cerebral cortex. Such results could show the right hemisphere as an integrator, able to put together inputs into a whole pattern to analyze; whereas, the left hemisphere analyzes according to individual bit information.

The decrease in accuracy due to contrast and stimulus duration time decreases correlates with the theory of the corpus callosum as a limited communications channel dependent on amount of stimulus information available.

The small number of subjects used in this experiment could appear to limit the scope of the results. However, the data is extremely consistent throughout the various types of subjects. Likewise, data was repeatable for a subject with as much as six weeks delay in time, pointing to an accurate basic experimental paradigm. Thus, the data base herein should be sound for further studies of the processing of information within the human peripheral visual system.

VI. Recommendations

As stated in the Conclusions, this report shows significant variations in the ability of the human visual system to perceive spatial presentations which correlate with location of the presentation in the visual field. Further data are required to fill in all areas of the visual field. By completing such data, recommended fields of vision for spatial presentations could be suggested.

Also, the perception based on location should be studied in relation to design concepts of such items as cockpit display units, where peripheral perception could be used to maximize human performance.

Increasing the data in all areas of the periphery could also provide more insight into the overall type of information processing inherent to each of the cerebral hemispheres, leading to a better model of pattern recognition.

Bibliography

1. Berlucchi, G., and G. Rizzolatti. "Binocularly Driven Neurons in Visual Cortex of Split-Chiasm Cats." Science, 159: 308-310 (1968).

2. Cohen, G. "Hemisphere Differences in the Effects of Cuing in Visual Recognition Tasks." Journal of Experimental Psychology, 1: 366-373 (1975).

3. Cornsweet, T. N. Visual Perception. New York: Academic Press, 1970.

4. Cowger, R. I. A Measurement of the Anisotropic Modulation Transfer Function of the Extrafoveal Human Visual System. Unpublished Thesis, Wright-Patterson Air Force Base, Ohio: Air Force Institute of Technology, December, 1973.

5. Gazzaniga, M. "One Brain -- Two Minds?" American Scientist, 60: 311-317 (1972).

6. Gazzaniga, M., J. Bogen, and R. Sperry. "Observations on Visual Perception After Disconnection of the Cerebral Hemispheres in Man." Brain, 88: 221-236 (1965).

7. Gazzaniga, M., and R. Sperry. "Language After Section of Cerebral Commissures." Brain, 99: 131-148 (1967).

8. Gross, M. "Hemispheric Specialization for Processing of Visually Presented Verbal and Spatial Stimuli." Perception and Psychophysics, 12: 357-363 (1972).

9. Guidry, R. A High Resolution Measurement of the Anisotropic Modulation Transfer Function of the Human Visual System. Unpublished Thesis, Wright-Patterson Air Force Base, Ohio: Air Force Institute of Technology, June, 1973.

10. Hilz, R., and C. Cavonius. "Functional Organization of the Peripheral Retina: Sensitivity to Periodic Stimuli." Vision Research, 14: 1333-1337 (1975).

11. Isseroff, A., A. Carmon, and J. Nachshon. "Dissociation of Hemifield Reaction Time Differences From Verbal Stimulus Directionality." Journal of Experimental Psychology, 103: 145-149 (1974).

12. Kimura, D. "The Asymmetry of the Human Brain." Scientific American, 228: 70-78 (1973).

13. Klatzky, R. "Interhemispheric Transfer of Test Stimulus Representations in Memory Scanning." Psychonomic Science, 21: 201-203 (1970).

14. Sakai, J. T. A Measure of Foveal Sensitivity in an Expanded Field of Visual Attention. Unpublished Thesis, Wright-Patterson Air Force Base, Ohio: Air Force Institute of Technology, June, 1976.

15. Selby, S. Standard Mathematical Tables. Cleveland, Ohio: CRC Press, Inc., 1975.

16. Teitelbaum, H., S. Sharpless, and R. Bych. "Role of Somatosensory Cortex in Interhemispheric Transfer of Tactile Habits." Journal of Comparative and Physiological Psychology, 66: 623-632 (1968).

17. White, M. "Does Cerebral Dominance Offer a Sufficient Explanation for Laterality Differences in Tachistoscopic Recognition?" Perceptual and Motor Skills, 36: 479-485 (1973).

18. Yarbus, A. L. Eye Movements and Vision. New York: Plenum Press, 1967.

Appendix A

Z-Axis Stimulus Timing

Sakai (Ref 14:58-59) used the following equation as a relationship of the output duration of the SN74L121, a one-shot monostable multivibrator, to the values of the external capacitor and resistor in the stimulus timer. This enabled him to determine the values of external resistor and capacitors required to yield specific stimulus durations ($t_{W(out)}$) for the design of the stimulus timing mechanism.

$$t_{W(out)} = C_T R_T \log_e 2 \qquad (2)$$

The block diagram of the stimulus switch and stimulus duration timer is found in Fig. 12.

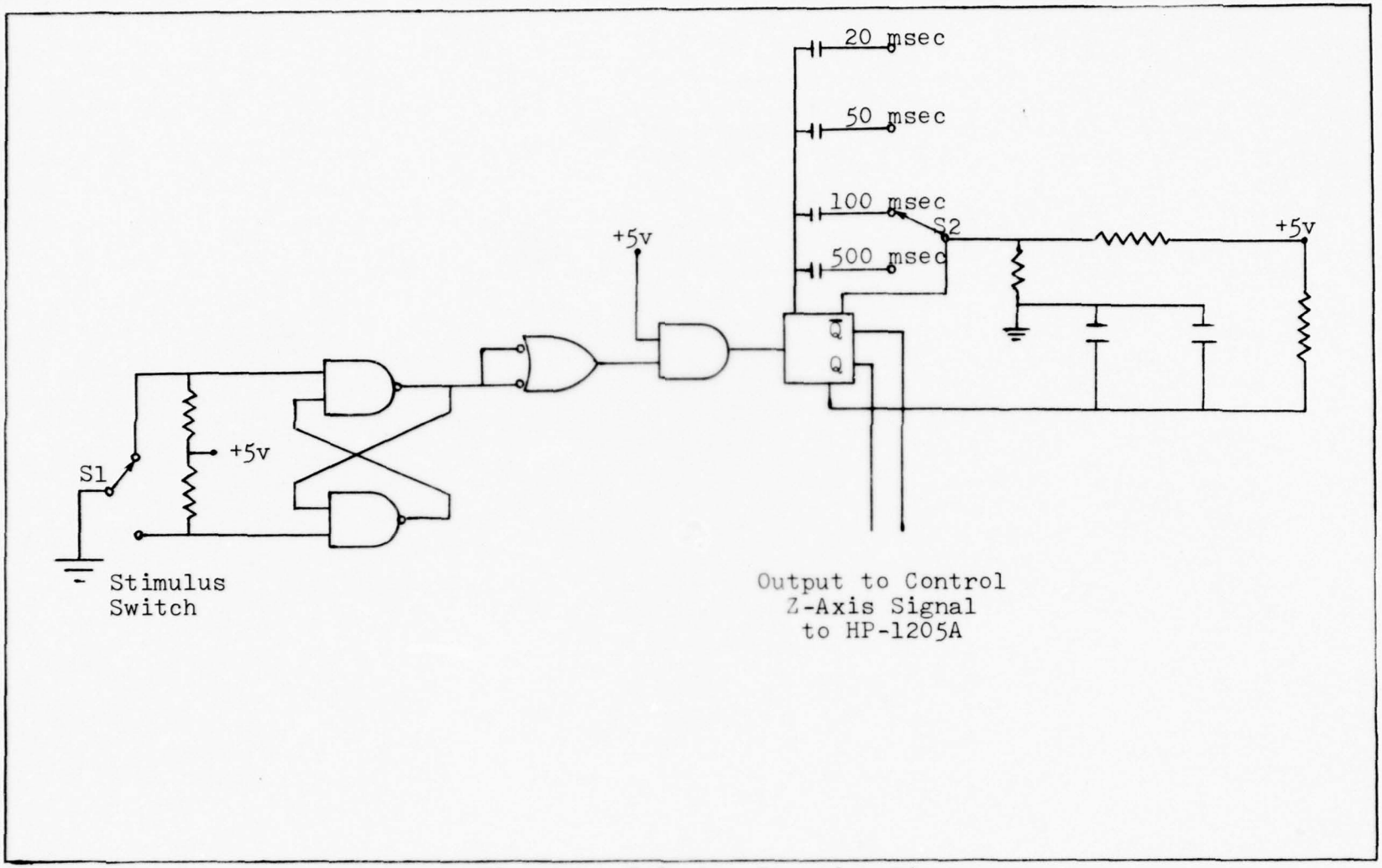

Fig. 12. Stimulus Duration Timer.

Appendix B

Accuracy Values (%): MK, 500 MSEC

Table III
Accuracy: MK, 500 msec

Contrast (Volts)	Peripheral Scope Position 1	2	3	4	5
6.00	100.0	100.0	100.0	100.0	94.2
3.00	100.0	100.0	100.0	100.0	(96.2)
1.00	100.0	100.0	100.0	100.0	99.2
0.50	100.0	100.0	(99.3)	(98.0)	(99.0)
0.25	100.0	100.0	98.7	95.0	98.4
0.15	100.0	100.0	(97.3)	(89.5)	(95.1)
0.10	100.0	100.0	96.2	85.0	92.5
0.05	100.0	100.0	51.2	40.0	64.2

	6	7	8
6.00	98.3	100.0	100.0
3.00	99.2	(100.0)	100.0
1.00	96.7	100.0	95.0
0.50	(98.0)	100.0	95.0
0.25	99.2	100.0	100.0
0.15	(97.8)	(96.7)	(89.8)
0.10	96.7	92.5	81.7
0.05	85.8	77.5	75.0

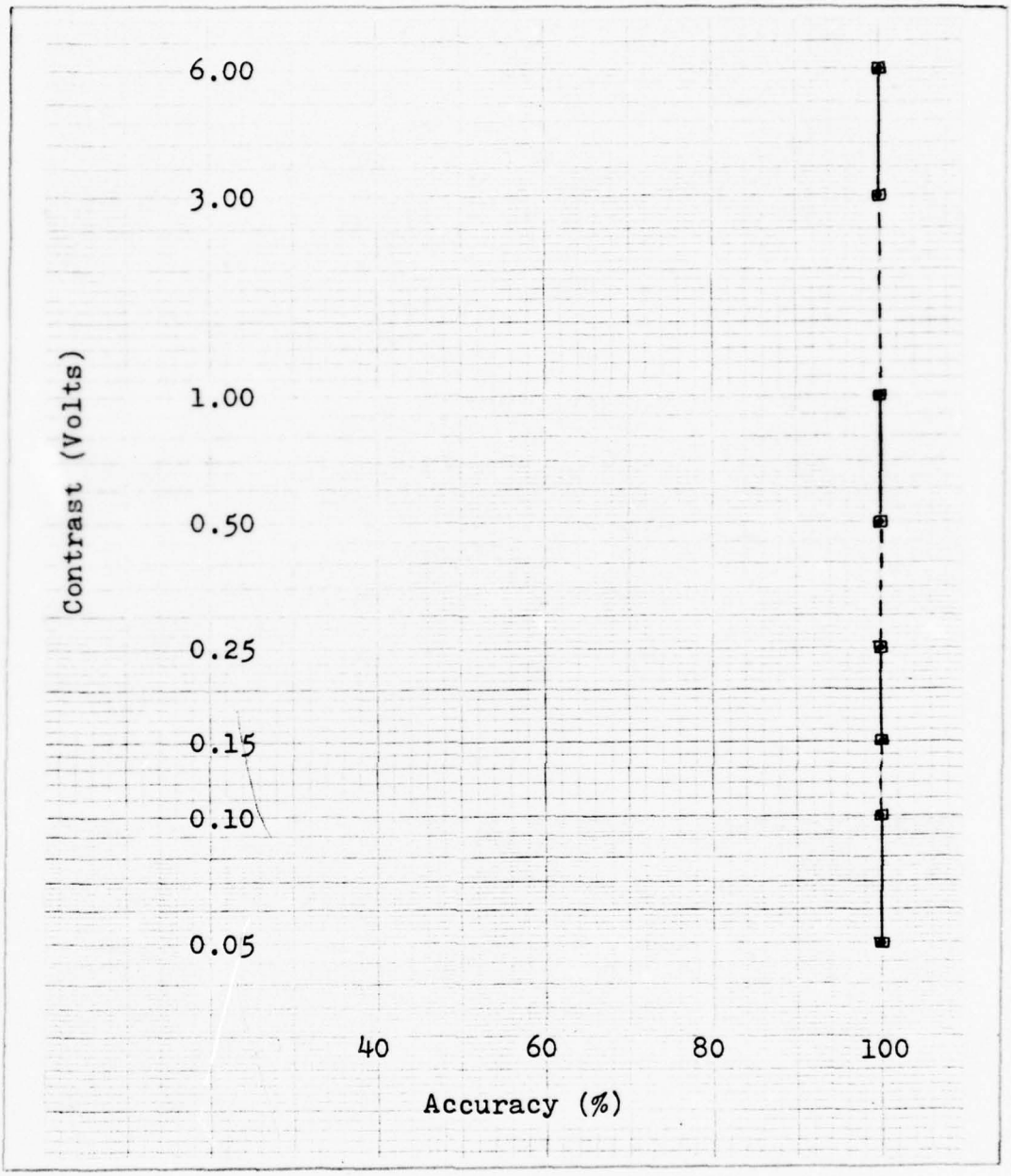

Fig. 13. Plot of Accuracy: MK, 500 msec, Positions 1 (——) and 2 (- -).

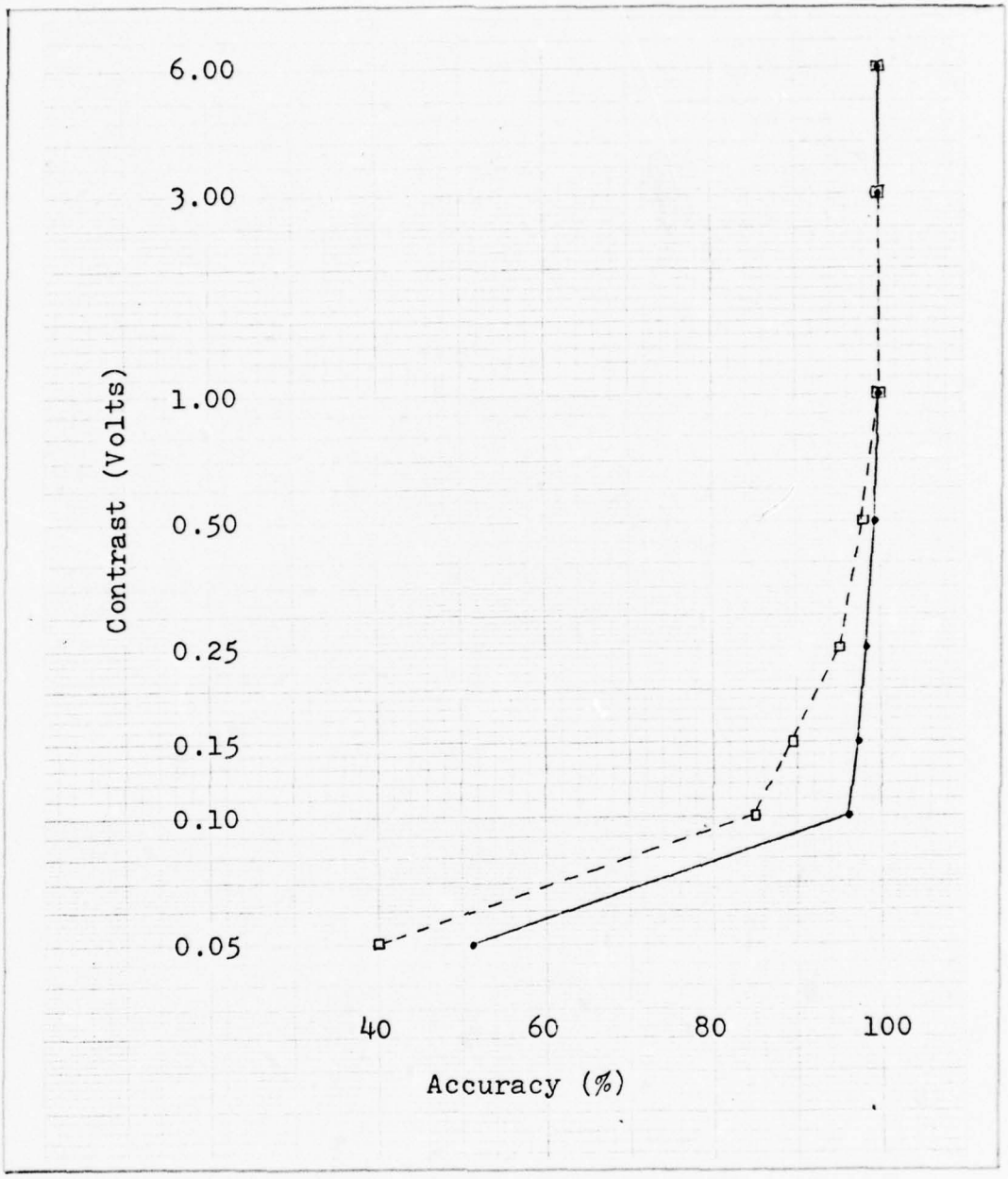

Fig. 14. Plot of Accuracy: MK, 500 msec, Positions 3 (——) and 4 (- -).

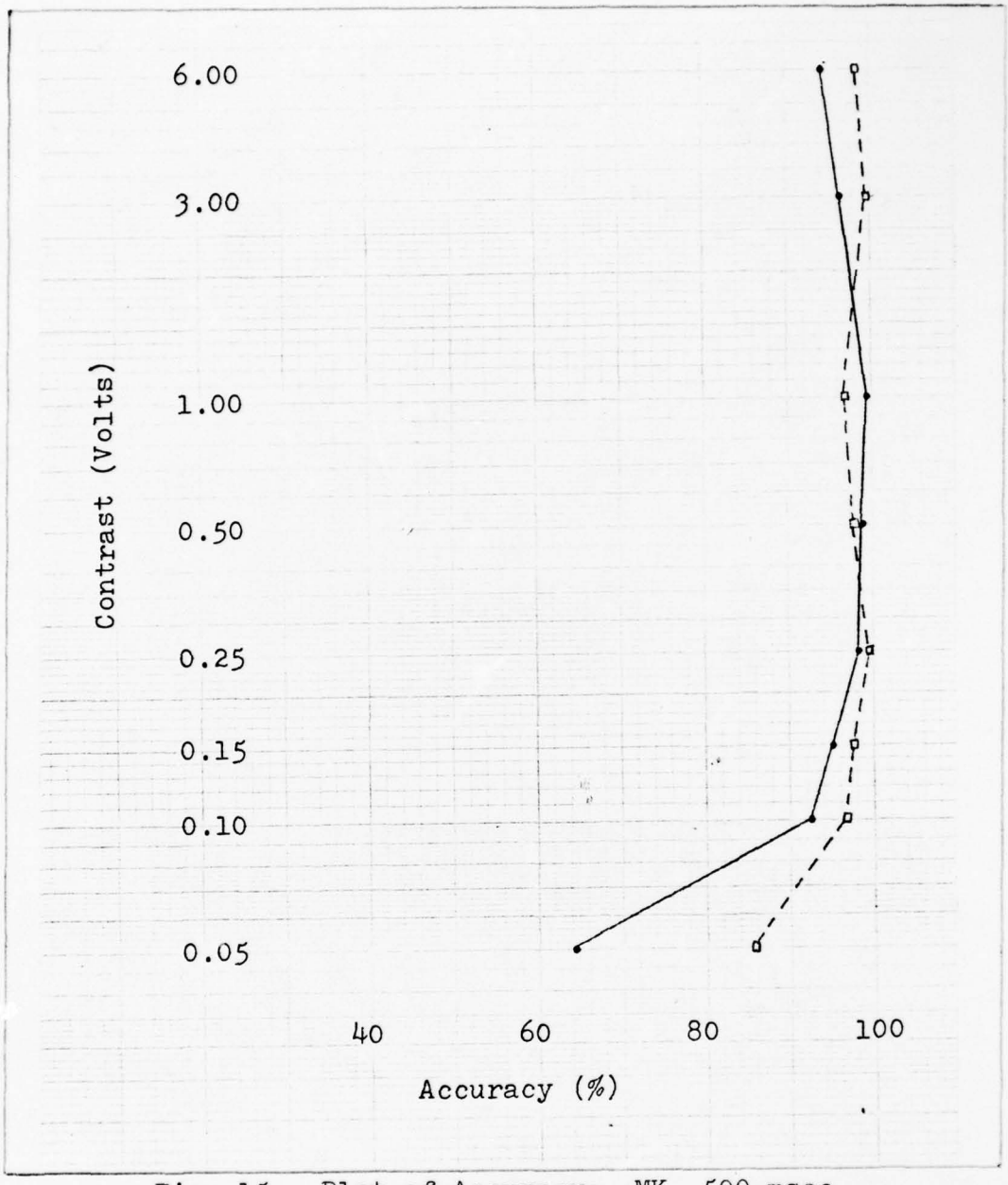

Fig. 15. Plot of Accuracy: MK, 500 msec, Positions 5 (——) and 6 (- -).

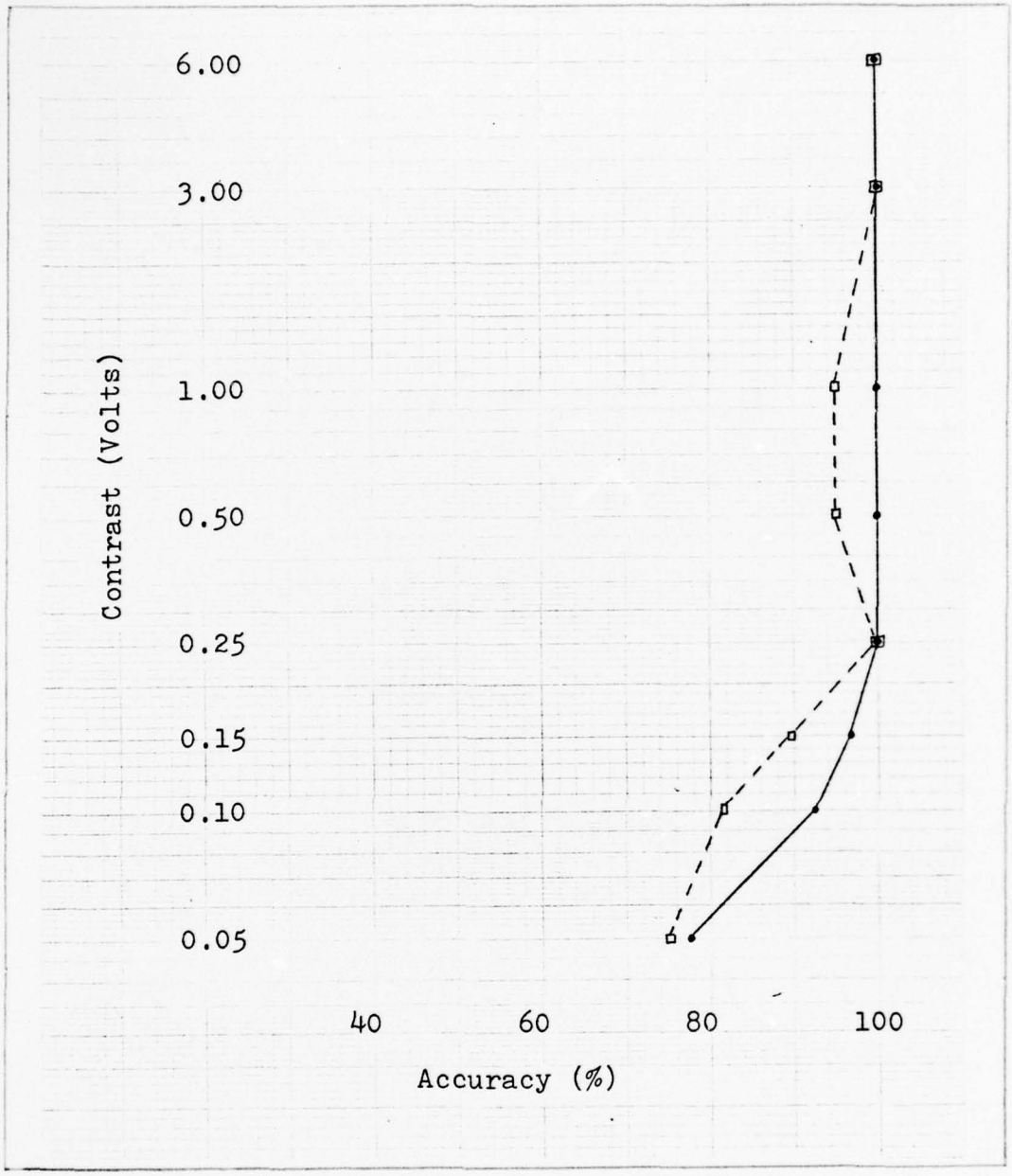

Fig. 16. Plot of Accuracy: MK, 500 msec, Positions 7 (——) and 8 (- -).

Appendix C

Accuracy Values (%): MK, 100 MSEC

Table IV
Accuracy: MK, 100 msec

Contrast (Volts)	Peripheral Scope Position 1	2	3	4	5
6.00	100.0	100.0	100.0	100.0	84.2
3.00	100.0	100.0	100.0	100.0	(85.1)
1.00	100.0	100.0	100.0	100.0	86.7
0.50	100.0	100.0	(100.0)	100.0	84.2
0.25	100.0	100.0	100.0	100.0	90.0
0.15	100.0	100.0	(81.0)	(83.1)	(74.5)
0.10	100.0	100.0	66.2	70.0	52.5
0.05	95.0	97.5	47.5	50.0	(25.0)
	6	7	8	9	10
6.00	95.0	97.5	95.0	100.0	100.0
3.00	(96.2)	(97.5)	(93.0)	(100.0)	(100.0)
1.00	98.3	97.5	90.0	100.0	100.0
0.50	95.0	94.1	97.5	(100.0)	(100.0)
0.25	96.9	92.5	95.8	100.0	100.0
0.15	(94.2)	(81.2)	(87.4)	(91.2)	(99.0)
0.10	95.0	72.5	80.8	84.0	98.0
0.05	78.3	(57.5)	(69.5)	62.0	100.0
	11	12	13	14	15
6.00	96.0	100.0	81.7	96.7	100.0
3.00	(96.8)	(100.0)	(81.7)	(96.7)	(100.0)
1.00	98.0	100.0	81.7	96.7	100.0
0.50	(93.9)	(99.0)	(72.5)	(97.5)	(100.0)
0.25	90.0	98.0	63.3	98.3	100.0
0.15	(71.5)	(90.0)	(56.5)	(80.5)	(100.0)
0.10	56.0	84.0	(51.2)	66.7	100.0
0.05	(50.0)	50.0	(42.0)	(43.0)	100.0

Table IV (Cont)

	16	17	18	19	20
6.00	100.0	100.0	100.0	100.0	100.0
3.00	(100.0)	(99.2)	(100.0)	(100.0)	(100.0)
1.00	100.0	98.0	100.0	100.0	100.0
0.50	(100.0)	(98.0)	(100.0)	(99.0)	(100.0)
0.25	100.0	98.0	100.0	98.0	100.0
0.15	(100.0)	(76.5)	(82.0)	(98.0)	(100.0)
0.10	100.0	60.0	68.0	98.0	100.0
0.05	96.0	50.0	50.0	90.0	82.0

	21	22
6.00	100.0	100.0
3.00	(100.0)	(100.0)
1.00	100.0	100.0
0.50	(100.0)	(98.0)
0.25	100.0	96.0
0.15	(94.5)	(89.5)
0.10	90.0	84.0
0.05	58.0	64.0

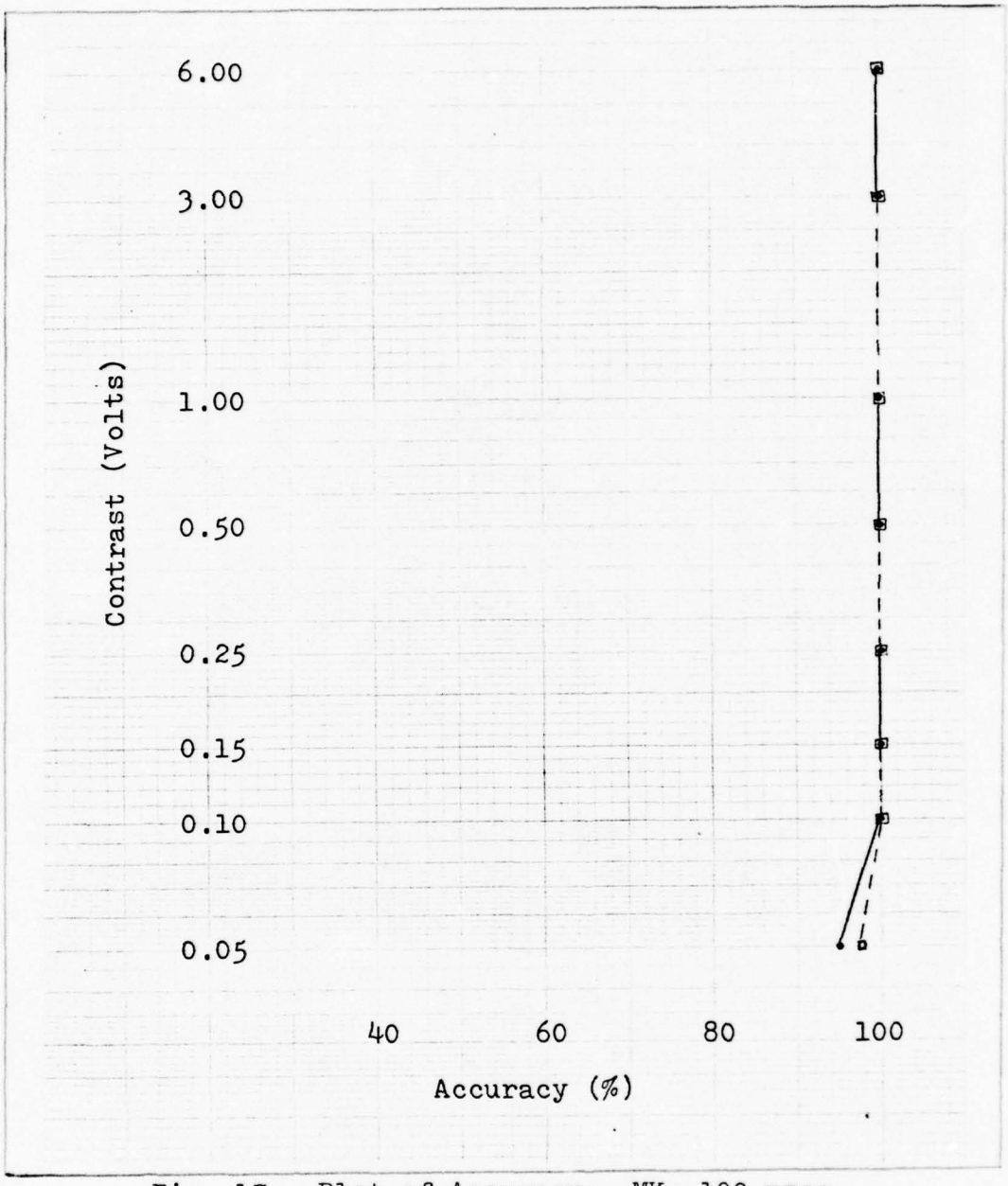

Fig. 17. Plot of Accuracy: MK, 100 msec, Positions 1 (——) and 2 (- -).

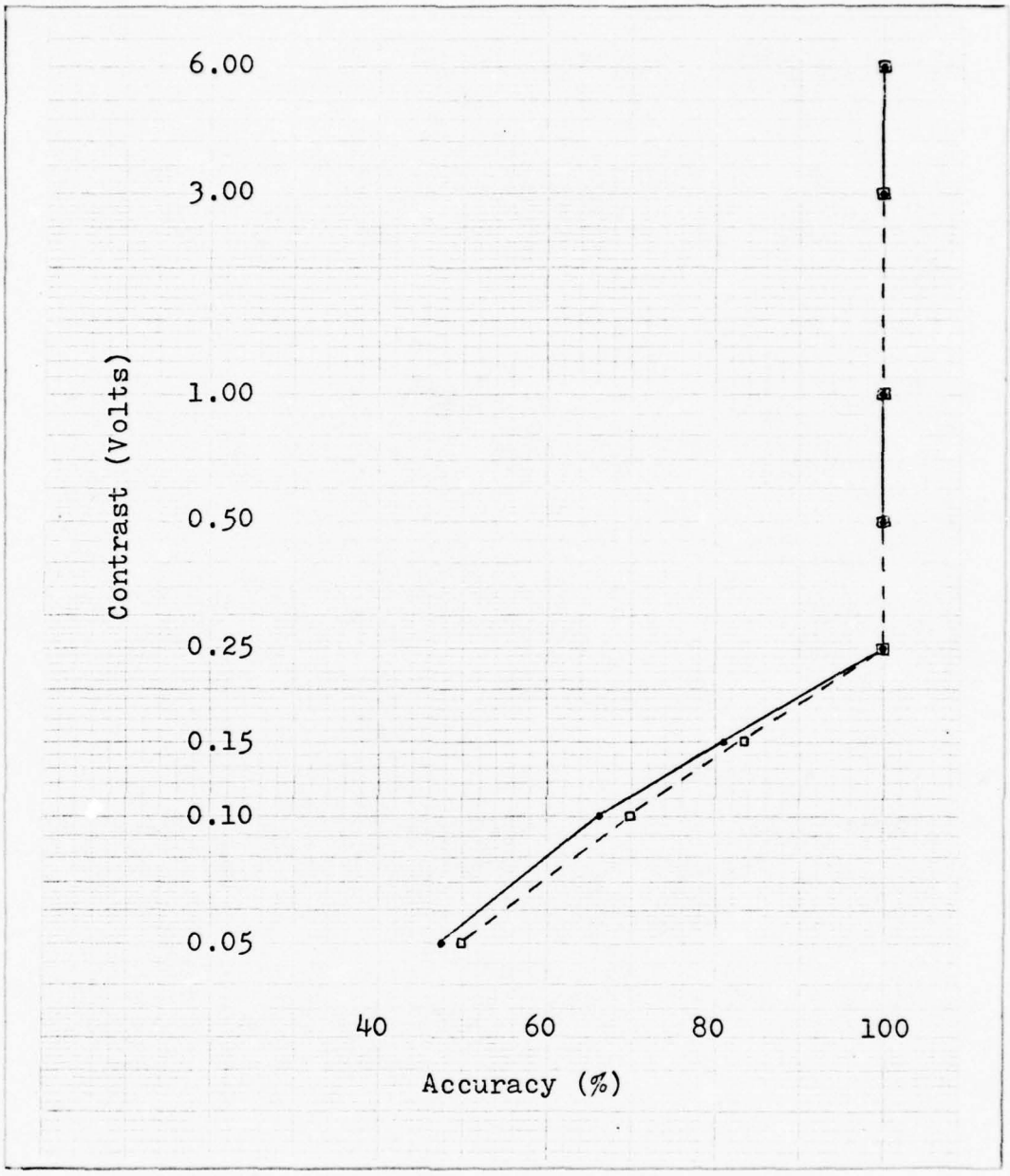

Fig. 18. Plot of Accuracy: MK, 100 msec, Positions 3 (——) and 4 (- -).

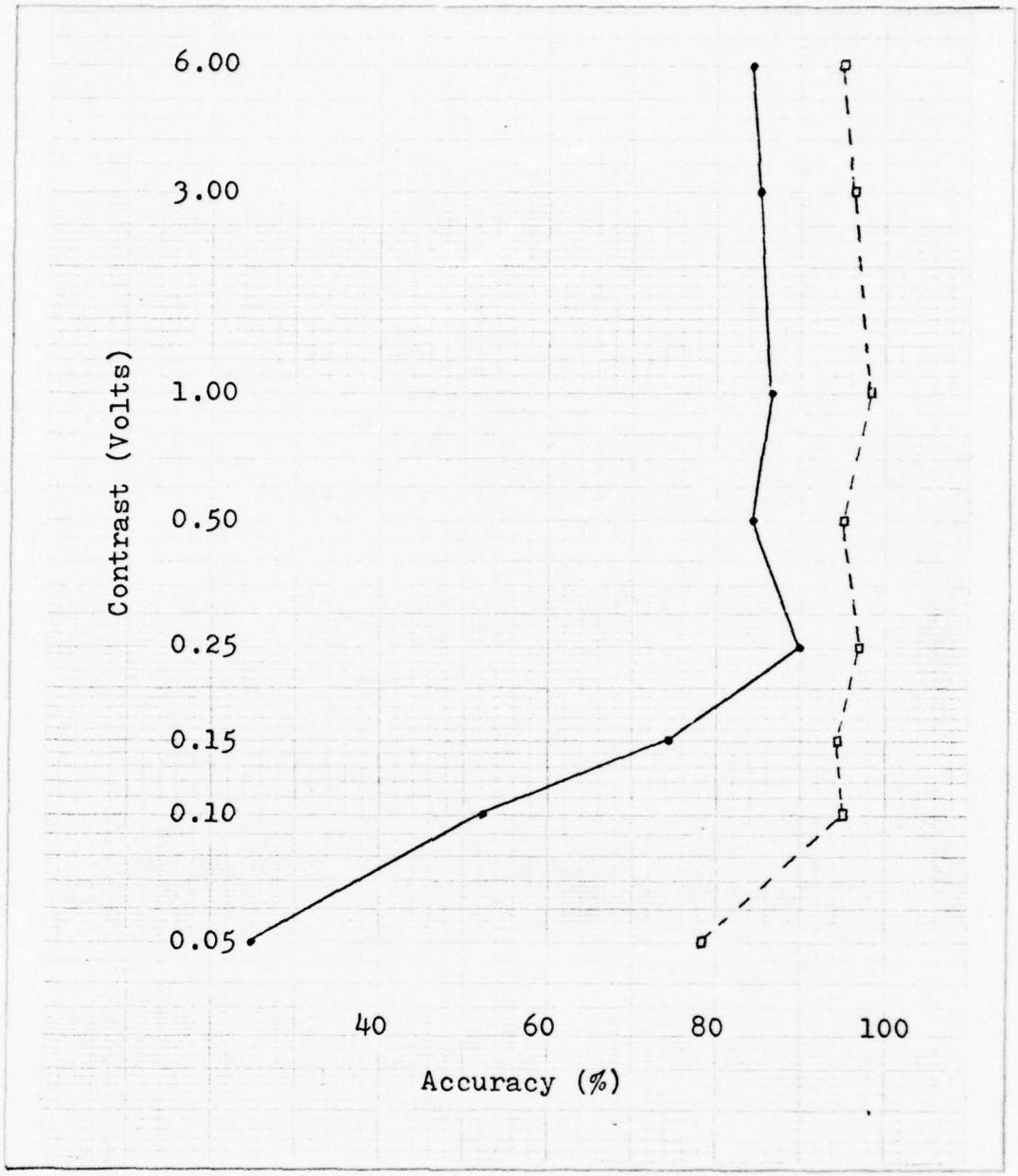

Fig. 19. Plot of Accuracy: MK, 100 msec, Positions 5 (——) and 6 (- -).

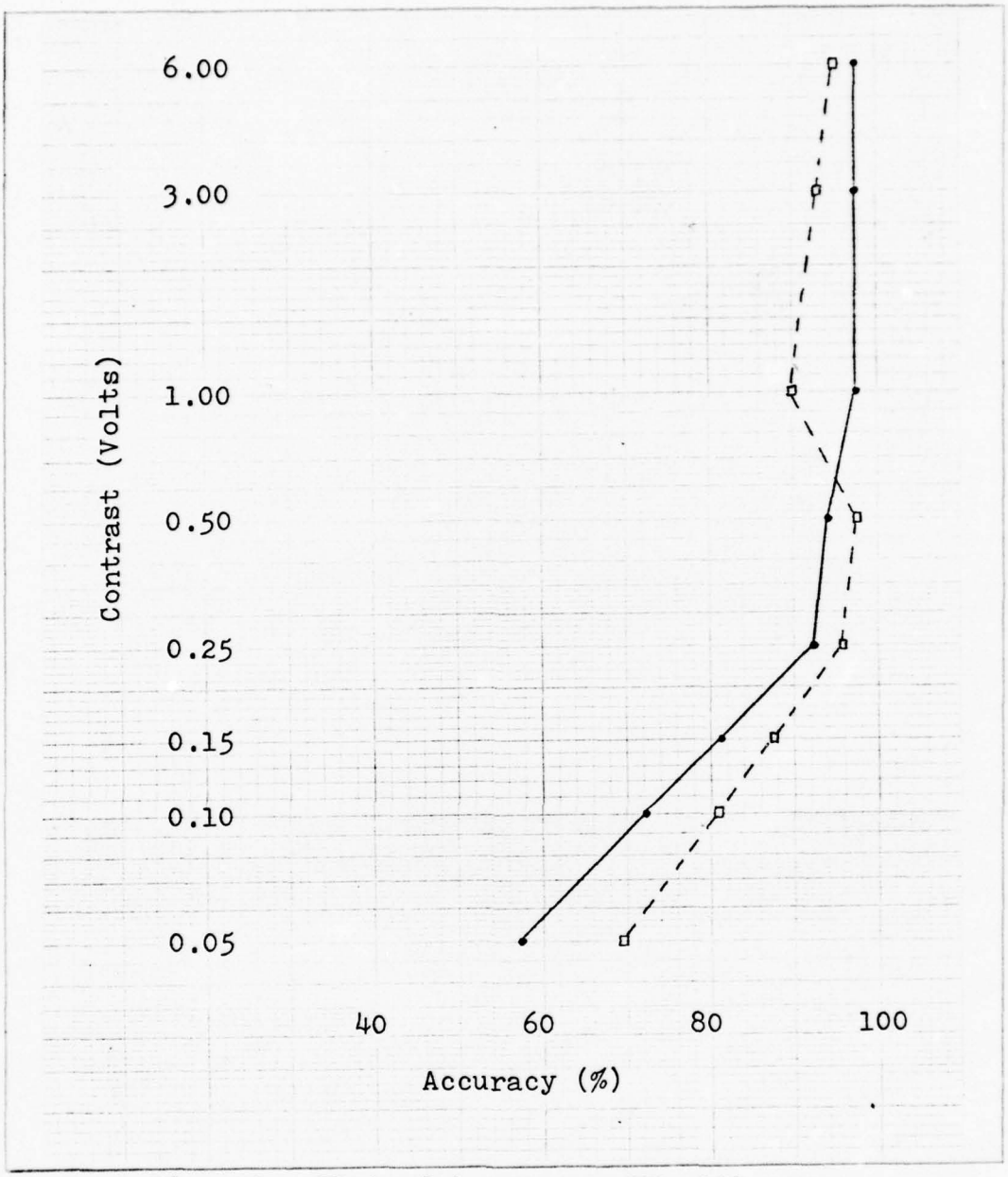

Fig. 20. Plot of Accuracy: MK, 100 msec, Positions 7 (——) and 8 (- -).

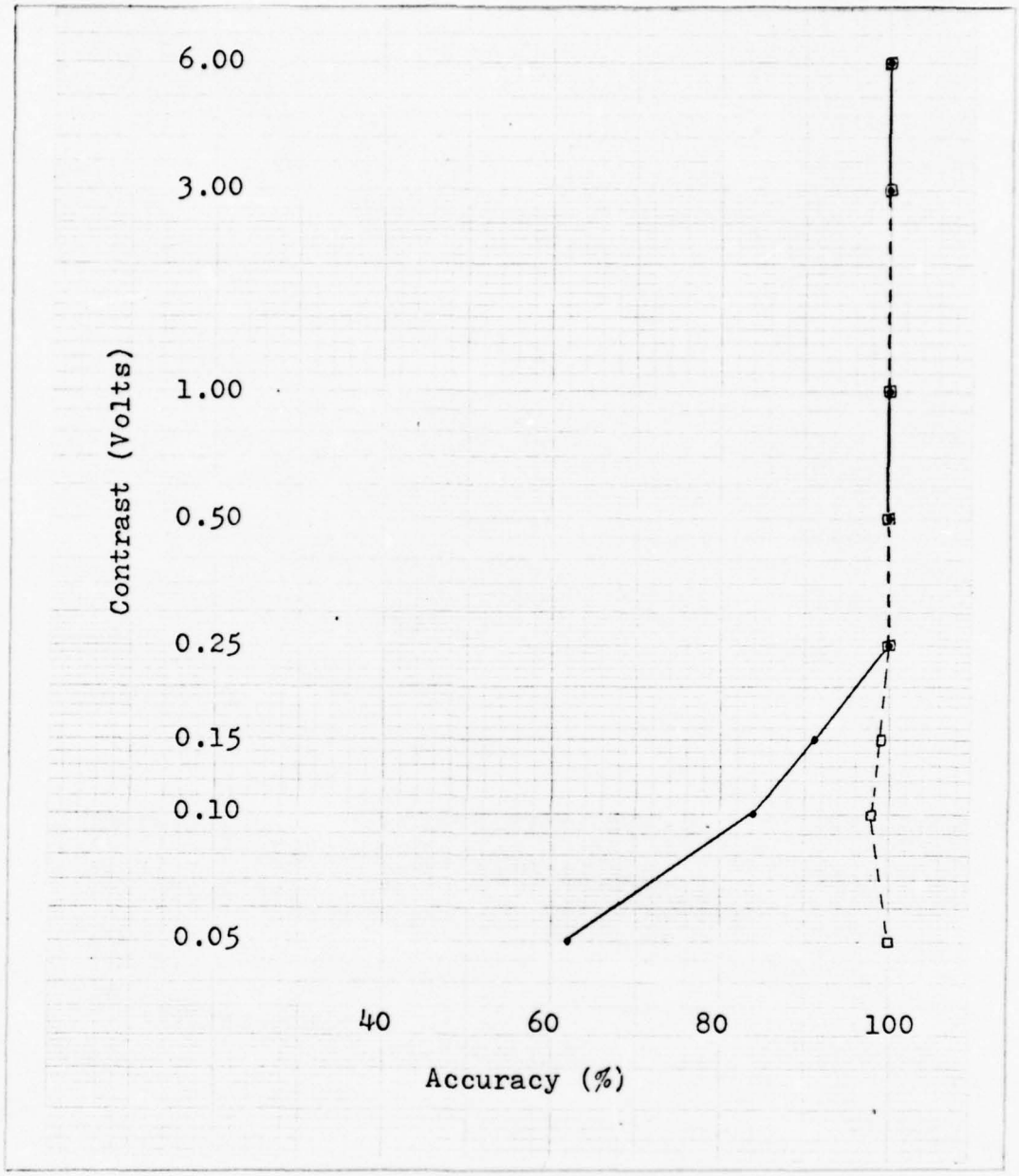

Fig. 21. Plot of Accuracy: MK, 100 msec, Positions 9 (——) and 10 (- -).

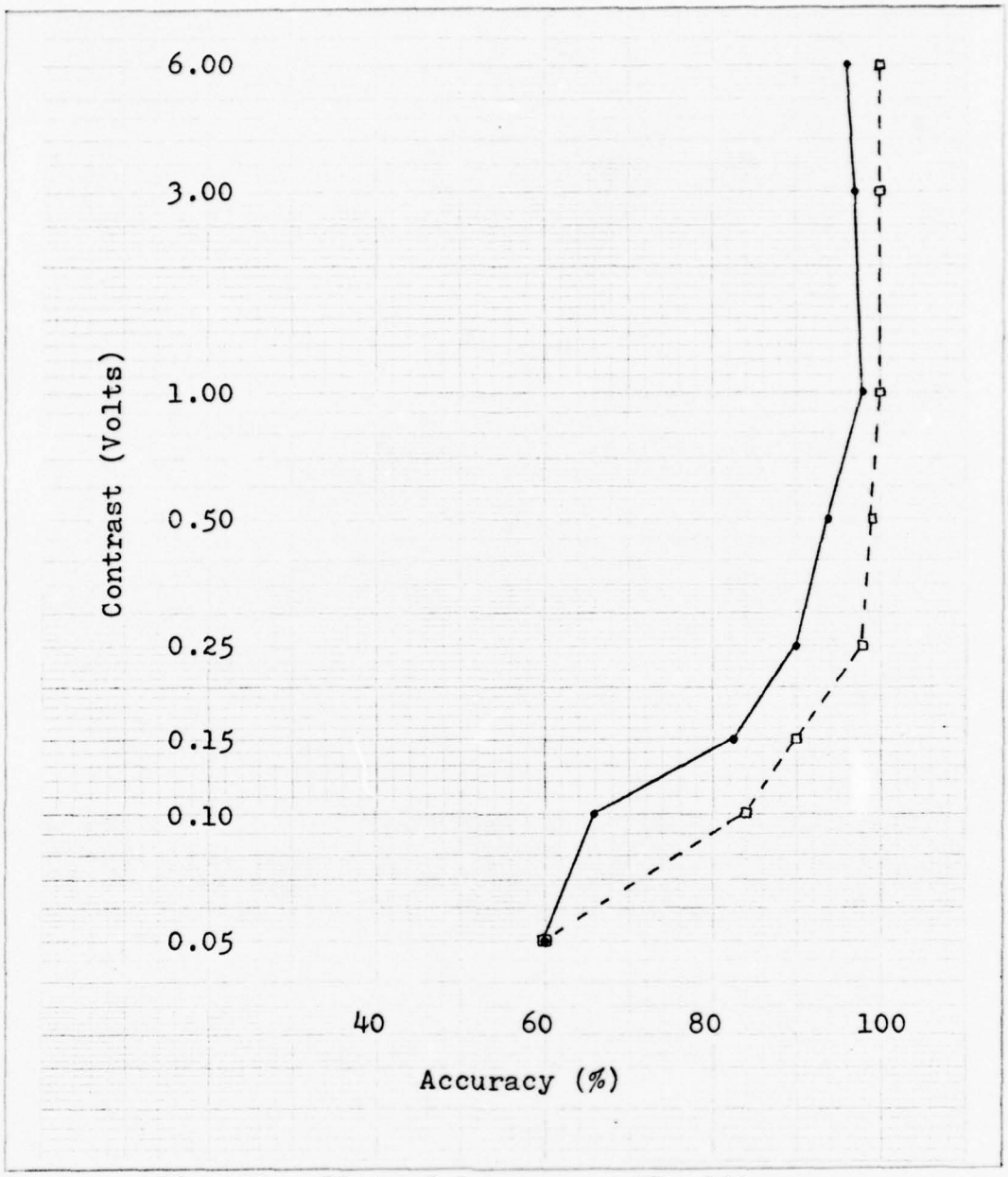

Fig. 22. Plot of Accuracy: MK, 100 msec, Positions 11 (——) and 12 (- -).

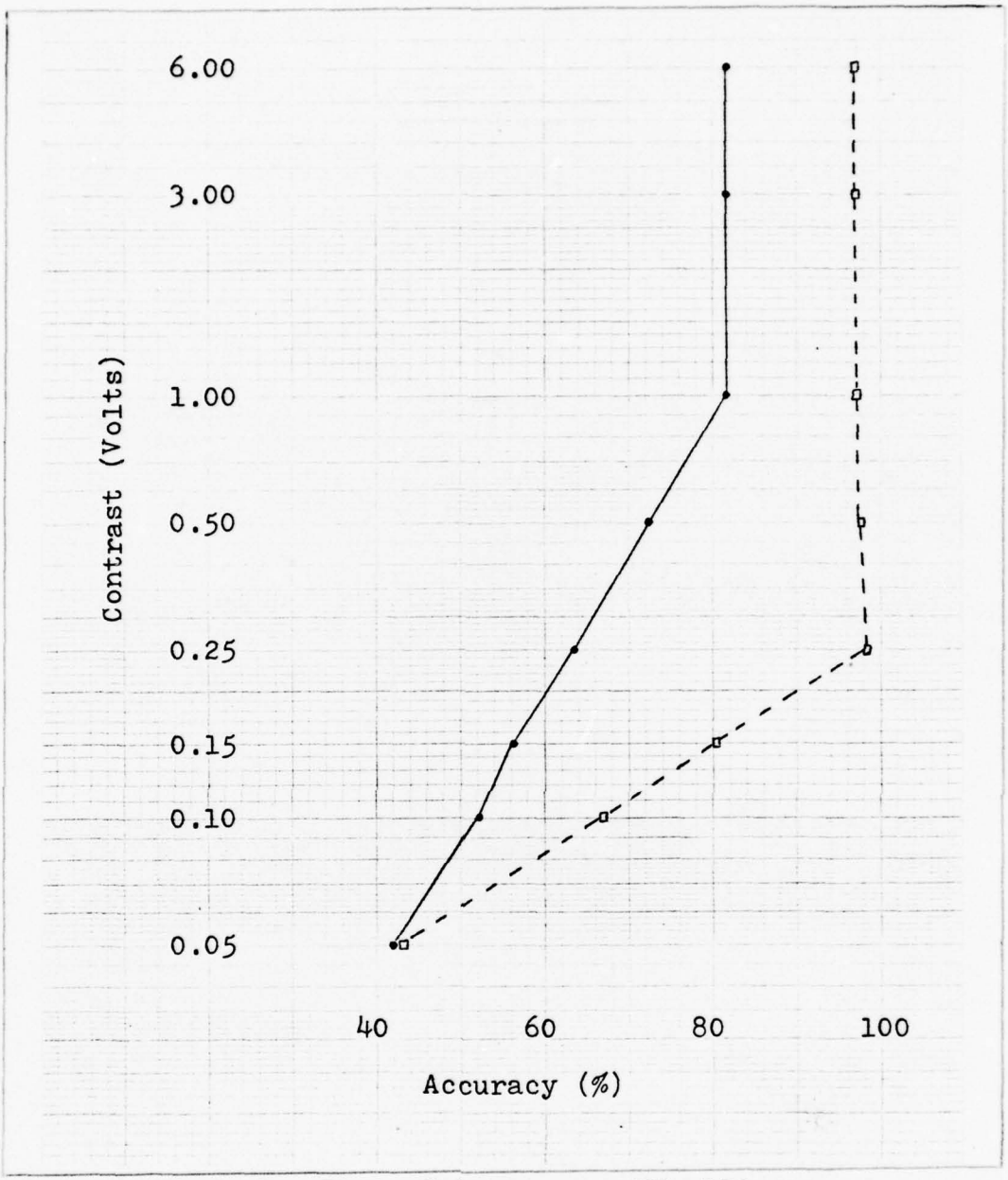

Fig. 23. Plot of Accuracy: MK, 100 msec, Positions 13 (——) and 14 (- -).

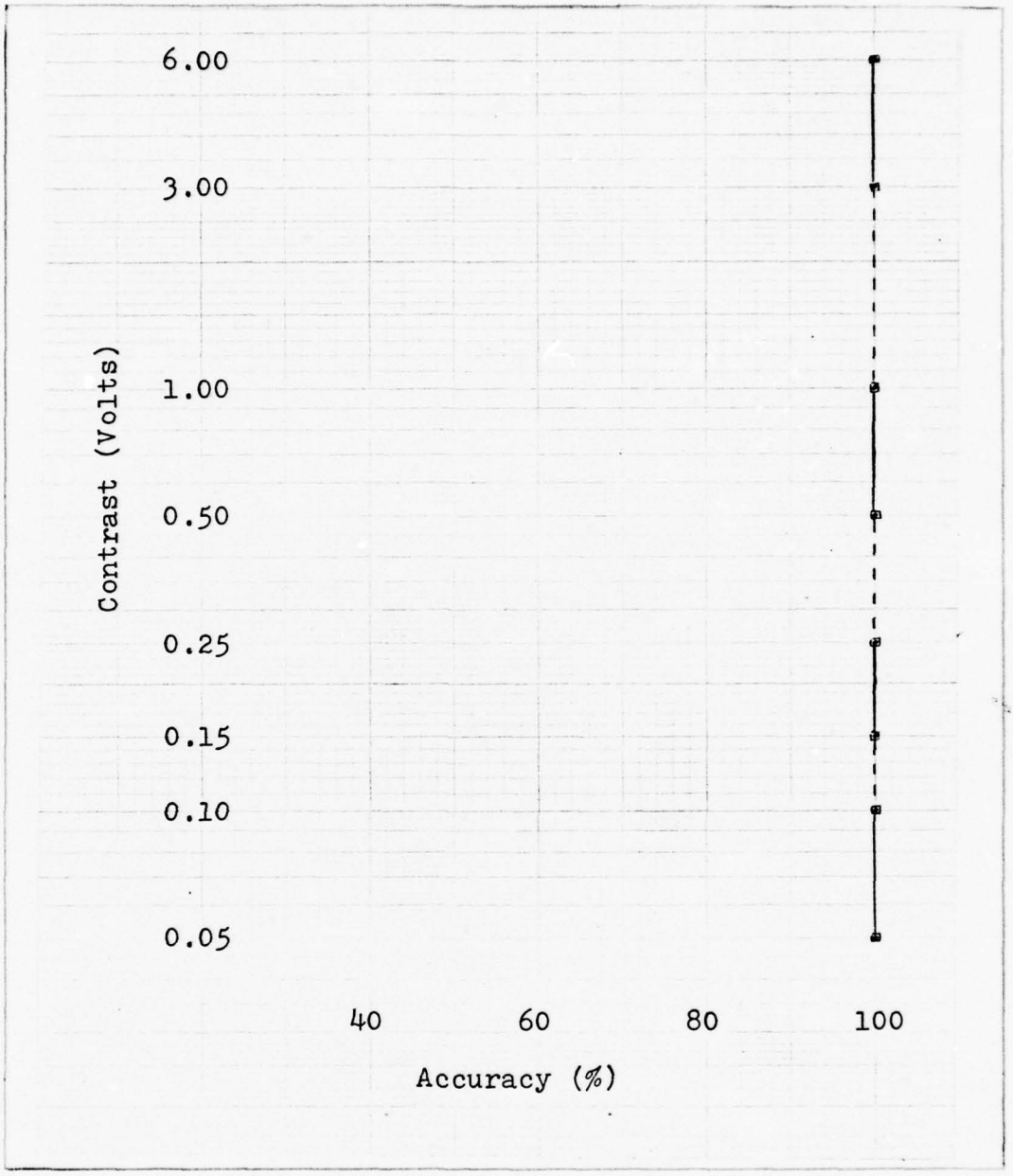

Fig. 24. Plot of Accuracy: MK, 100 msec, Positions 15 (——) and 16 (- -).

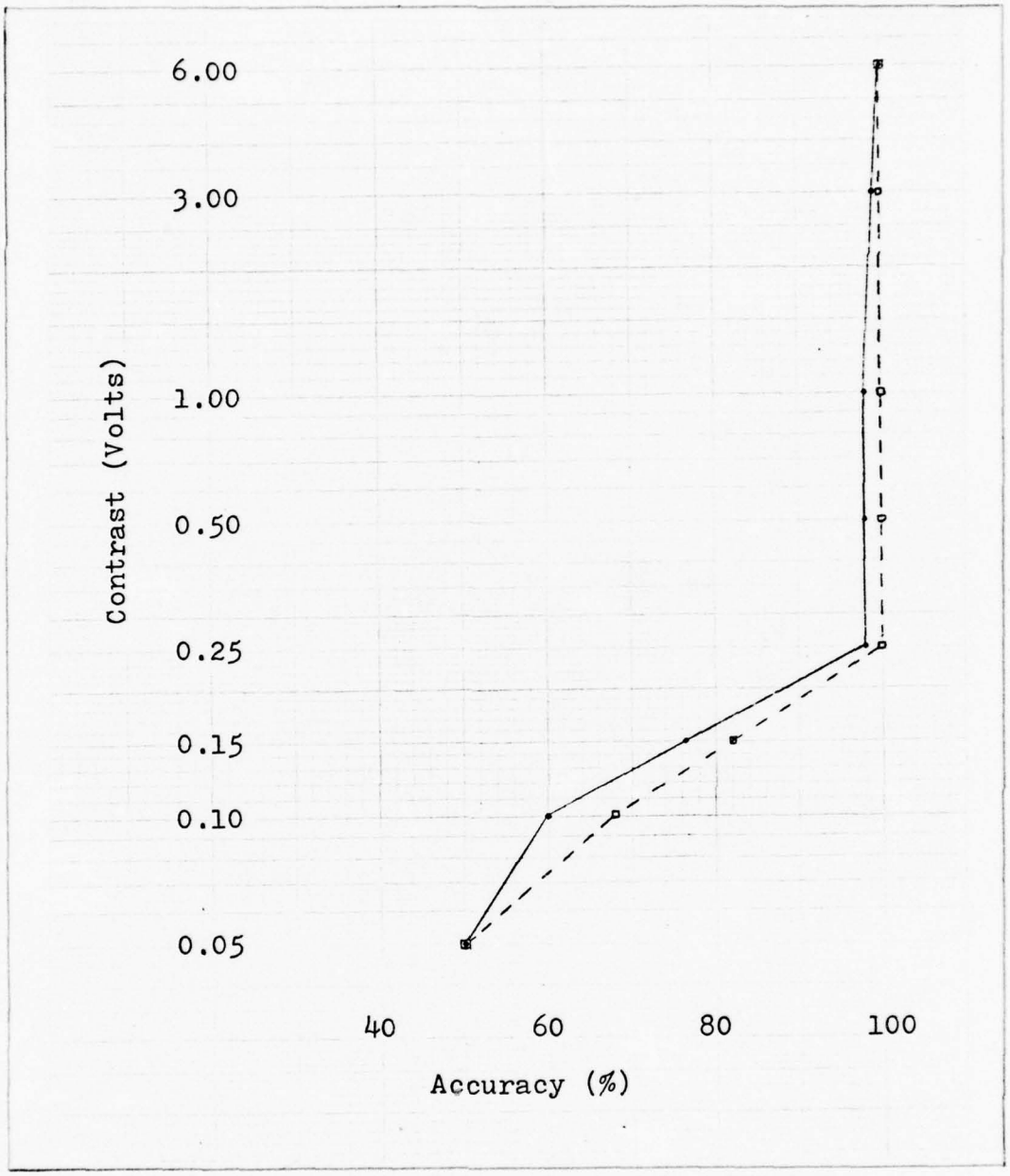

Fig. 25. Plot of Accuracy: MK, 100 msec, Positions 17 (——) and 18 (- -).

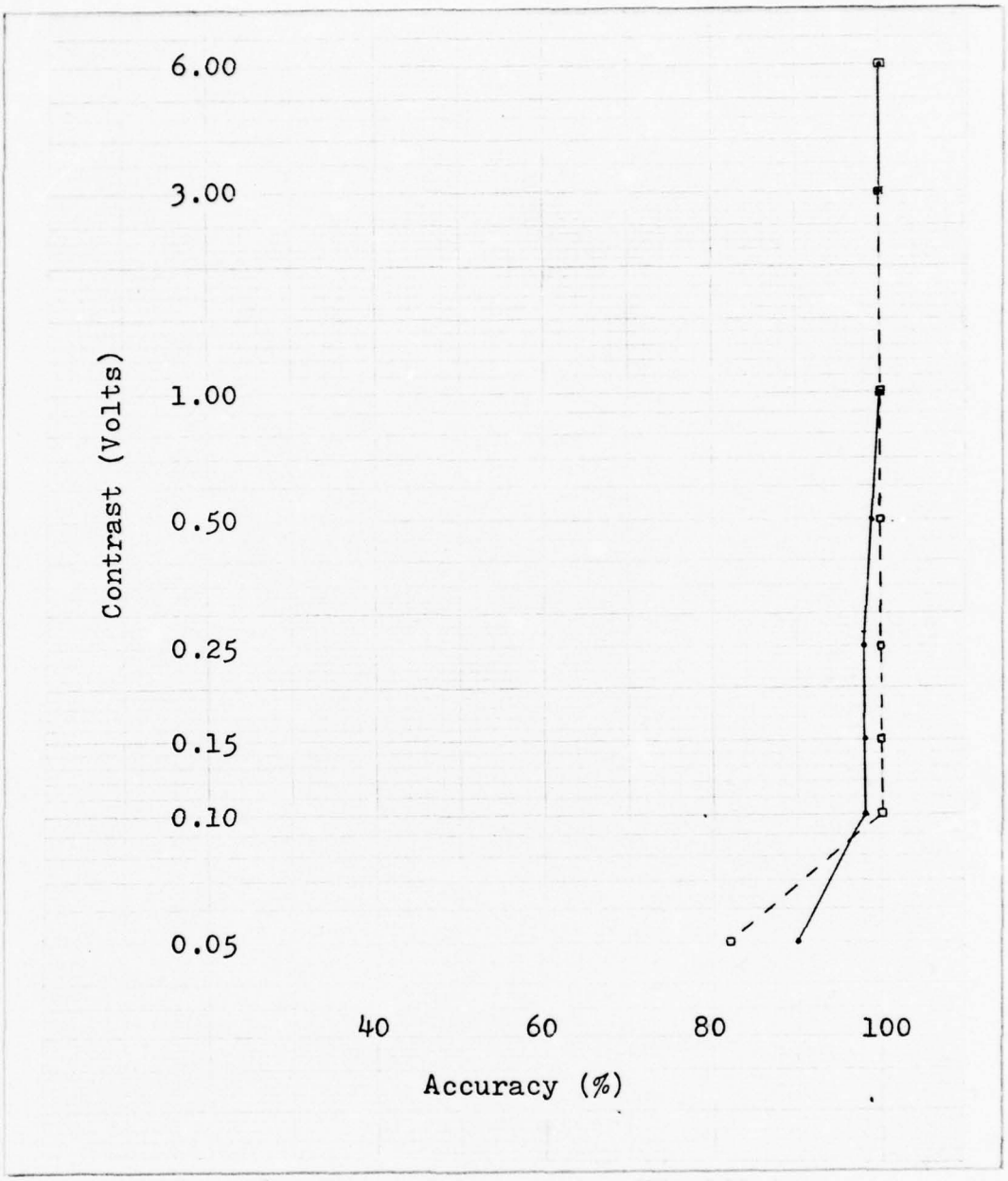

Fig. 26. Plot of Accuracy: MK, 100 msec, Positions 19 (——) and 20 (- -).

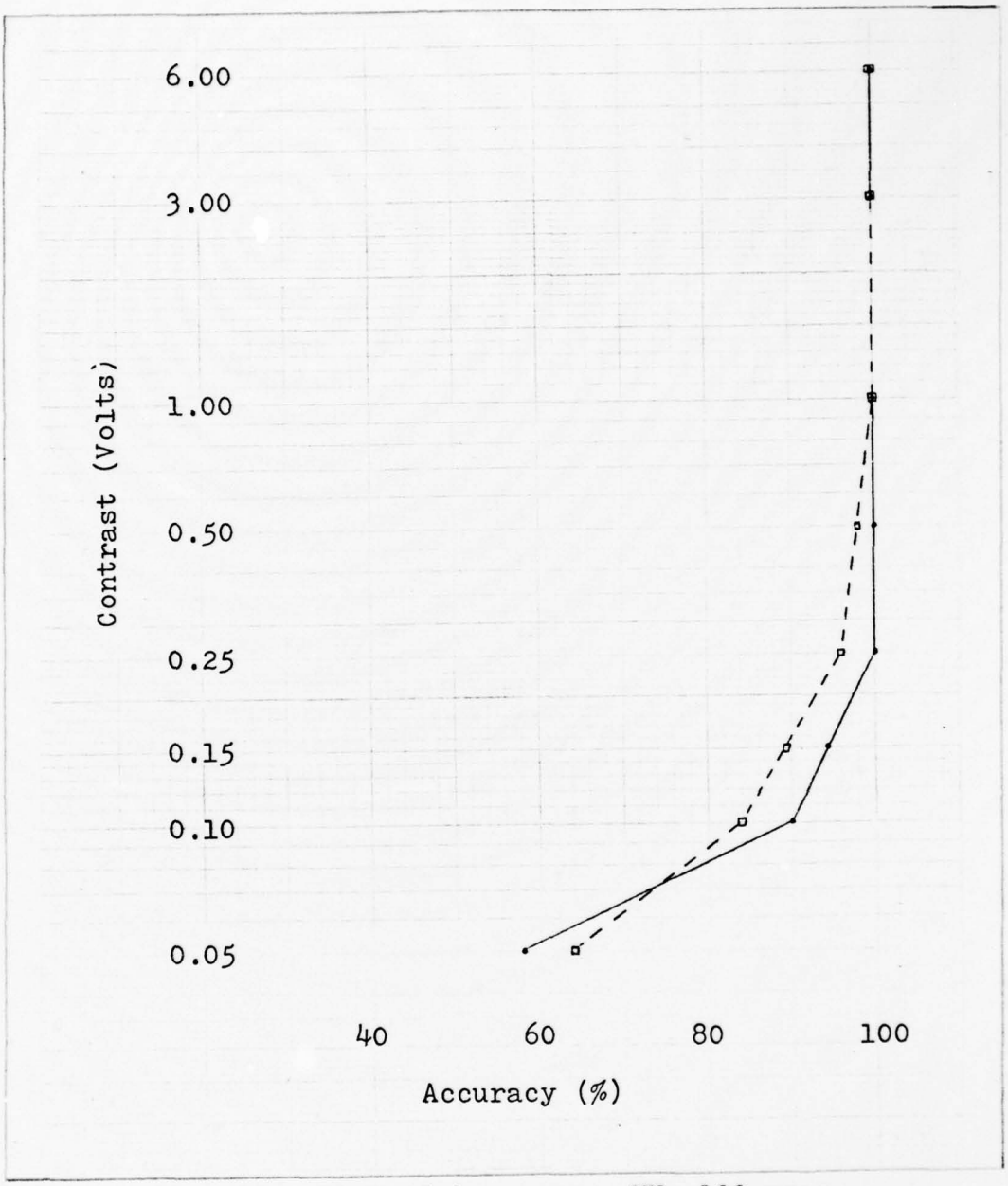

Fig. 27. Plot of Accuracy: MK, 100 msec, Positions 21 (——) and 22 (- -).

Appendix D

Accuracy Values (%): MK, 50 MSEC

Table V
Accuracy: MK, 50 msec

Contrast (Volts)	Peripheral Scope Position 1	2	3	4	5
6.00	100.0	100.0	100.0	100.0	90.0
3.00	100.0	100.0	100.0	100.0	90.0
1.00	100.0	100.0	100.0	100.0	87.5
0.50	100.0	100.0	(93.0)	95.0	84.2
0.25	100.0	100.0	86.2	(87.5)	71.6
0.15	(98.5)	(100.0)	(67.5)	(81.8)	(63.5)
0.10	97.5	100.0	52.5	77.5	58.5
0.05	71.2	87.5	(50.0)	50.0	(45.4)

	6	7	8
6.00	91.7	92.5	93.3
3.00	95.8	(93.2)	(92.0)
1.00	94.2	95.0	90.0
0.50	96.7	92.5	93.3
0.25	90.0	90.0	95.0
0.15	81.7	60.0	71.0
0.10	74.2	(36.0)	51.7
0.05	(69.0)	(25.0)	(25.0)

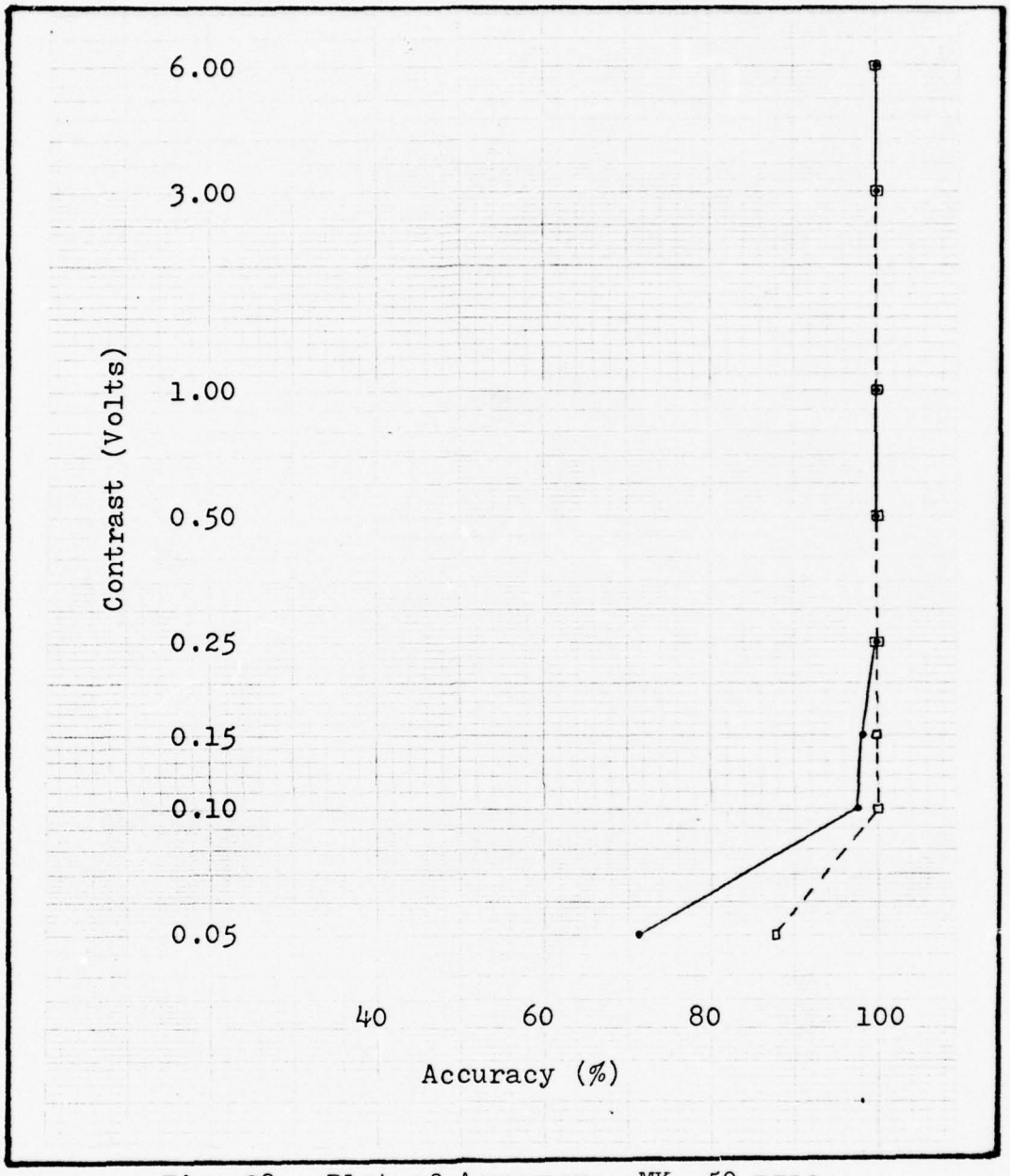

Fig. 28. Plot of Accuracy: MK, 50 msec, Positions 1 (——) and 2 (- -).

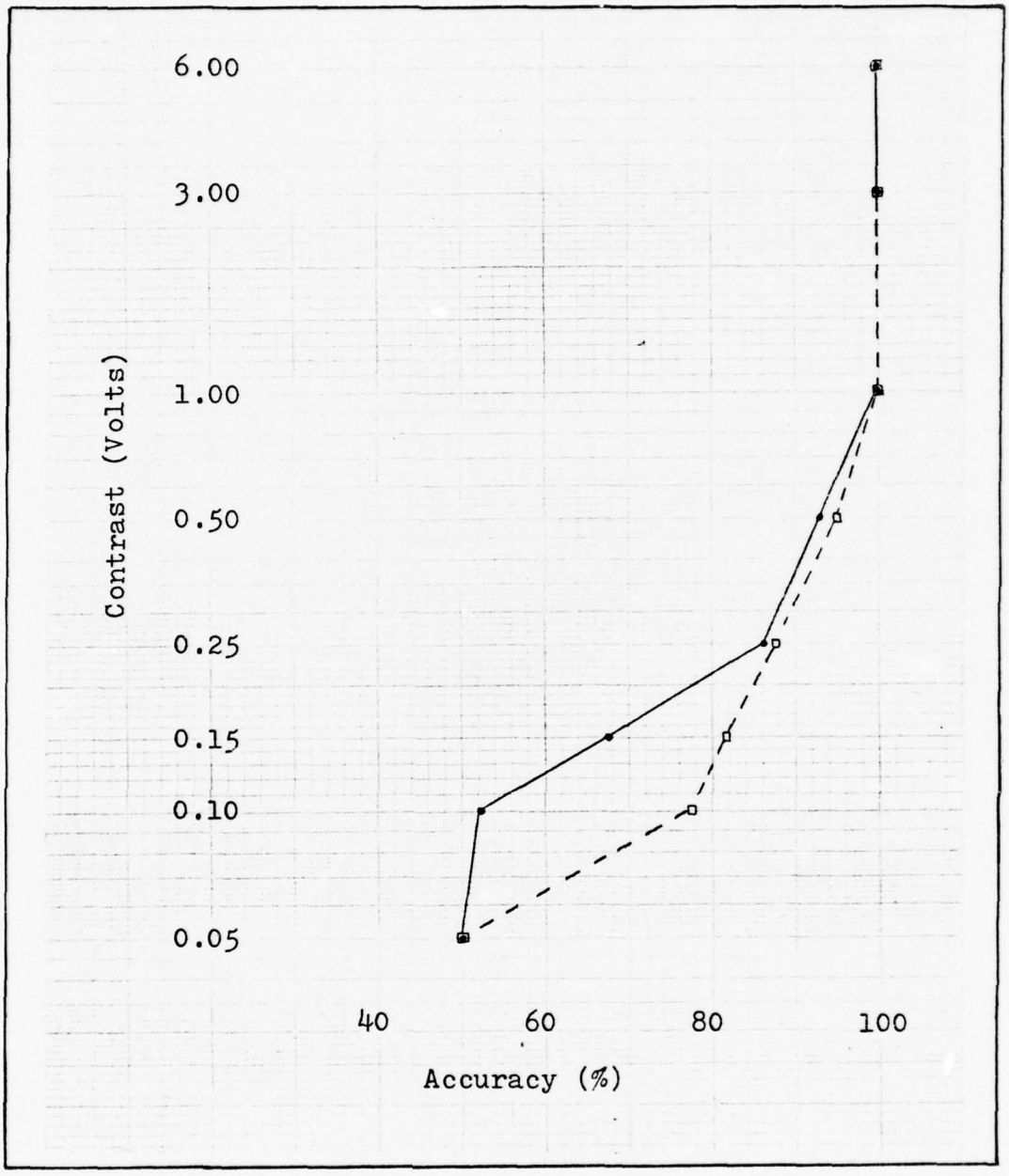

Fig. 29. Plot of Accuracy: MK, 50 msec, Positions 3 (——) and 4 (- -).

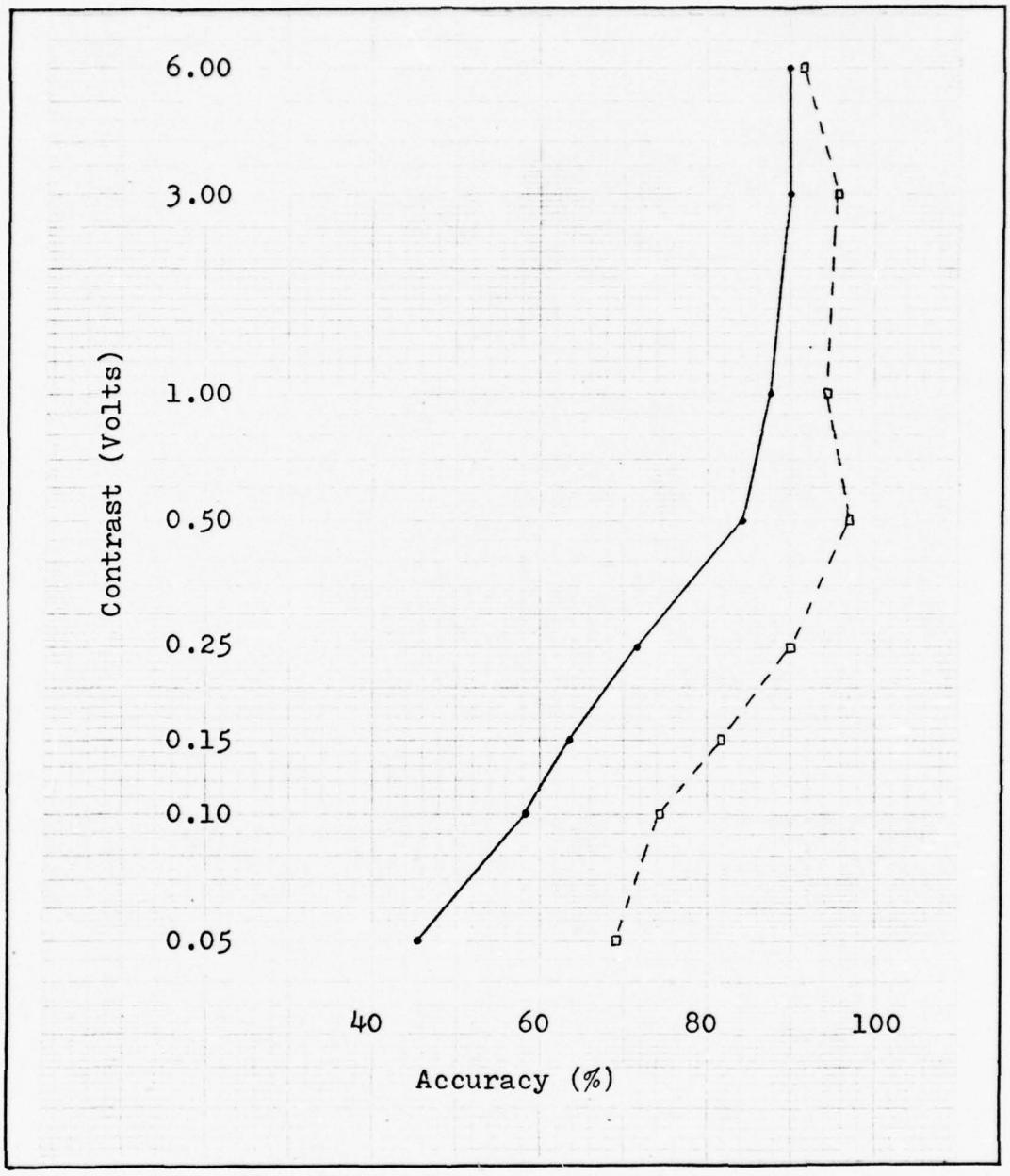

Fig. 30. Plot of Accuracy: MK, 50 msec, Positions 5 (——) and 6 (- -).

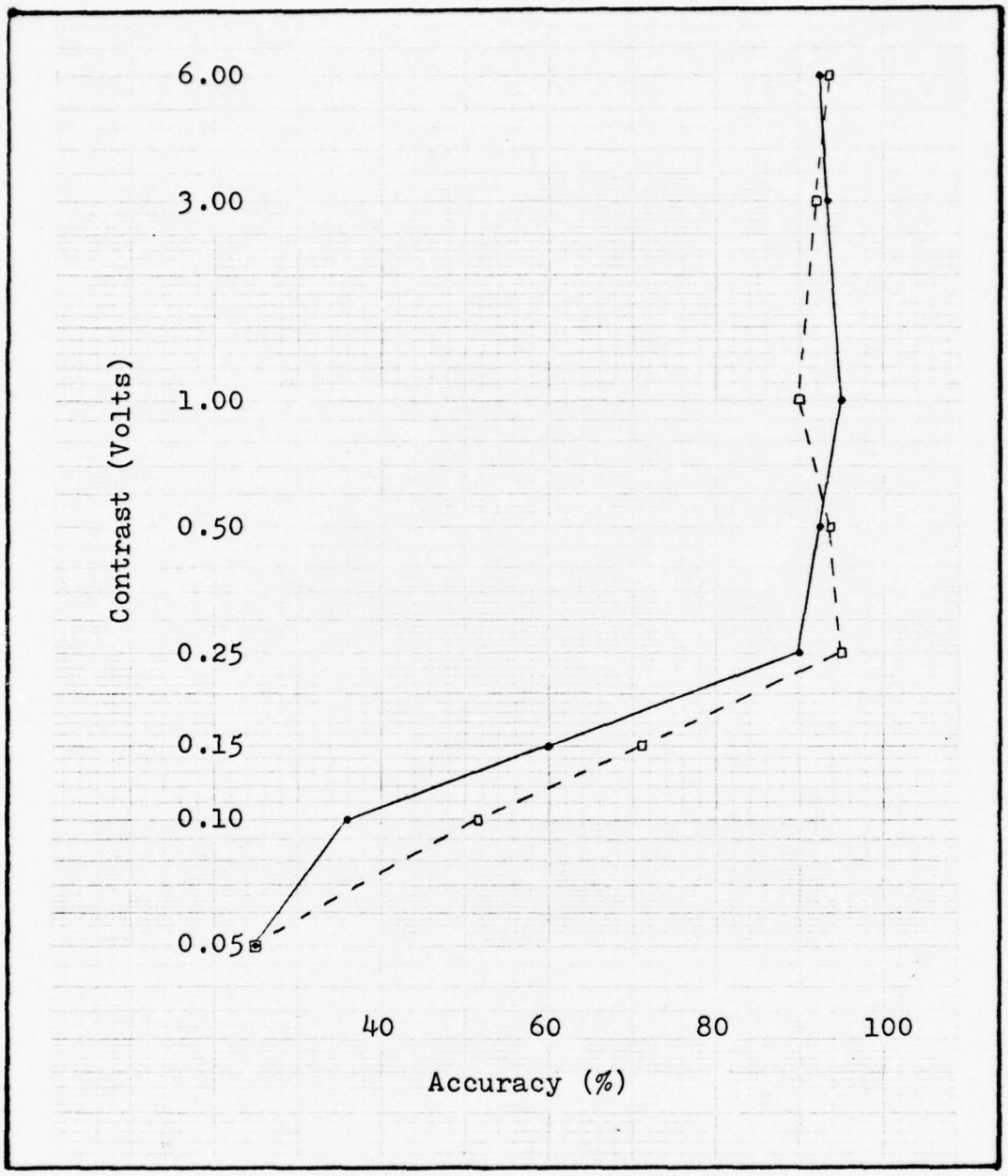

Fig. 31. Plot of Accuracy: MK, 50 msec, Positions 7(——) and 8 (- -).

Appendix E

Accuracy Values (%): MK, 20 MSEC

Table VI
Accuracy: MK, 20 msec

Contrast (Volts)	Peripheral Scope Position 1	2	3	4	5
6.00	100.0	100.0	100.0	97.5	85.0
3.00	100.0	100.0	(98.0)	92.5	80.8
1.00	100.0	100.0	95.0	90.0	77.5
0.50	100.0	100.0	71.2	60.0	67.5
0.25	97.5	97.5	55.0	50.0	52.5
0.15	(71.0)	(72.5)	(52.2)	(50.0)	(41.0)
0.10	50.0	52.5	(50.0)	(50.0)	(32.1)
0.05	(50.0)	(50.0)	(50.0)	(50.0)	(25.0)

Contrast (Volts)	6	7	8
6.00	94.2	95.0	95.0
3.00	96.7	(93.0)	(94.2)
1.00	95.0	90.0	93.3
0.50	93.3	85.0	80.0
0.25	85.8	(25.0)	41.7
0.15	(63.7)	(25.0)	(25.0)
0.10	(46.0)	(25.0)	(25.0)
0.05	(25.0)	(25.0)	(25.0)

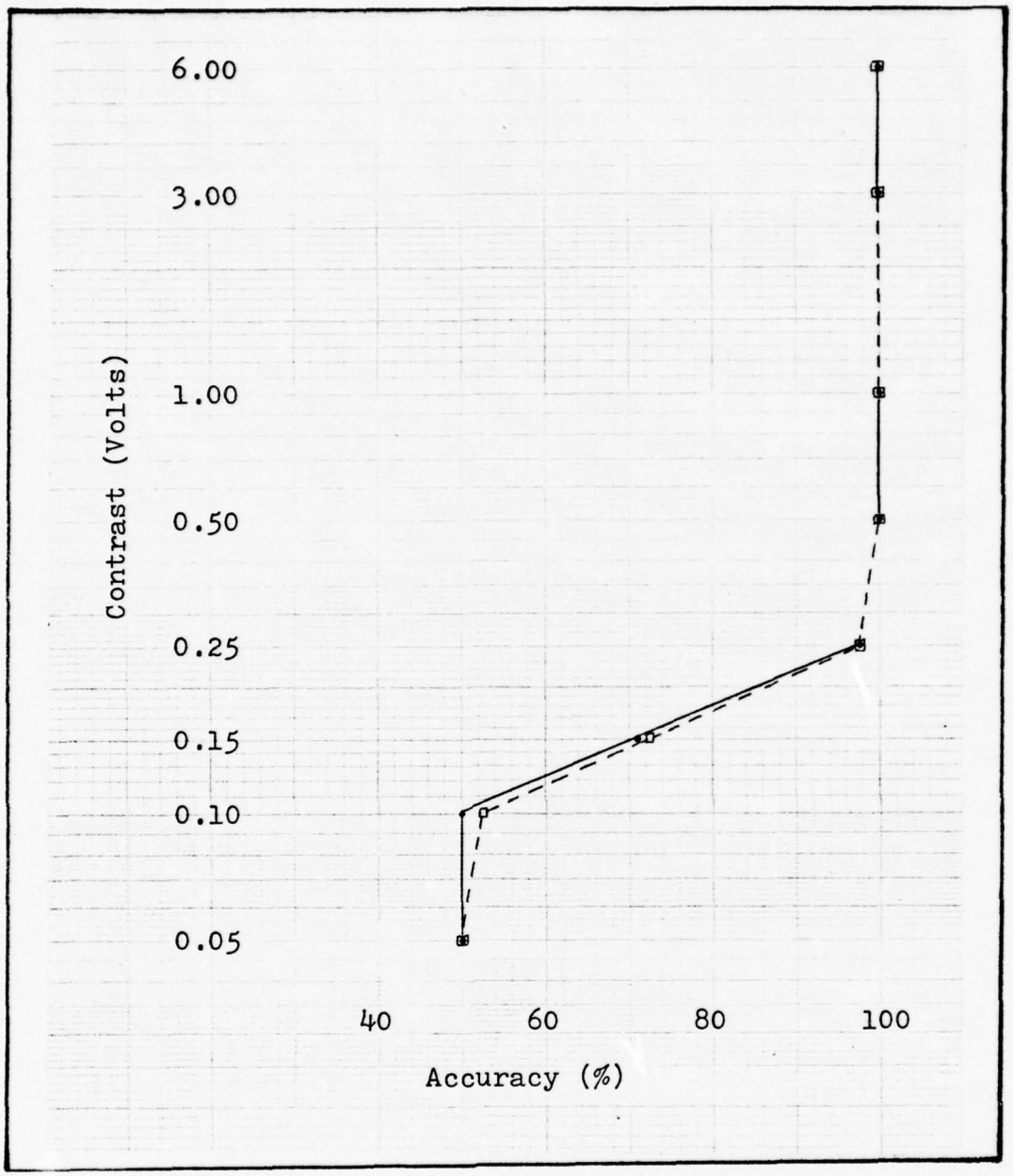

Fig. 32. Plot of Accuracy: MK, 20 msec, Positions 1 (——) and 2 (- -).

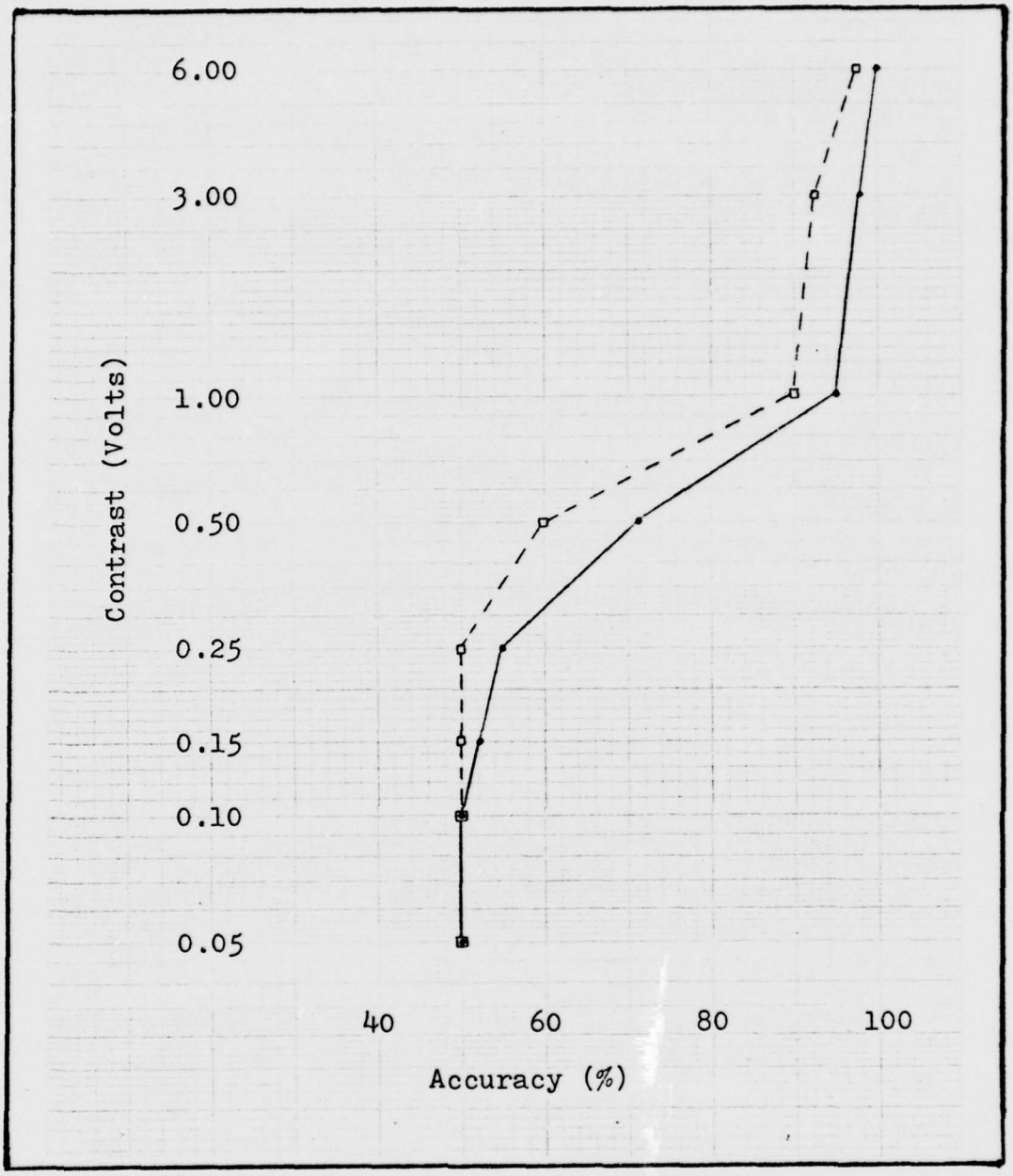

Fig. 33. Plot of Accuracy: MK, 20 msec, Positions 3 (——) and 4 (- -).

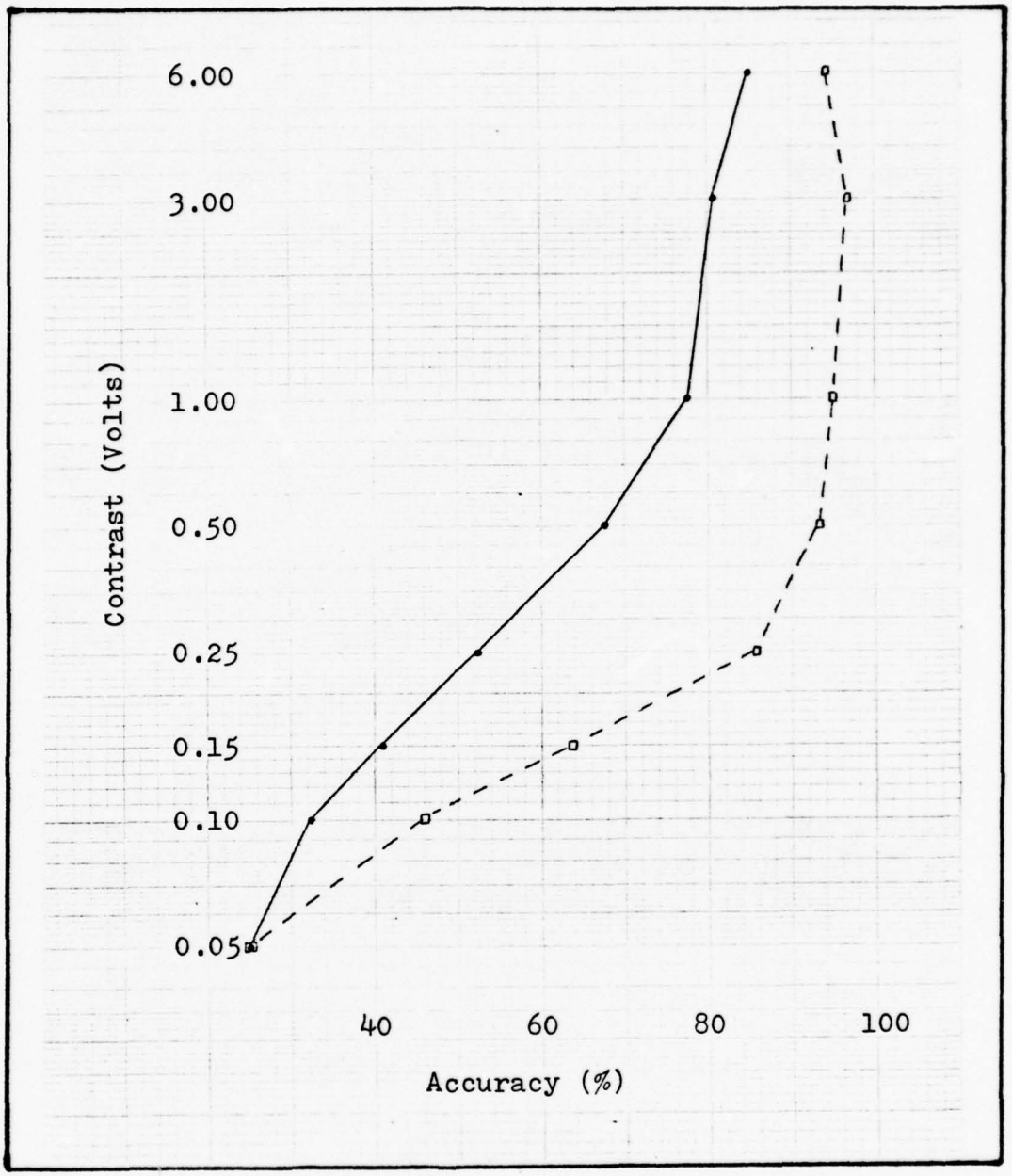

Fig. 34. Plot of Accuracy: MK, 20 msec, Positions 5 (——) and 6 (- -).

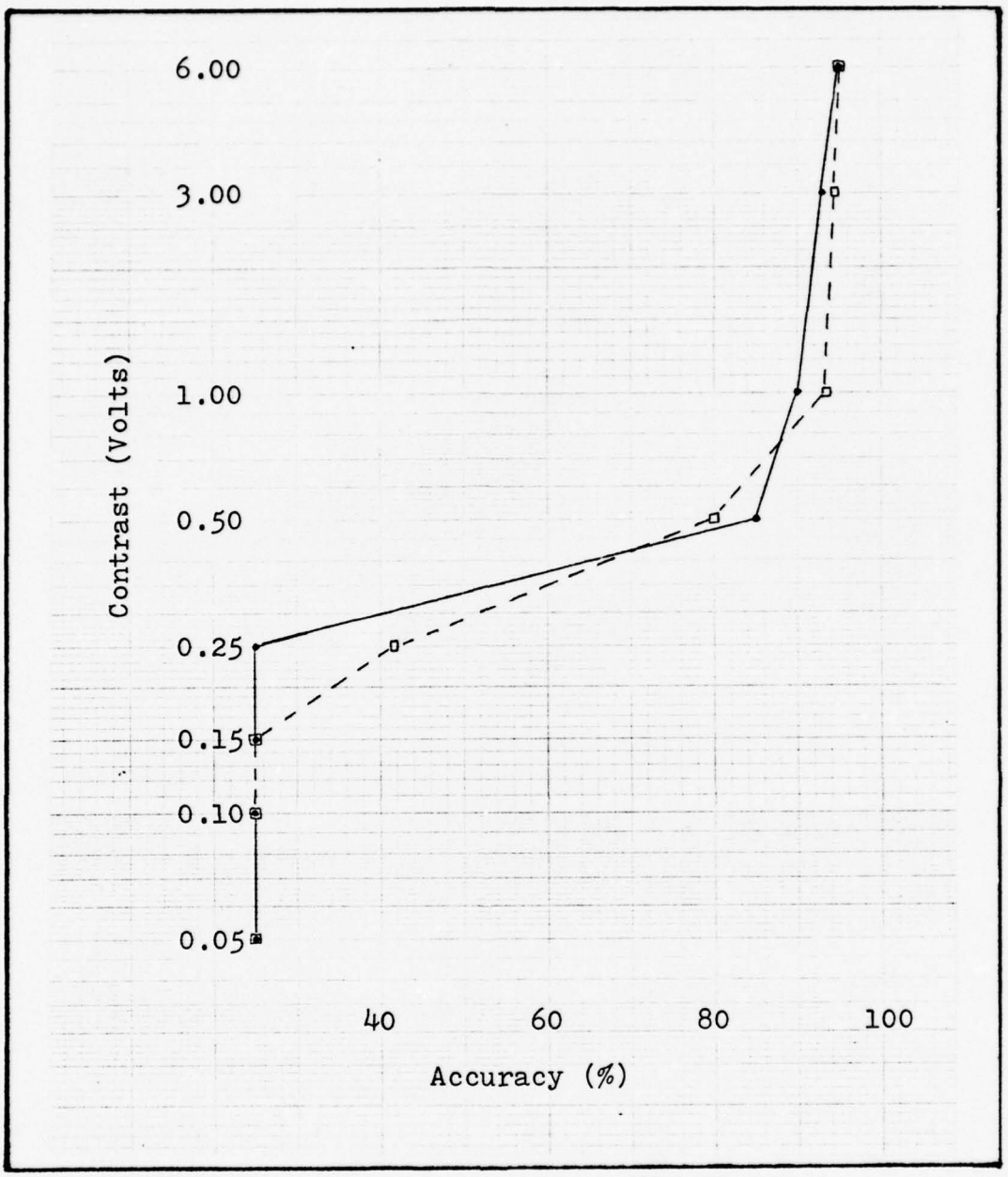

Fig. 35. Plot of Accuracy: MK, 20 msec, Positions 7 (——) and 8 (- -).

Appendix F

Accuracy Values (%): KB, 500 MSEC

Table VII
Accuracy: KB, 500 msec

Contrast (Volts)	Peripheral Scope Position 1	2	3
6.00	100.0	100.0	100.0
3.00	100.0	100.0	(100.0)
1.00	100.0	100.0	100.0
0.50	100.0	100.0	(100.0)
0.25	100.0	100.0	100.0
0.15	100.0	100.0	(84.8)
0.10	100.0	100.0	72.5
0.05	97.5	100.0	37.5

	4	5	6
6.00	100.0	98.7	93.8
3.00	100.0	(99.2)	93.4
1.00	100.0	100.0	99.2
0.50	(99.2)	(99.2)	95.8
0.25	(98.5)	98.7	96.7
0.15	(98.0)	(87.7)	98.3
0.10	97.5	78.7	96.7
0.05	52.5	53.7	77.5

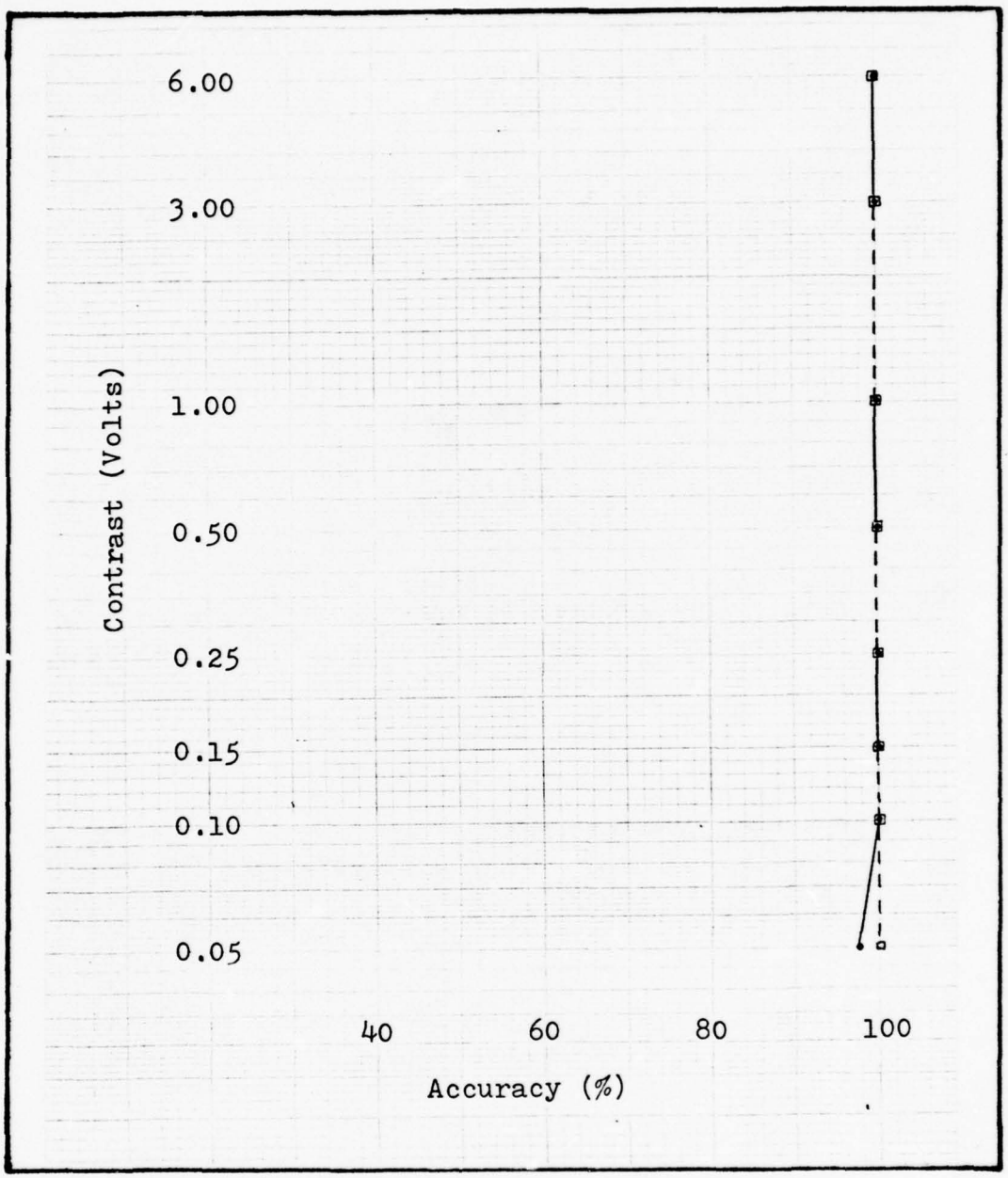

Fig. 36. Plot of Accuracy: KB, 500 msec, Positions 1 (——) and 2 (- -).

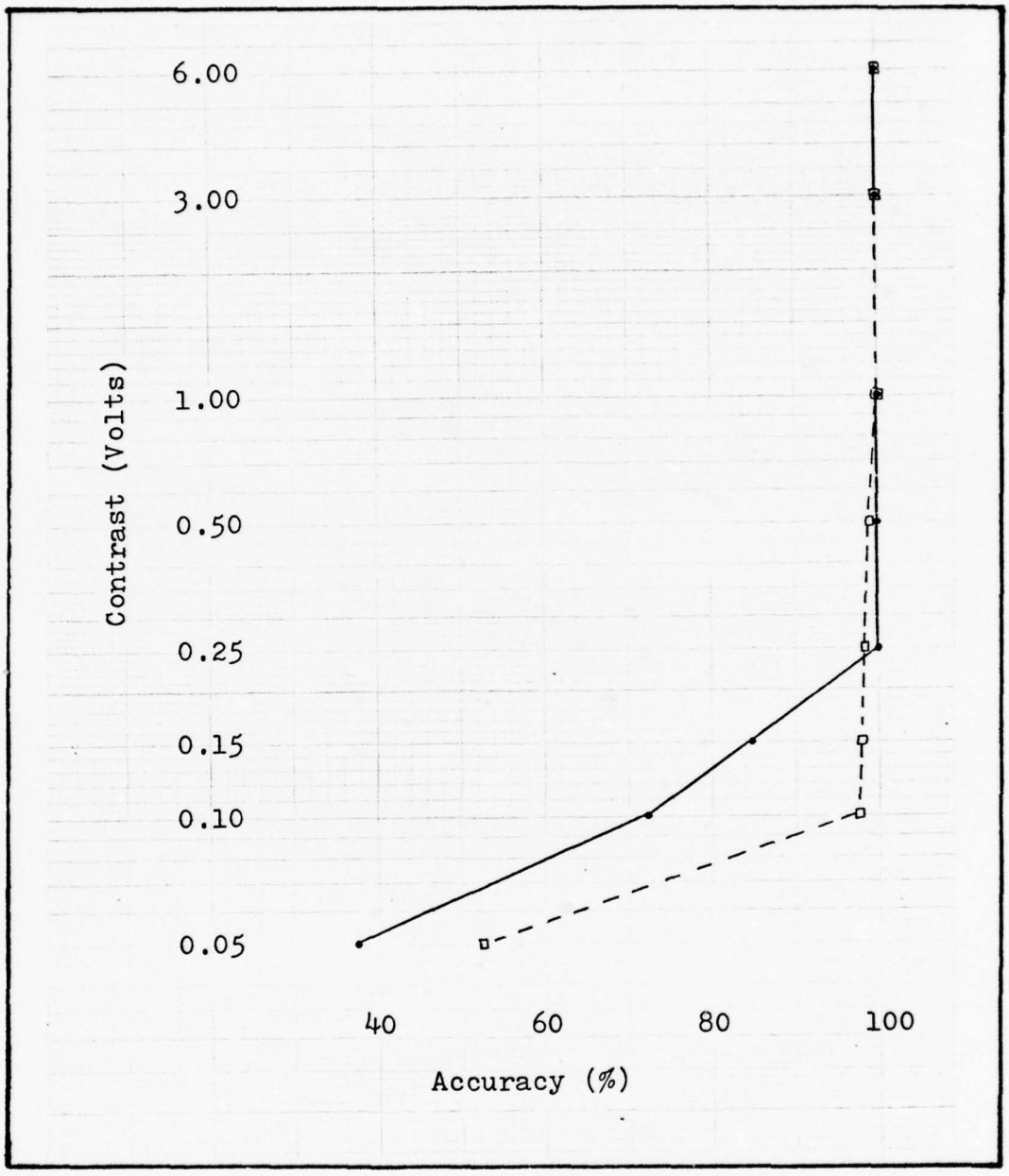

Fig. 37. Plot of Accuracy: KB, 500 msec, Positions 3 (——) and 4 (- -).

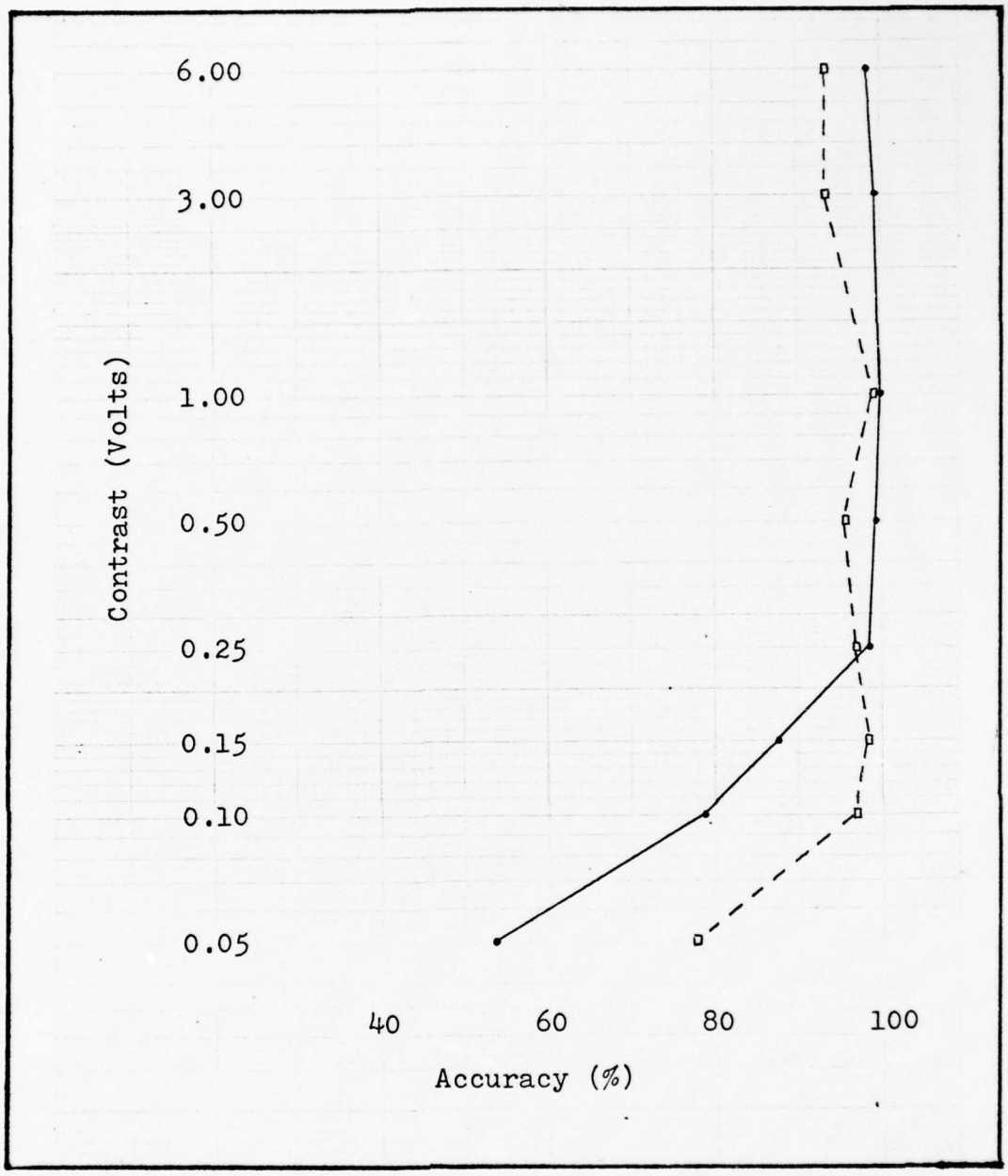

Fig. 38. Plot of Accuracy: KB, 500 msec, Positions 5 (——) and 6 (- -).

Appendix G

Accuracy Values (%): KB, 100 MSEC

Table VIII
Accuracy: KB, 100 msec

Contrast (Volts)	Peripheral Scope Position 1	2	3
6.00	100.0	100.0	100.0
3.00	(100.0)	(100.0)	(100.0)
1.00	100.0	100.0	100.0
0.50	(100.0)	(100.0)	100.0
0.25	100.0	100.0	92.5
0.15	(100.0)	(100.0)	(74.0)
0.10	100.0	100.0	60.0
0.05	95.0	100.0	(50.0)

	4	5	6
6.00	100.0	80.0	95.8
3.00	(100.0)	(85.2)	95.8
1.00	100.0	93.7	96.7
0.50	(100.0)	87.5	93.3
0.25	100.0	77.5	92.5
0.15	(98.5)	(65.0)	(93.8)
0.10	(97.5)	51.2	93.3
0.05	75.0	(25.0)	70.0

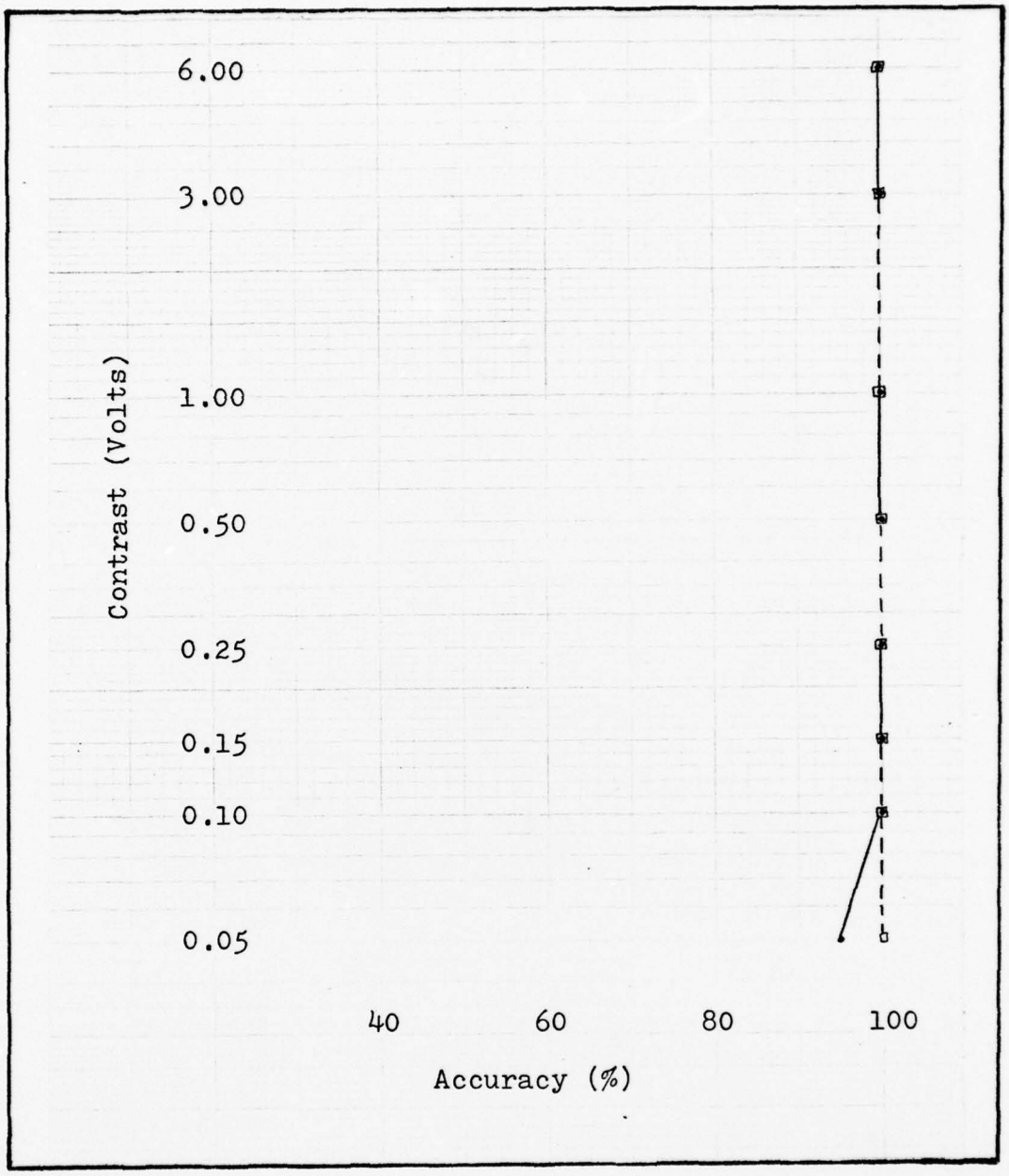

Fig. 39. Plot of Accuracy: KB, 100 msec, Positions 1 (——) and 2 (- -).

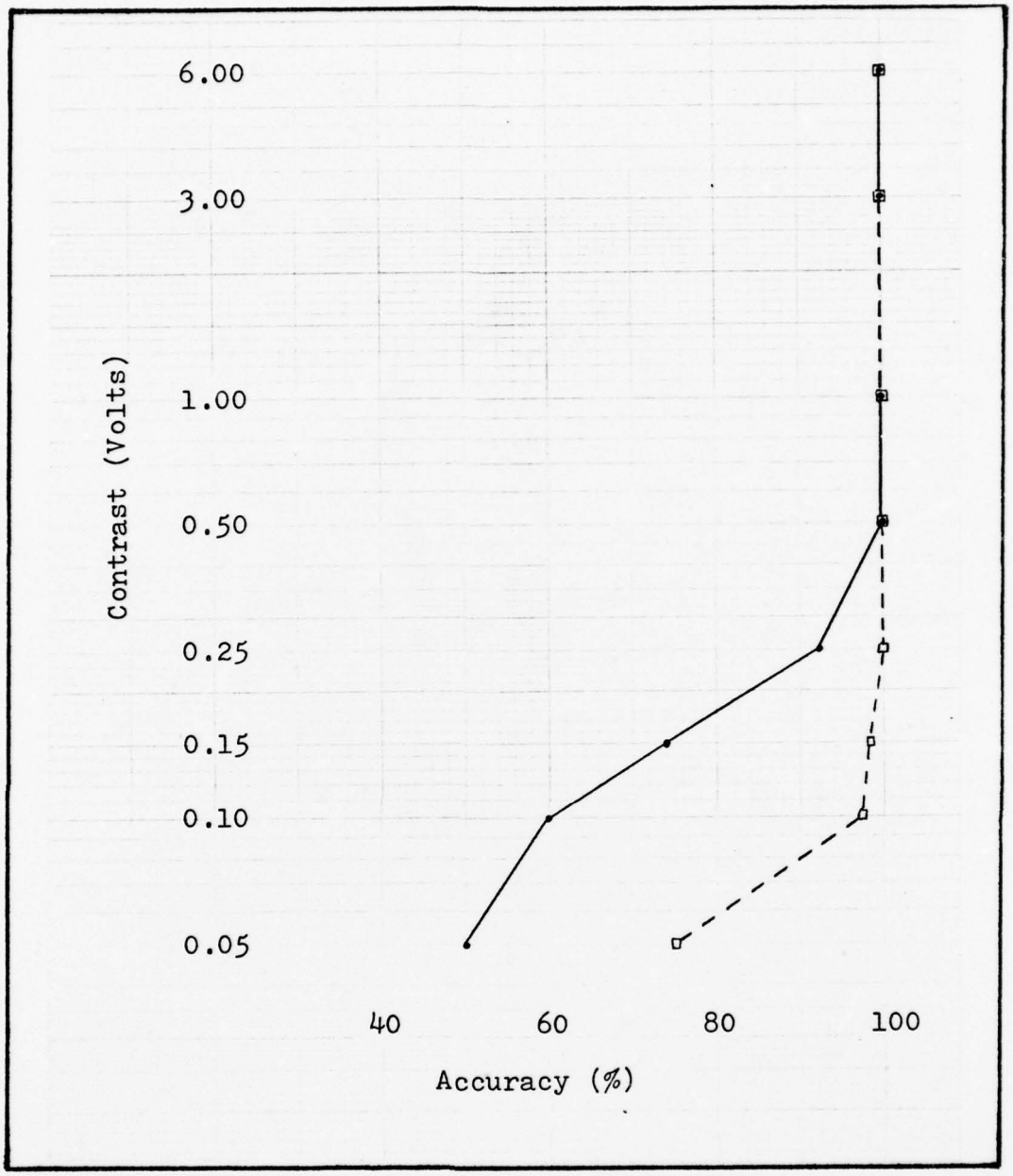

Fig. 40. Plot of Accuracy: KB, 100 msec, Positions 3 (——) and 4 (- -).

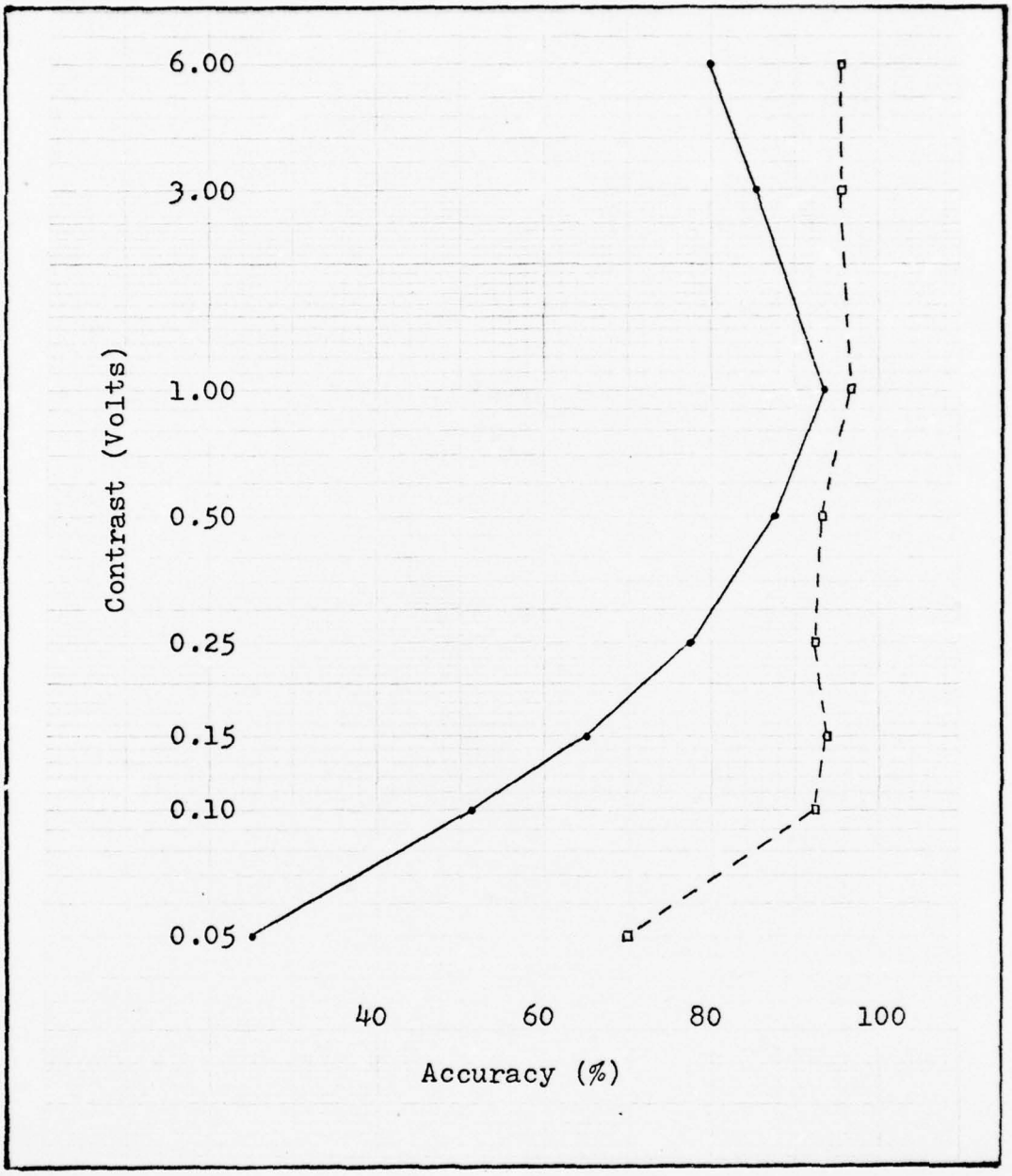

Fig. 41. Plot of Accuracy: KB, 100 msec, Positions 5 (——) and 6 (- -).

Appendix H

Accuracy Values (%): KB, 50 MSEC

Table IX
Accuracy: KB, 50 msec

Contrast (Volts)	Peripheral Scope Position 1	2	3
6.00	100.0	100.0	100.0
3.00	(100.0)	(100.0)	(99.0)
1.00	100.0	100.0	97.5
0.50	(100.0)	(100.0)	95.0
0.25	100.0	100.0	85.0
0.15	(97.2)	(98.5)	(67.0)
0.10	95.0	97.5	52.5
0.05	77.5	95.0	(50.0)

	4	5	6
6.00	100.0	87.5	97.5
3.00	(100.0)	(86.0)	96.7
1.00	100.0	88.7	95.0
0.50	100.0	80.0	95.0
0.25	(88.0)	61.2	90.0
0.15	(79.2)	(57.8)	83.3
0.10	72.5	55.0	72.5
0.05	50.0	(50.2)	(54.0)

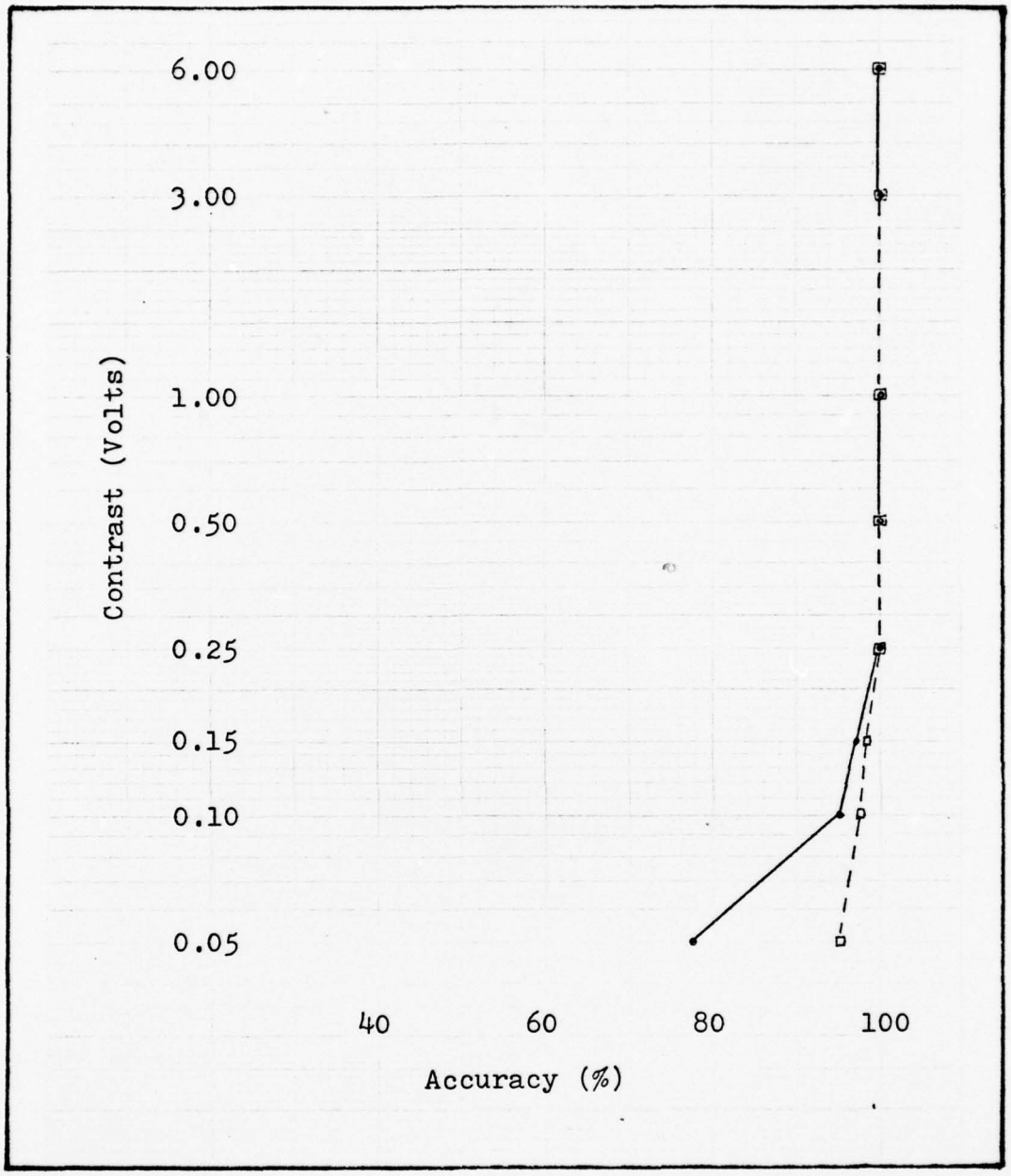

Fig. 42. Plot of Accuracy: KB, 50 msec, Positions 1 (——) and 2 (- -).

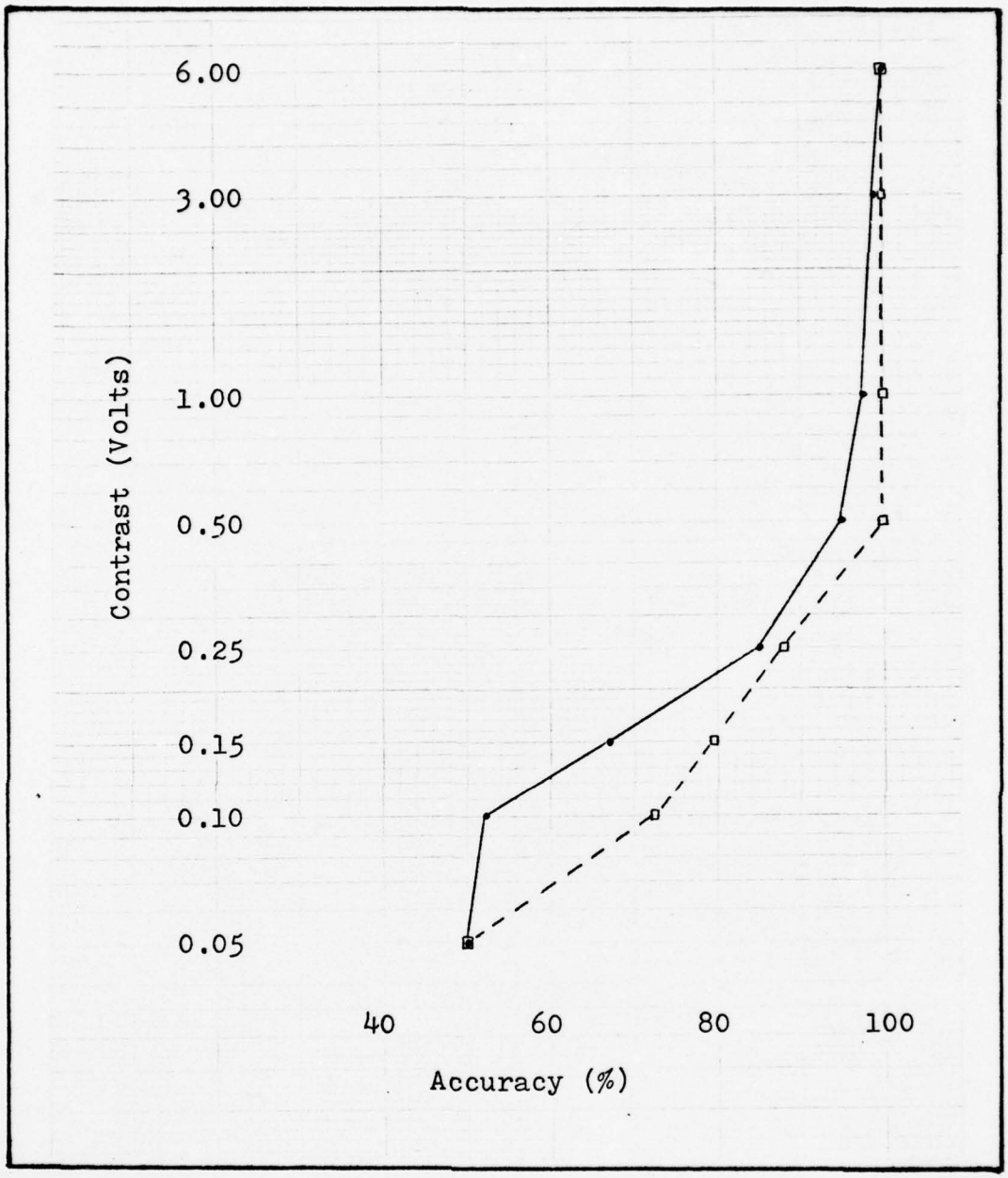

Fig. 43. Plot of Accuracy: KB, 50 msec, Positions 3 (——) and 4 (- -).

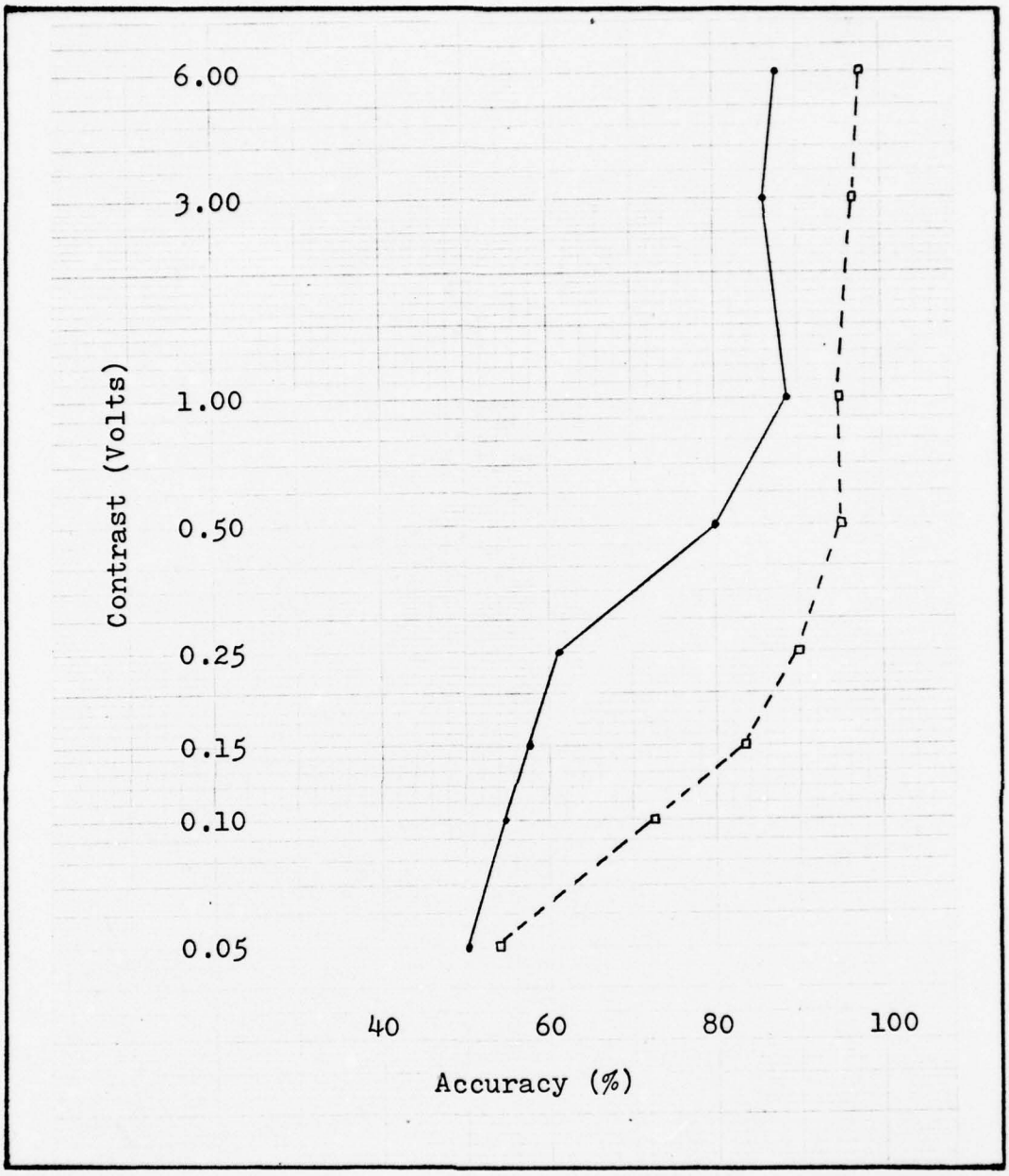

Fig. 44. Plot of Accuracy: KB, 50 msec, Positions 5 (——) and 6 (- -).

Appendix I

Accuracy Values (%): KB, 20 MSEC

Table X
Accuracy: KB, 20 msec

Contrast (Volts)	Peripheral Scope Position 1	2	3
6.00	100.0	100.0	100.0
3.00	(100.0)	(100.0)	(93.0)
1.00	100.0	100.0	82.5
0.50	100.0	100.0	70.0
0.25	97.5	97.5	55.0
0.15	(71.8)	(72.0)	(50.0)
0.10	50.0	52.5	(50.0)
0.05	(50.0)	(50.0)	(50.0)

	4	5	6
6.00	100.0	80.0	96.7
3.00	(99.0)	61.2	98.3
1.00	97.5	63.7	95.8
0.50	100.0	57.5	90.8
0.25	67.5	48.7	76.7
0.15	(50.0)	(42.0)	(62.0)
0.10	(50.0)	(36.8)	(51.6)
0.05	(50.0)	(27.8)	(31.5)

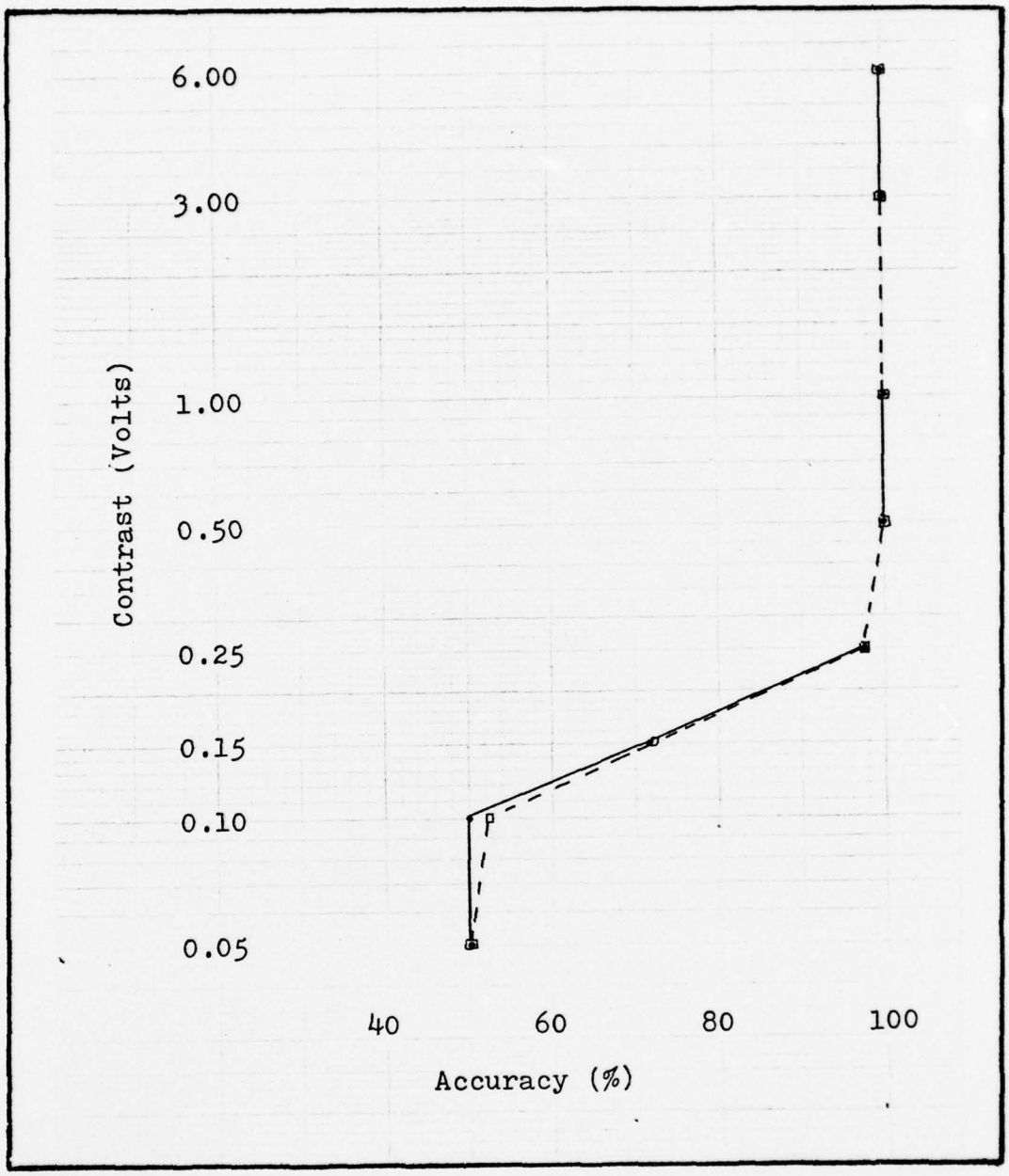

Fig. 45. Plot of Accuracy: KB, 20 msec, Positions 1 (——) and 2 (- -).

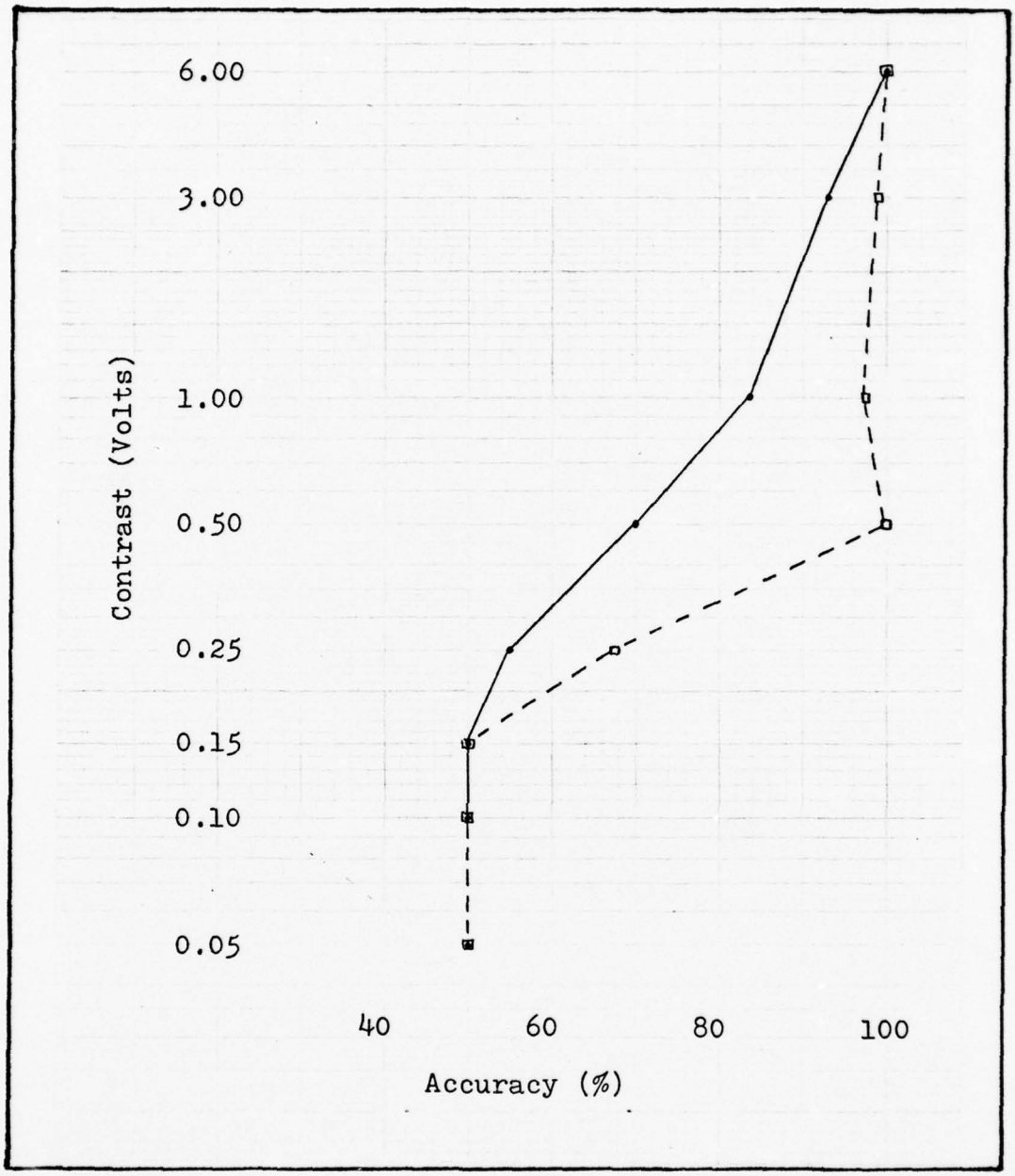

Fig. 46. Plot of Accuracy: KB, 20 msec, Positions 3 (——) and 4 (- -).

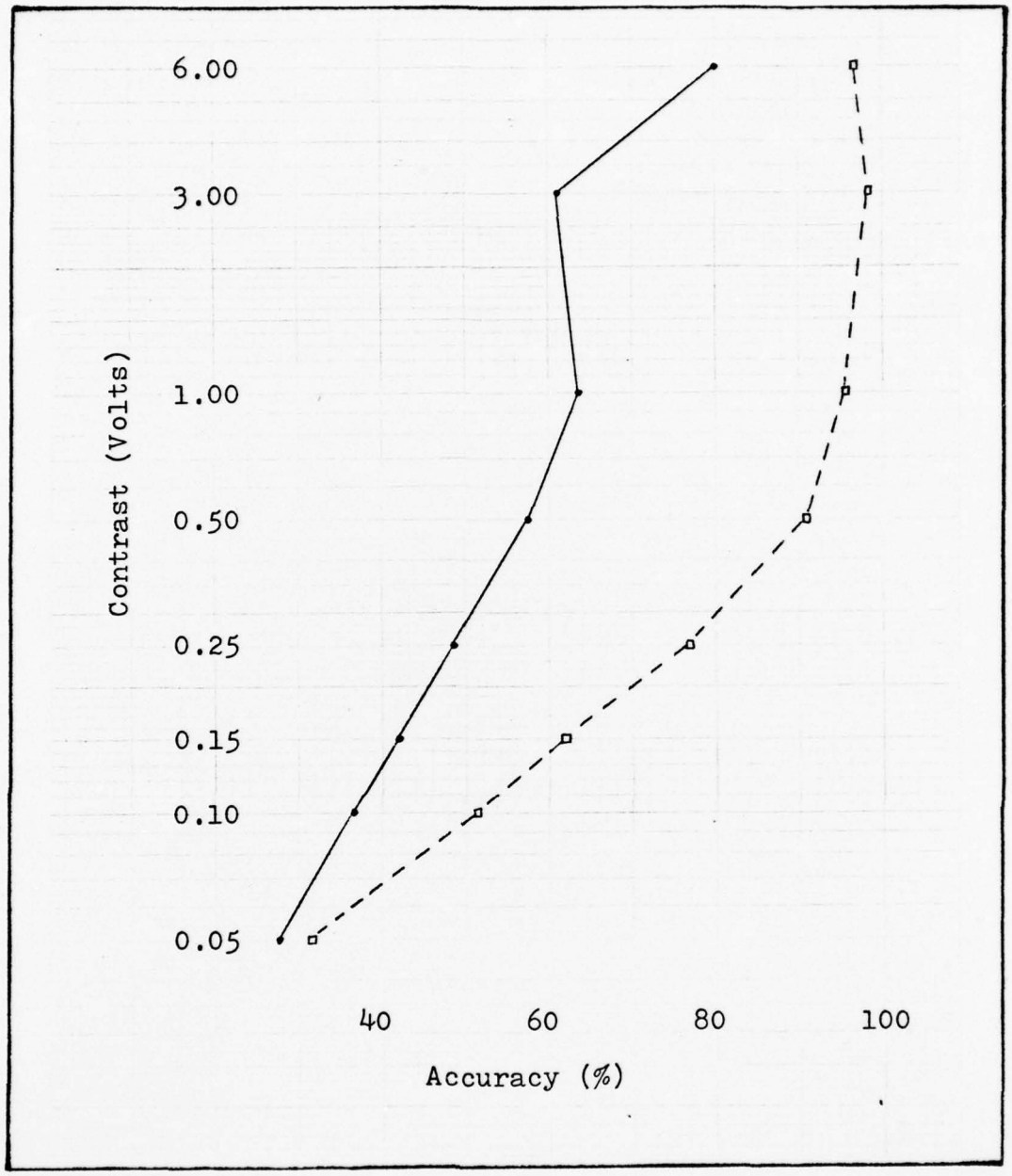

Fig. 47. Plot of Accuracy: KB, 20 msec, Positions 5 (——) and 6 (- -).

Appendix J

Accuracy Values (%): JK, 500 MSEC

Table XI
Accuracy: JK, 500 msec

Contrast (Volts)	Peripheral Scope Position 1	2	3
6.00	100.0	100.0	100.0
3.00	(100.0)	(100.0)	(100.0)
1.00	100.0	100.0	100.0
0.50	(100.0)	(100.0)	(97.5)
0.25	100.0	100.0	95.0
0.15	(100.0)	(98.5)	(88.0)
0.10	100.0	97.5	82.5
0.05	92.5	97.5	70.0
	4	5	6
6.00	100.0	87.5	88.8
3.00	(100.0)	(85.6)	(90.5)
1.00	100.0	82.5	93.8
0.50	(100.0)	(75.5)	(91.2)
0.25	100.0	68.8	(89.1)
0.15	(95.8)	(59.8)	87.5
0.10	92.5	52.5	75.0
0.05	75.0	41.2	52.5

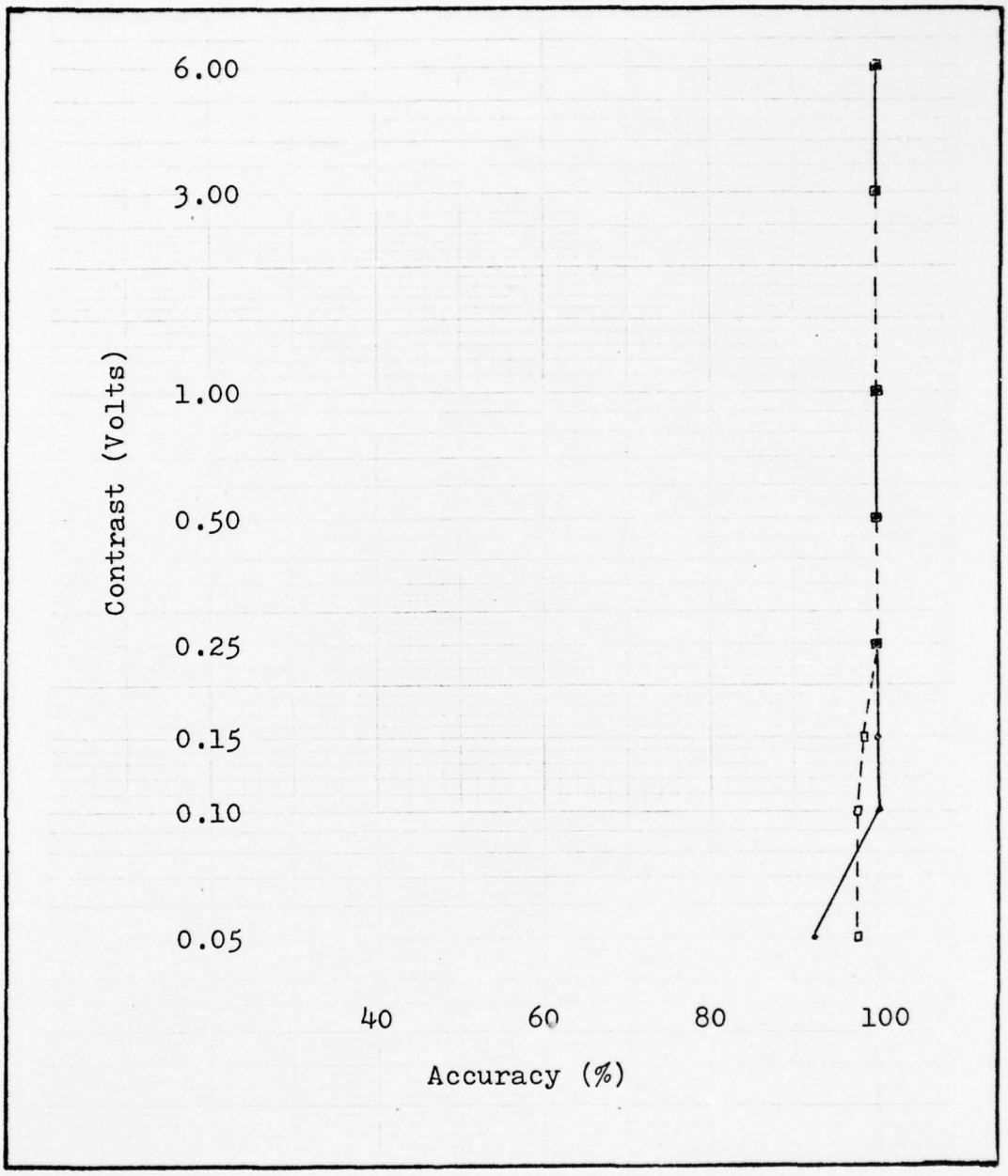

Fig. 48. Plot of Accuracy: JK, 500 msec, Positions 1 (——) and 2 (- -).

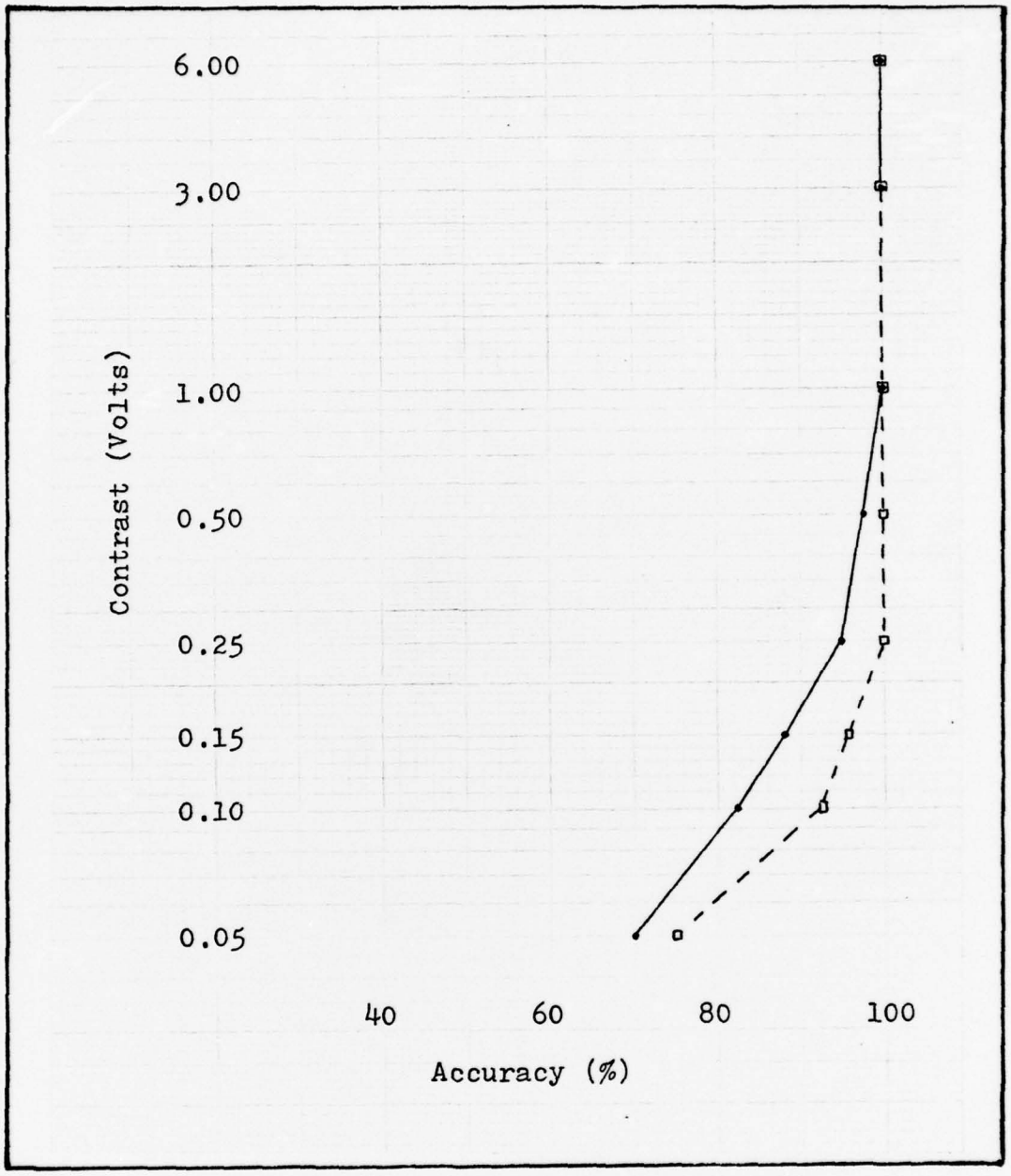

Fig. 49. Plot of Accuracy: JK, 500 msec, Positions 3 (——) and 4 (- -).

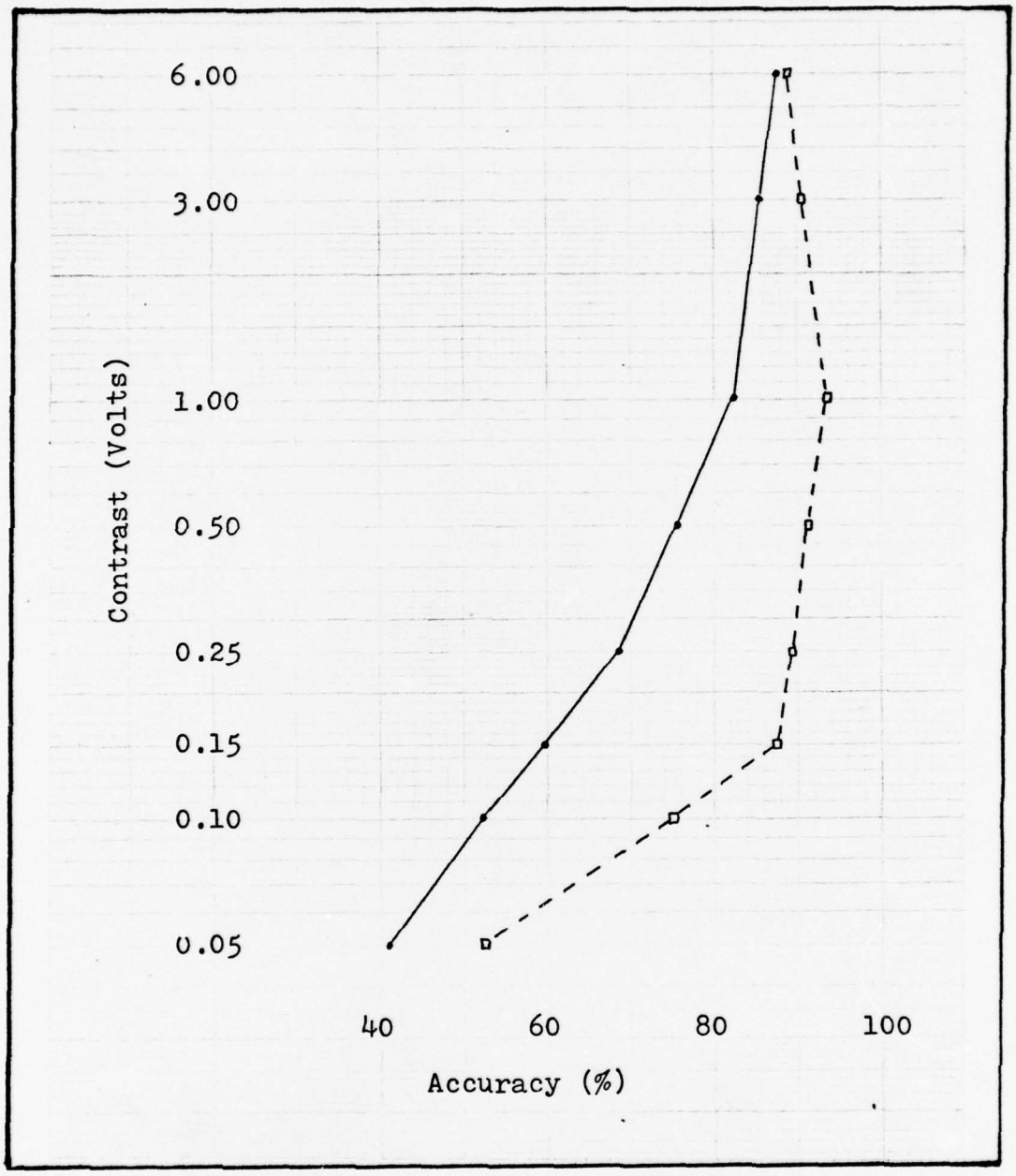

Fig. 50. Plot of Accuracy: JK, 500 msec, Positions 5 (——) and 6 (- -).

Appendix K

Accuracy Values (%): JK, 100 MSEC

Table XII
Accuracy: JK, 100 msec

Contrast (Volts)	Peripheral Scope Position 1	2	3
6.00	100.0	100.0	100.0
3.00	(100.0)	(98.3)	(100.0)
1.00	100.0	97.5	100.0
0.50	(100.0)	(97.5)	(100.0)
0.25	100.0	97.5	100.0
0.15	(100.0)	(97.5)	(84.5)
0.10	100.0	97.5	72.5
0.05	90.0	92.5	70.0
	4	5	6
6.00	100.0	57.5	88.8
3.00	(100.0)	(57.1)	(89.2)
1.00	100.0	56.3	90.0
0.50	(100.0)	(52.0)	(88.8)
0.25	100.0	47.5	87.5
0.15	(92.8)	(53.0)	(82.0)
0.10	85.0	42.5	71.2
0.05	47.5	(25.0)	47.5

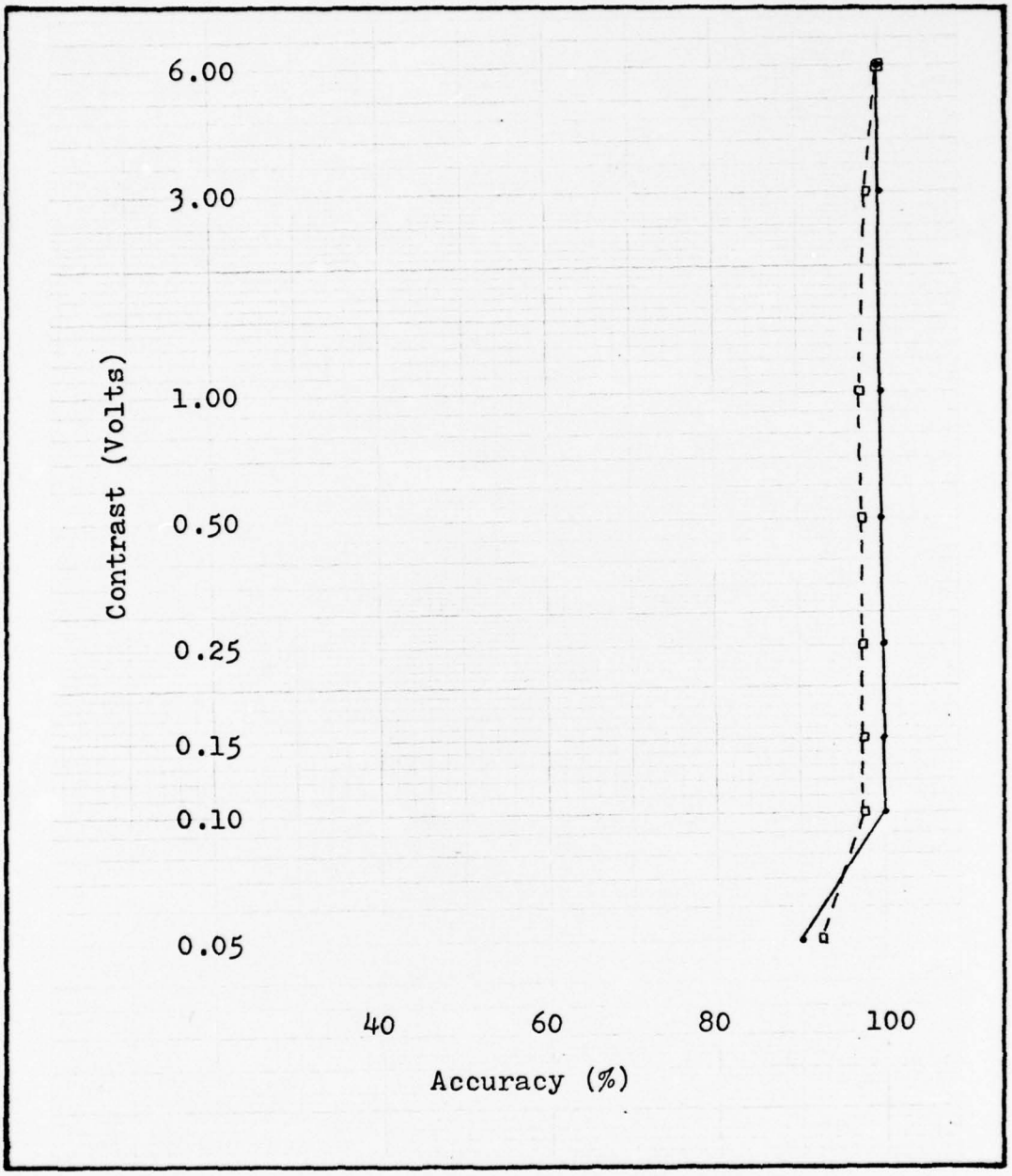

Fig. 51. Plot of Accuracy: JK, 100 msec, Positions 1 (——) and 2 (- -).

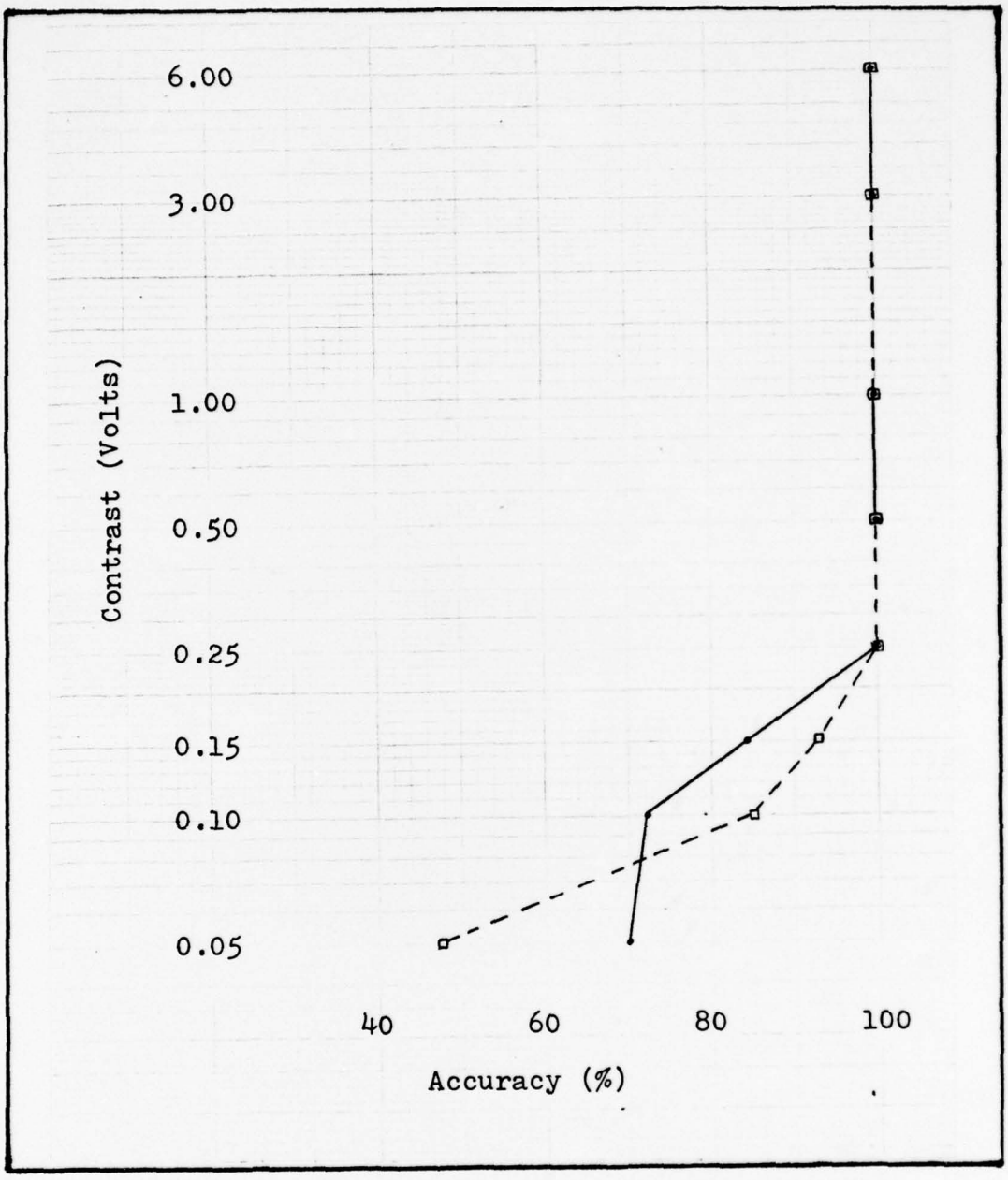

Fig. 52. Plot of Accuracy: JK, 100 msec, Positions 3 (——) and 4 (- -).

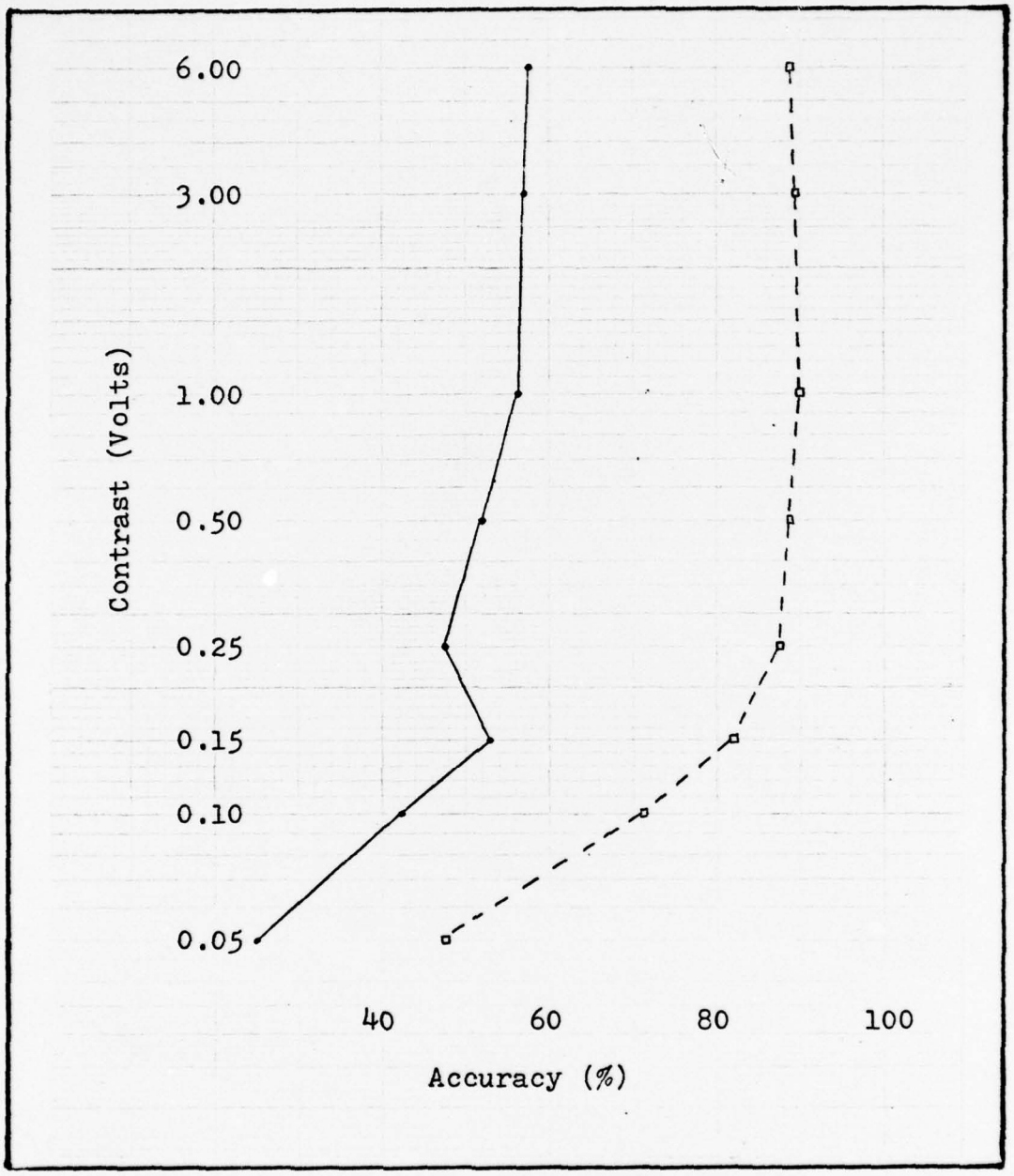

Fig. 53. Plot of Accuracy: JK, 100 msec, Positions 5 (——) and 6 (- -).

Appendix L

Accuracy Values (%): JK, 50 MSEC

Table XIII
Accuracy: JK, 50 msec

Contrast (Volts)	Peripheral Scope Position 1	2	3
6.00	100.0	100.0	100.0
3.00	(100.0)	(100.0)	(99.0)
1.00	100.0	100.0	97.5
0.50	(100.0)	(100.0)	(83.8)
0.25	100.0	100.0	70.0
0.15	(100.0)	(100.0)	(67.2)
0.10	100.0	100.0	65.0
0.05	75.0	70.0	52.5

	4	5	6
6.00	100.0	50.0	90.0
3.00	(100.0)	56.3	(88.0)
1.00	100.0	47.5	85.0
0.50	(98.8)	55.0	(85.0)
0.25	97.5	52.5	85.0
0.15	(93.2)	(45.0)	71.2
0.10	90.0	38.8	61.2
0.05	55.0	(28.1)	(44.0)

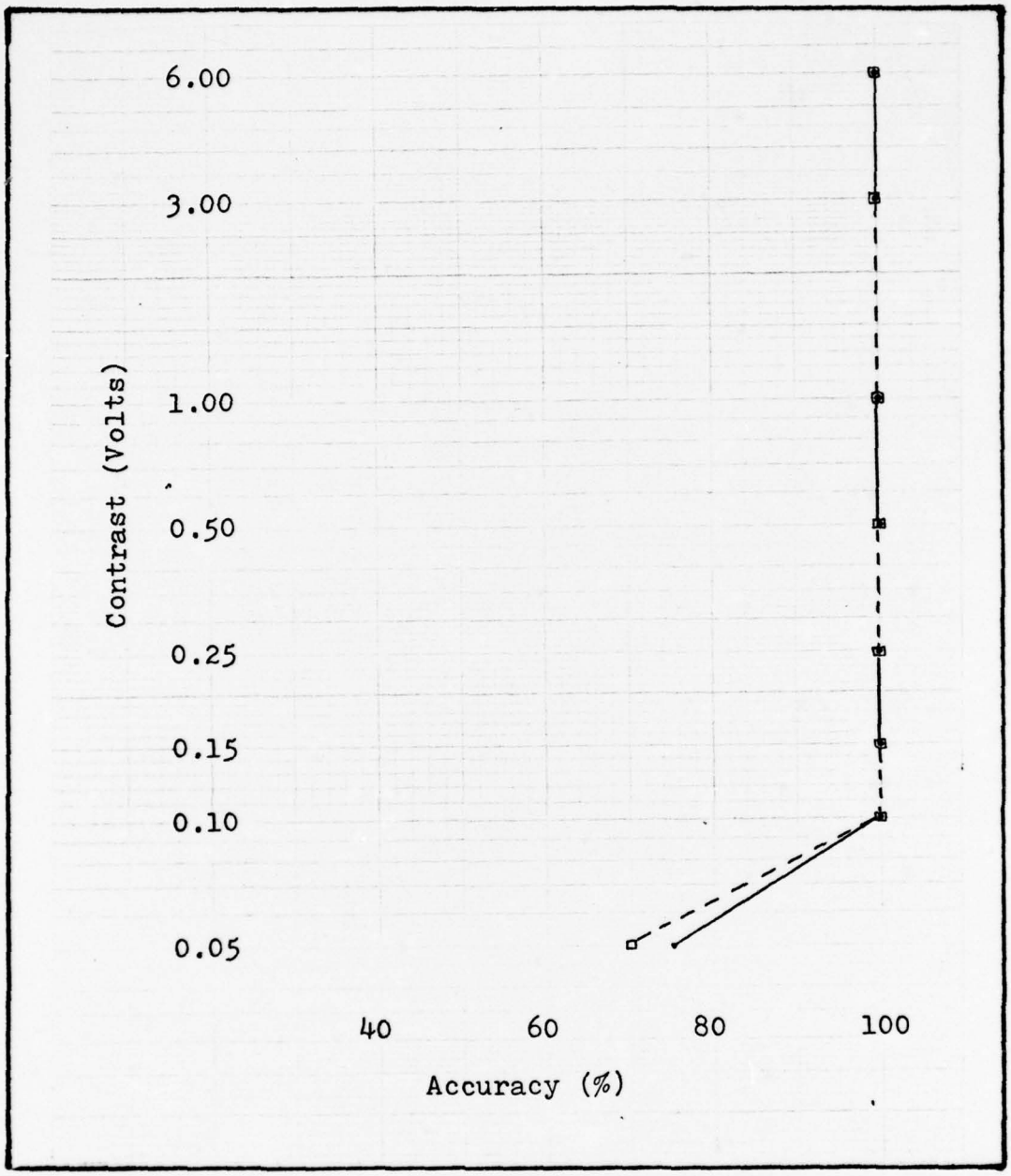

Fig. 54. Plot of Accuracy: JK, 50 msec, Positions 1 (——) and 2 (- -).

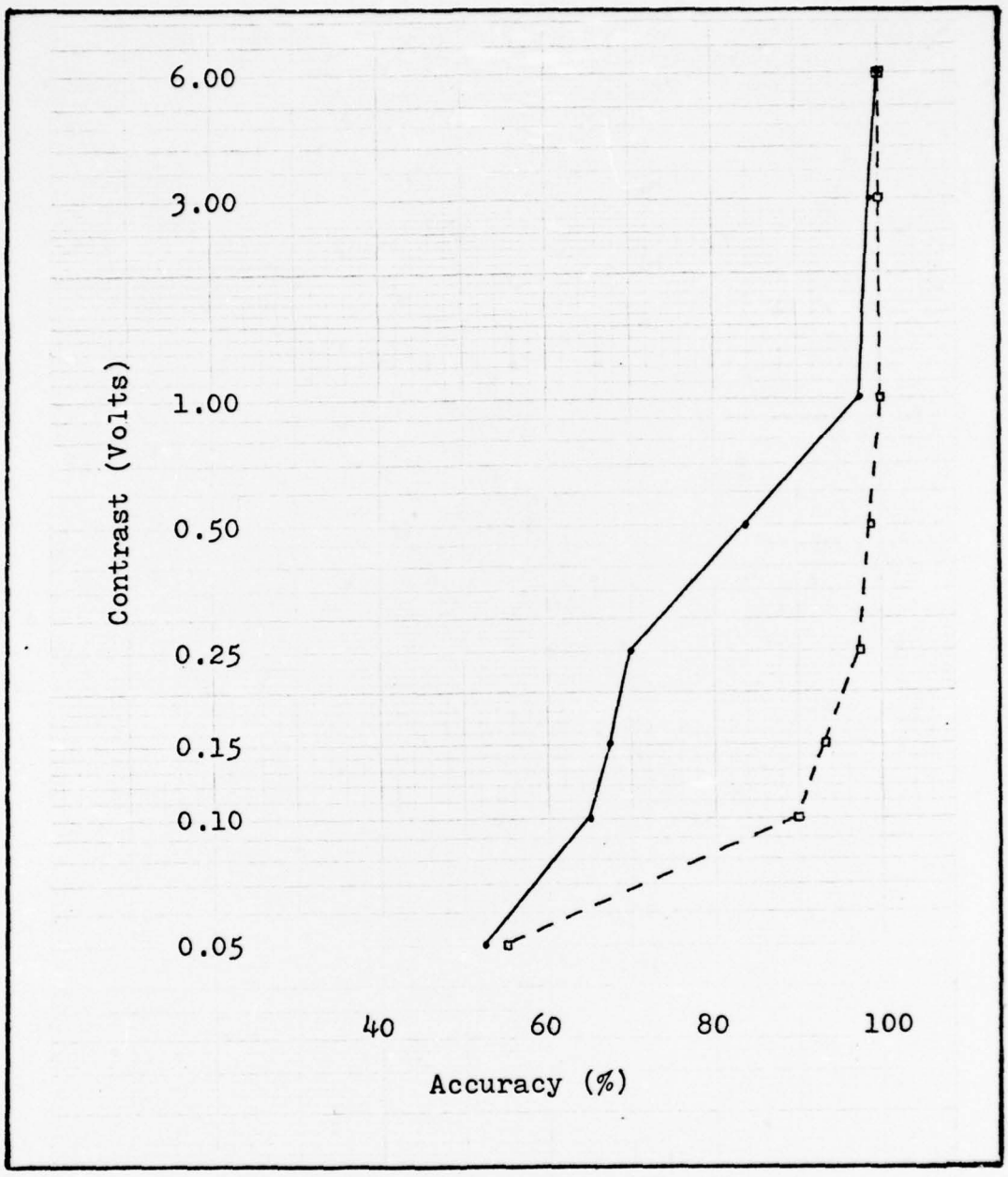

Fig. 55. Plot of Accuracy: JK, 50 msec, Positions 3 (——) and 4 (- -).

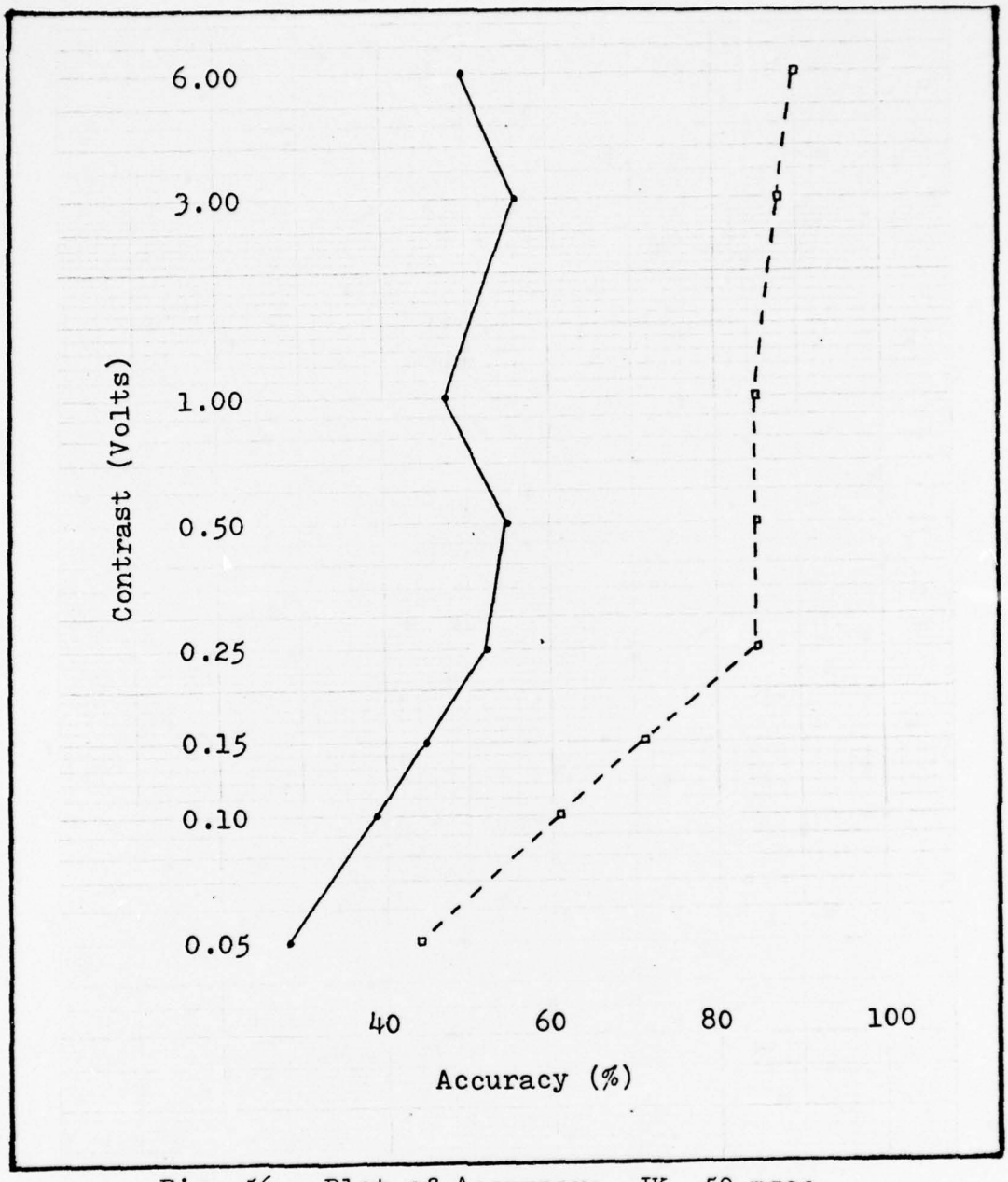

Fig. 56. Plot of Accuracy: JK, 50 msec, Positions 5 (——) and 6 (- -).

Appendix M

Accuracy Values (%): JK, 20 MSEC

Table XIV
Accuracy: JK, 20 msec

Contrast (Volts)	Peripheral Scope Position 1	2	3
6.00	100.0	100.0	100.0
3.00	(100.0)	(100.0)	(97.0)
1.00	(100.0)	100.0	92.5
0.50	100.0	(100.0)	(76.2)
0.25	95.0	100.0	60.0
0.15	(78.1)	(80.5)	45.0
0.10	65.0	65.0	67.5
0.05	(50.0)	(50.0)	(50.0)
	4	5	6
6.00	100.0	66.2	90.0
3.00	(99.0)	51.2	(88.0)
1.00	97.5	52.5	85.0
0.50	(93.8)	45.0	68.8
0.25	90.0	47.5	56.2
0.15	52.5	36.2	(48.0)
0.10	47.5	(27.0)	(41.2)
0.05	(47.5)	(25.0)	(29.8)

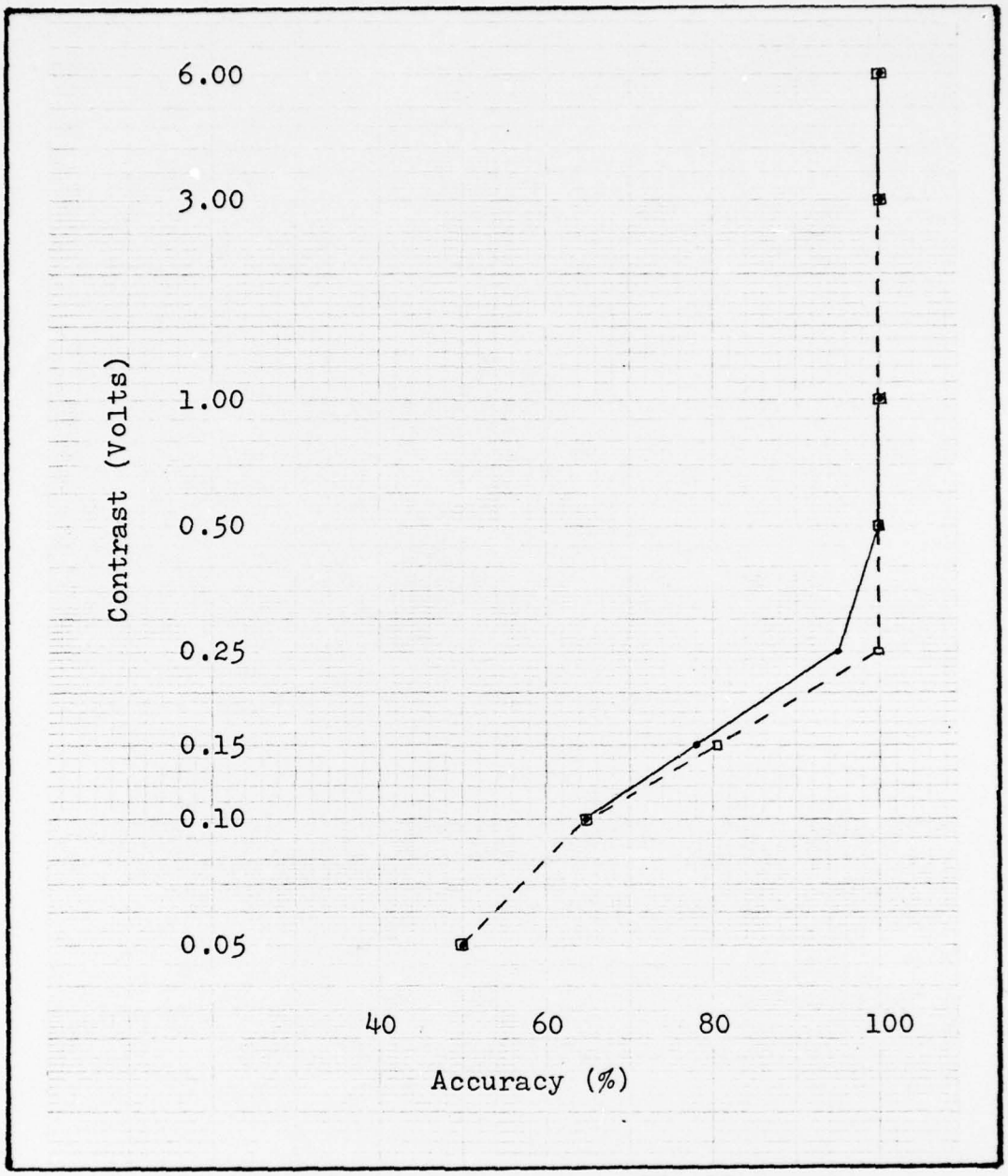

Fig. 57. Plot of Accuracy: JK, 20 msec, Positions 1 (——) and 2 (- -).

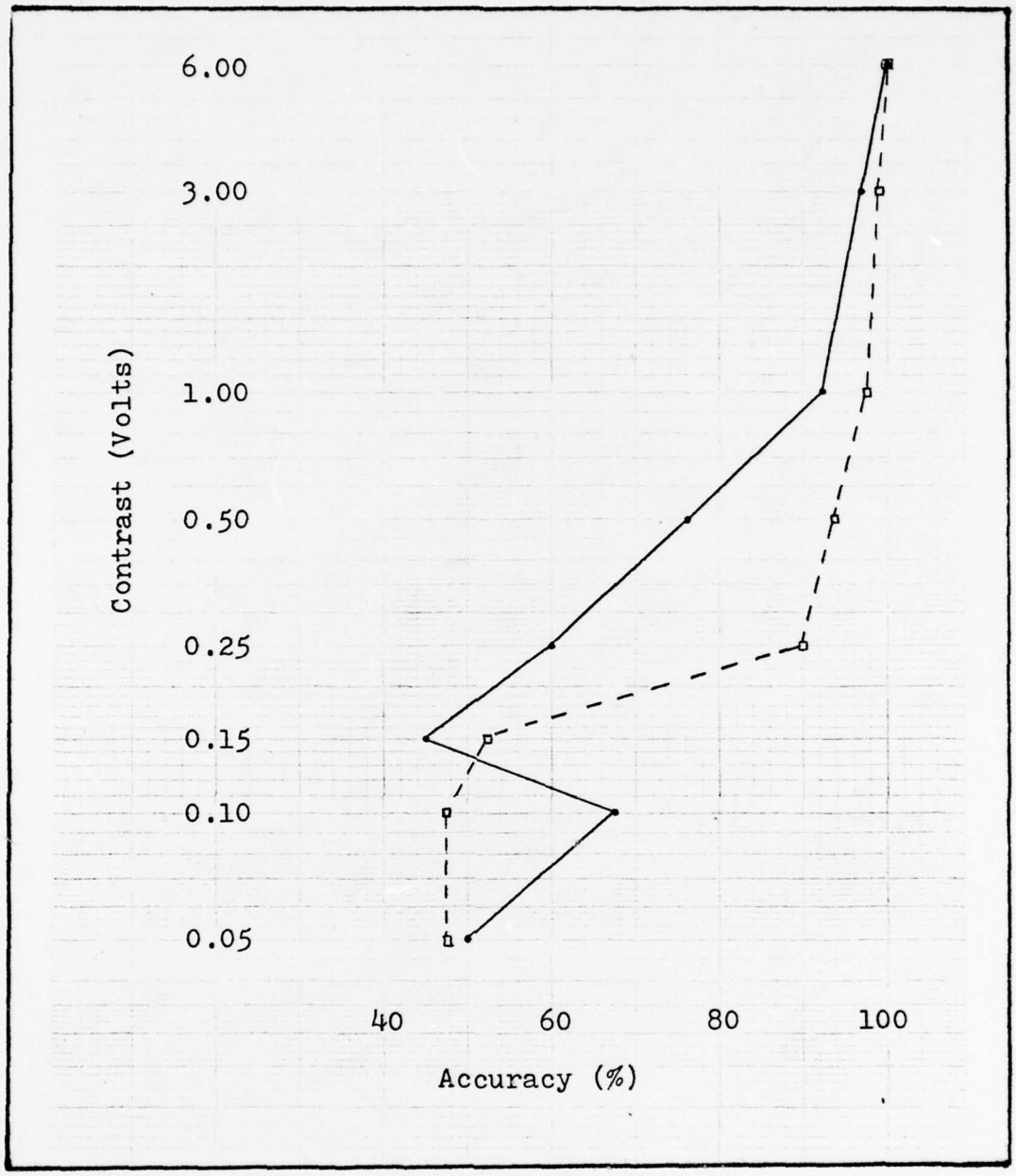

Fig. 58. Plot of Accuracy: JK, 20 msec, Positions 3 (——) and 4 (- -).

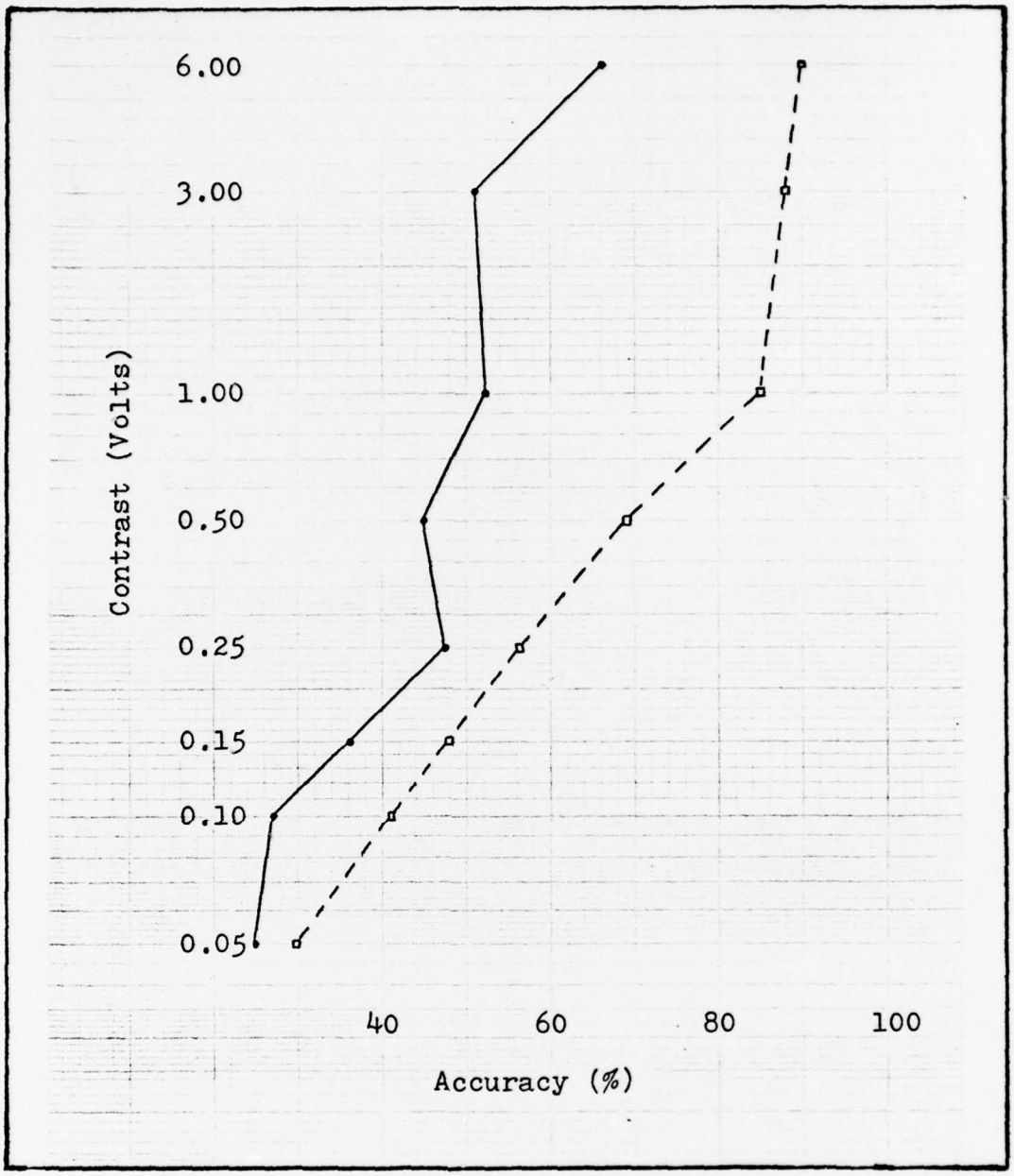

Fig. 59. Plot of Accuracy: JK, 20 msec, Positions 5 (——) and 6 (- -).

Appendix N

Accuracy Values (%): CH, 500 MSEC

Table XV
Accuracy: CH, 500 msec

Contrast (Volts)	Peripheral Scope Position 1	2	3
6.00	100.0	100.0	100.0
3.00	(100.0)	(100.0)	(100.0)
1.00	100.0	100.0	100.0
0.50	100.0	(100.0)	100.0
0.25	100.0	100.0	90.0
0.15	(100.0)	(100.0)	(84.2)
0.10	100.0	100.0	80.0
0.05	100.0	100.0	52.5

	4	5	6
6.00	100.0	93.8	98.8
3.00	(100.0)	(91.6)	(98.2)
1.00	100.0	87.5	97.5
0.50	(100.0)	(88.5)	(98.2)
0.25	100.0	90.0	98.8
0.15	(100.0)	(90.0)	(99.4)
0.10	100.0	90.0	100.0
0.05	50.0	68.8	75.0

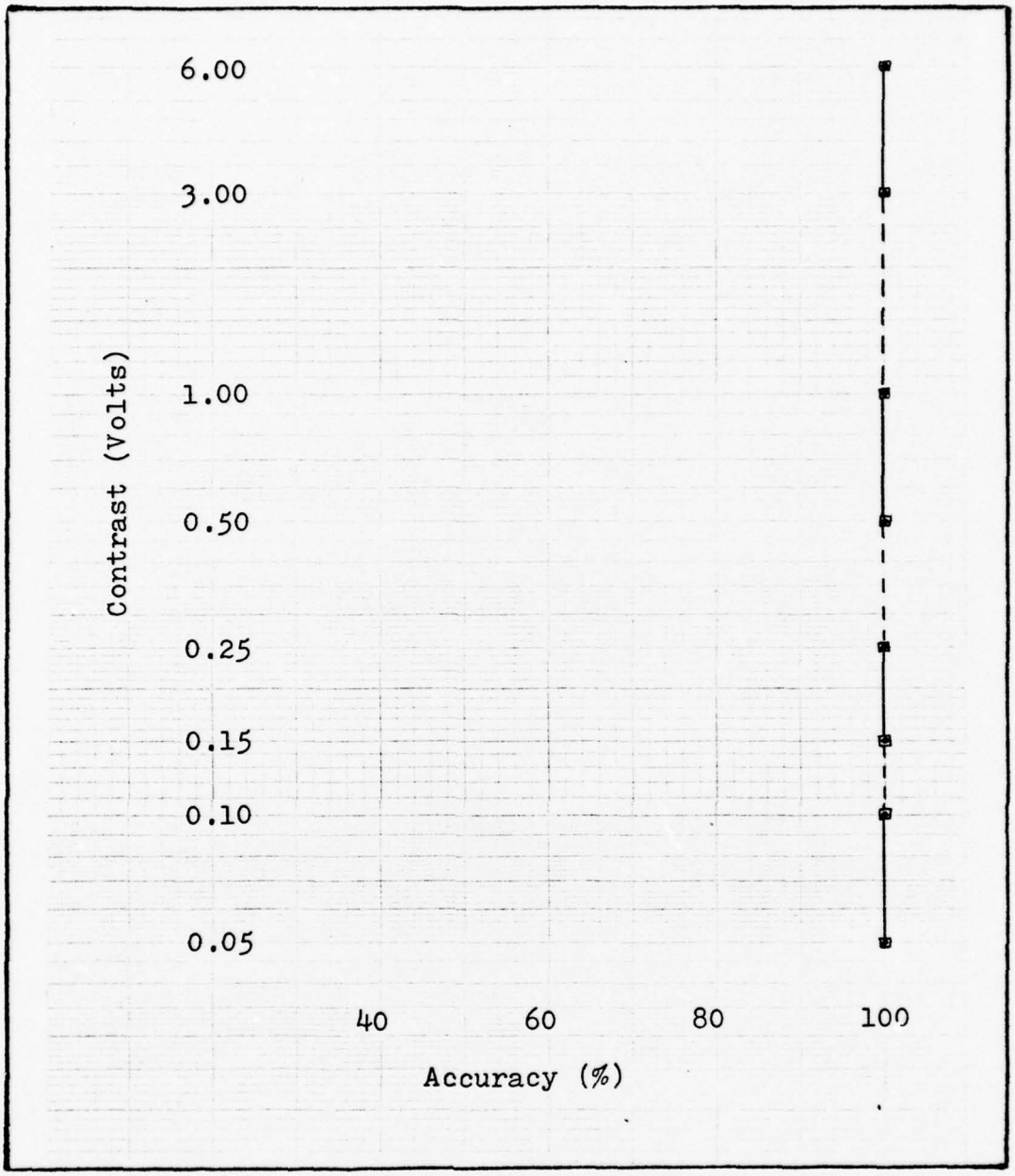

Fig. 60. Plot of Accuracy: CH, 500 msec, Positions 1 (——) and 2 (- -).

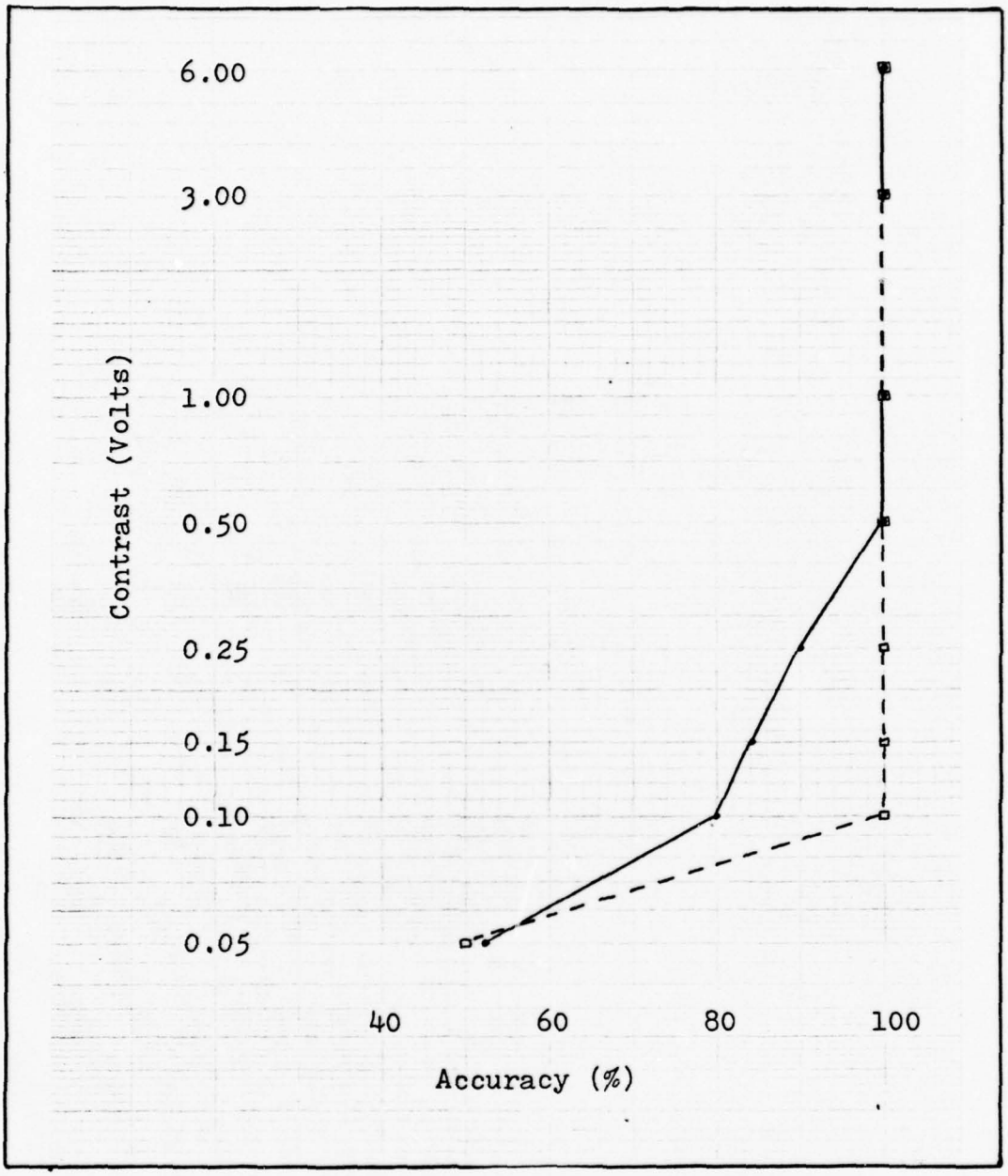

Fig. 61. Plot of Accuracy: CH, 500 msec, Positions 3 (——) and 4 (- -).

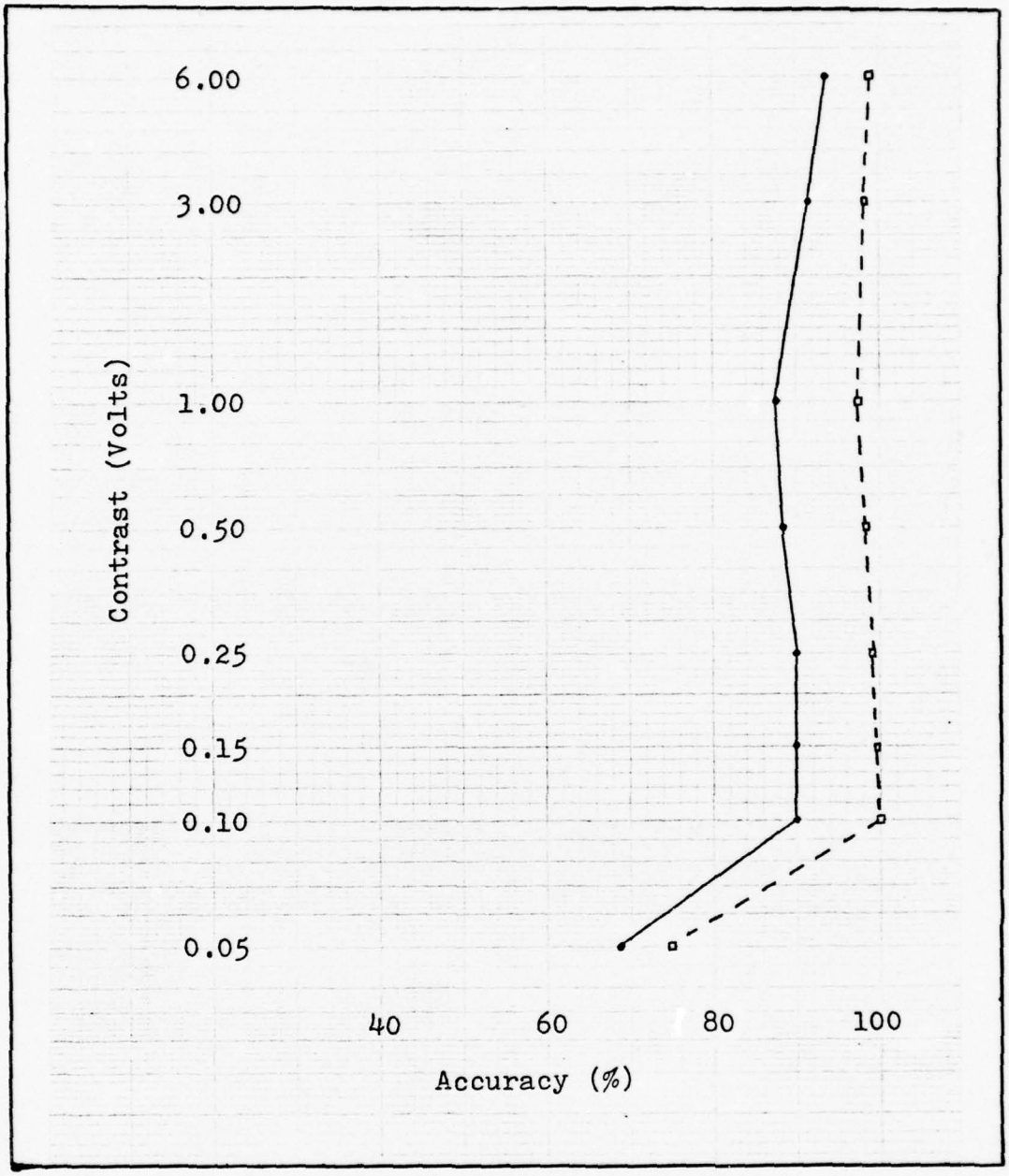

Fig. 62. Plot of Accuracy: CH, 500 msec, Positions 5 (——) and 6 (- -).

Appendix O

Accuracy Values (%): CH, 100 MSEC

Table XVI
Accuracy: CH, 100 msec

Contrast (Volts)	Peripheral Scope Position 1	2	3
6.00	100.0	100.0	100.0
3.00	(100.0)	(100.0)	(100.0)
1.00	100.0	100.0	100.0
0.50	100.0	(100.0)	97.5
0.25	(100.0)	100.0	92.5
0.15	(100.0)	(100.0)	(79.0)
0.10	100.0	100.0	50.0
0.05	97.5	92.5	(50.0)
	4	5	6
6.00	100.0	85.0	92.5
3.00	(100.0)	(85.0)	(92.0)
1.00	100.0	85.0	91.2
0.50	100.0	85.0	(91.8)
0.25	100.0	83.8	92.5
0.15	(87.5)	(70.0)	92.5
0.10	77.5	65.0	88.8
0.05	67.5	(42.8)	57.5

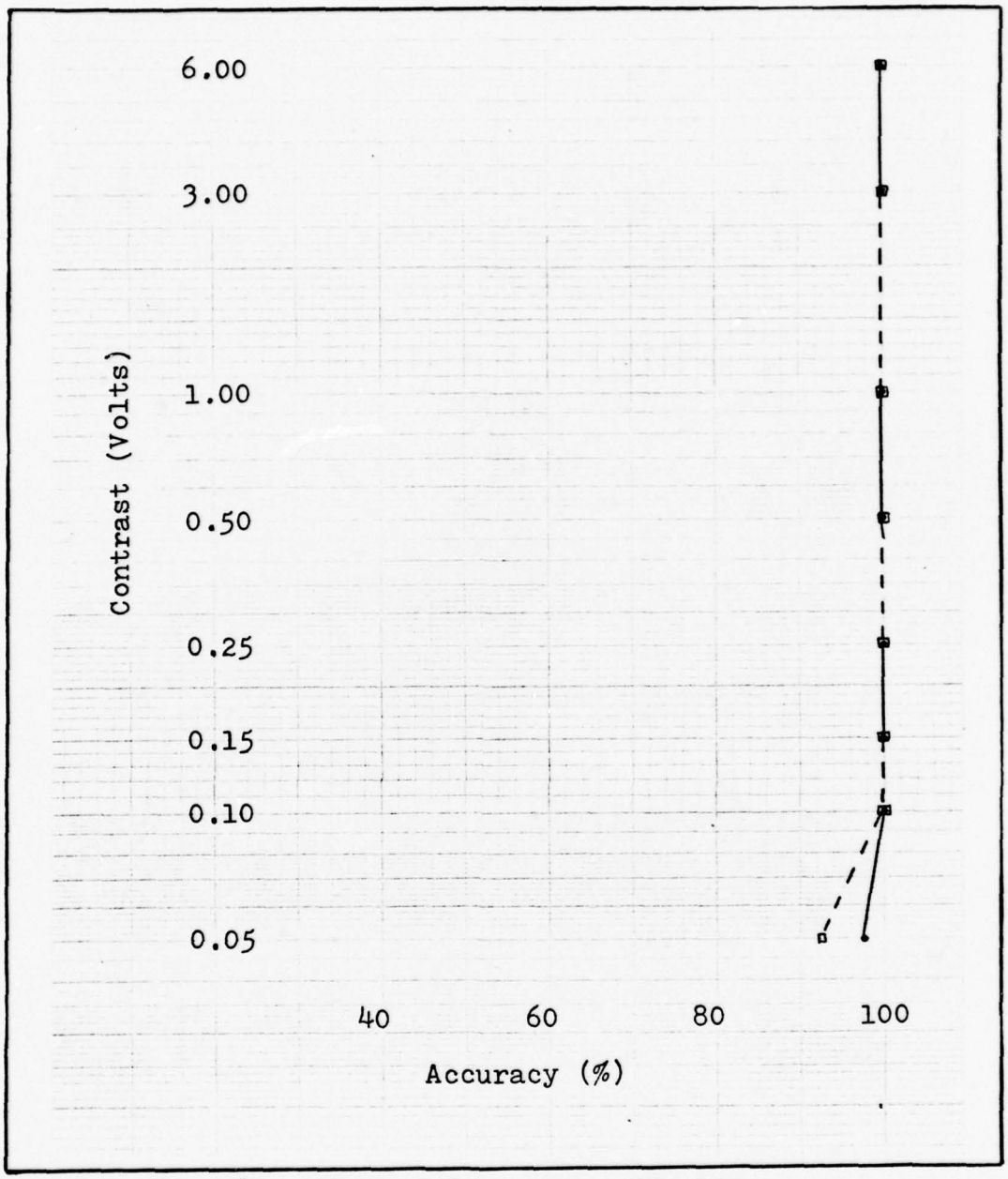

Fig. 63. Plot of Accuracy: CH, 100 msec, Positions 1 (——) and 2 (- -).

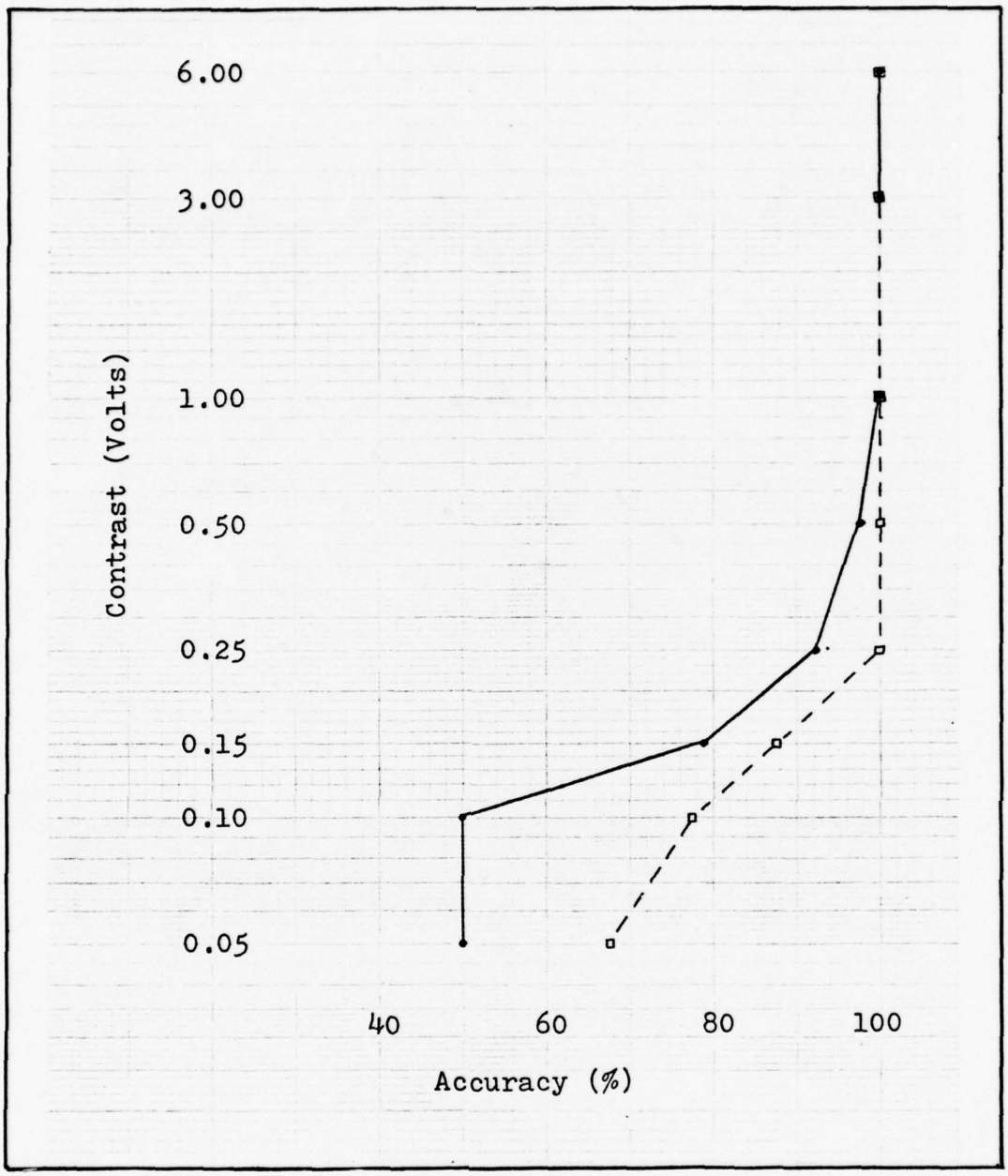

Fig. 64. Plot of Accuracy: CH, 100 msec, Positions 3 (——) and 4 (- -).

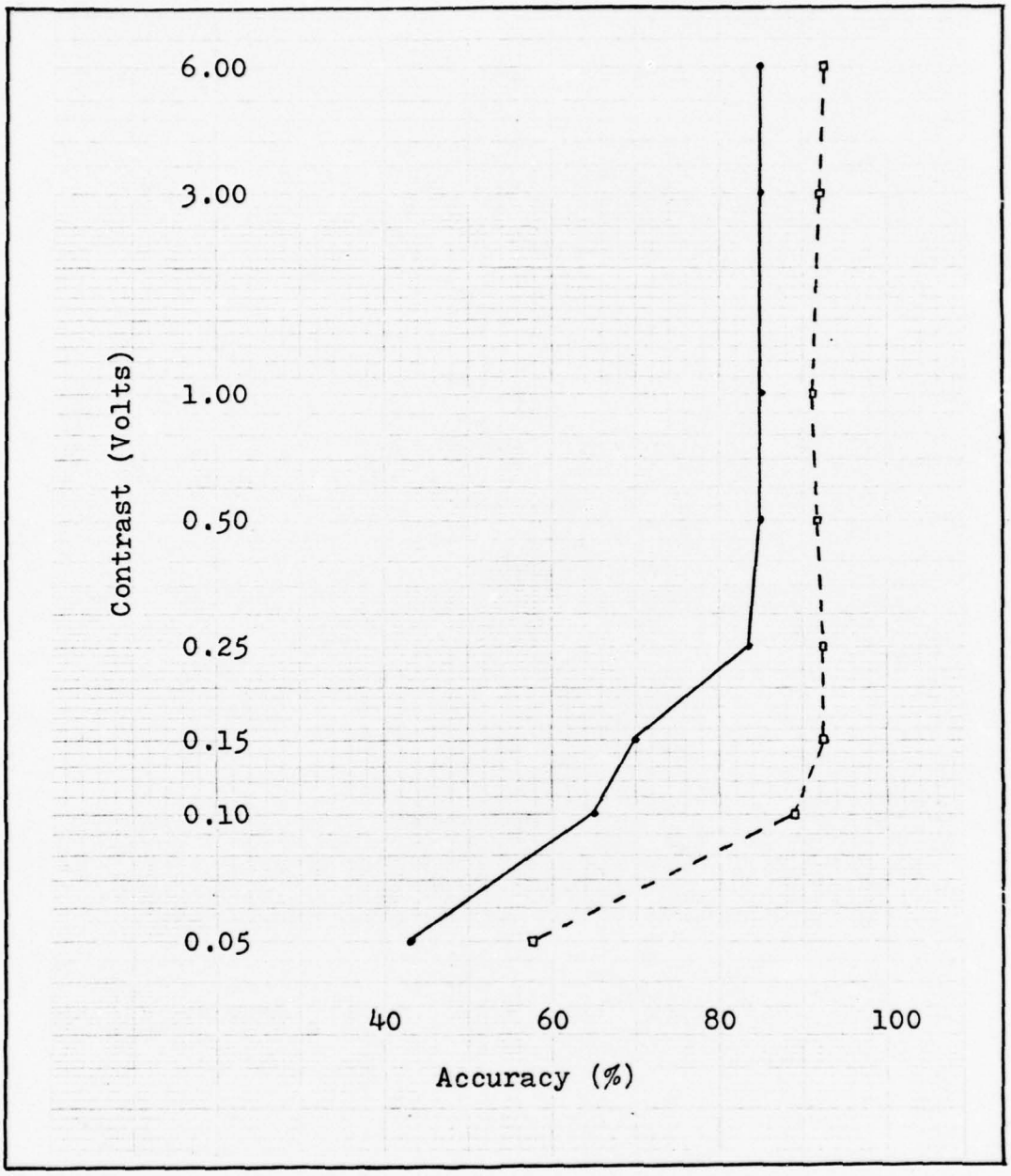

Fig. 65. Plot of Accuracy: CH, 100 msec, Positions 5 (——) and 6 (- -).

Appendix P

Accuracy Values (%): CH, 50 MSEC

Table XVII
Accuracy: CH, 50 msec

Contrast (Volts)	Peripheral Scope Position 1	2	3
6.00	(100.0)	100.0	100.0
3.00	(100.0)	(100.0)	(99.0)
1.00	100.0	100.0	97.5
0.50	(100.0)	(100.0)	87.5
0.25	100.0	100.0	85.0
0.15	(100.0)	(97.2)	(66.8)
0.10	100.0	95.0	52.5
0.05	75.0	75.0	(50.0)

	4	5	6
6.00	100.0	85.0	90.0
3.00	(100.0)	(83.0)	(89.5)
1.00	100.0	81.2	88.8
0.50	97.5	85.0	93.8
0.25	100.0	86.2	96.2
0.15	(90.0)	(69.7)	78.8
0.10	82.5	56.2	60.0
0.05	(47.5)	(33.5)	(28.0)

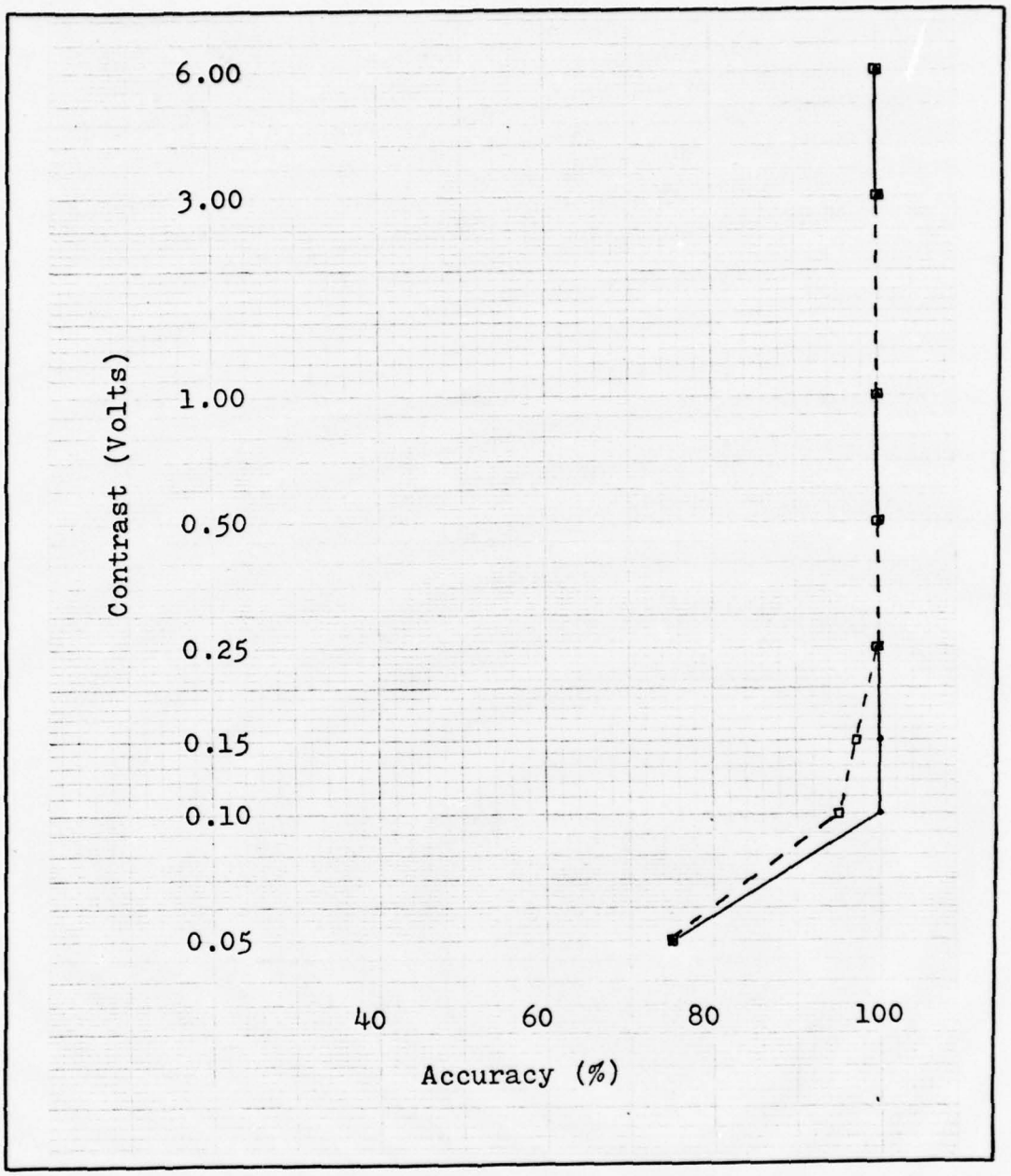

Fig. 66. Plot of Accuracy: CH, 50 msec, Positions 1 (——) and 2 (- -).

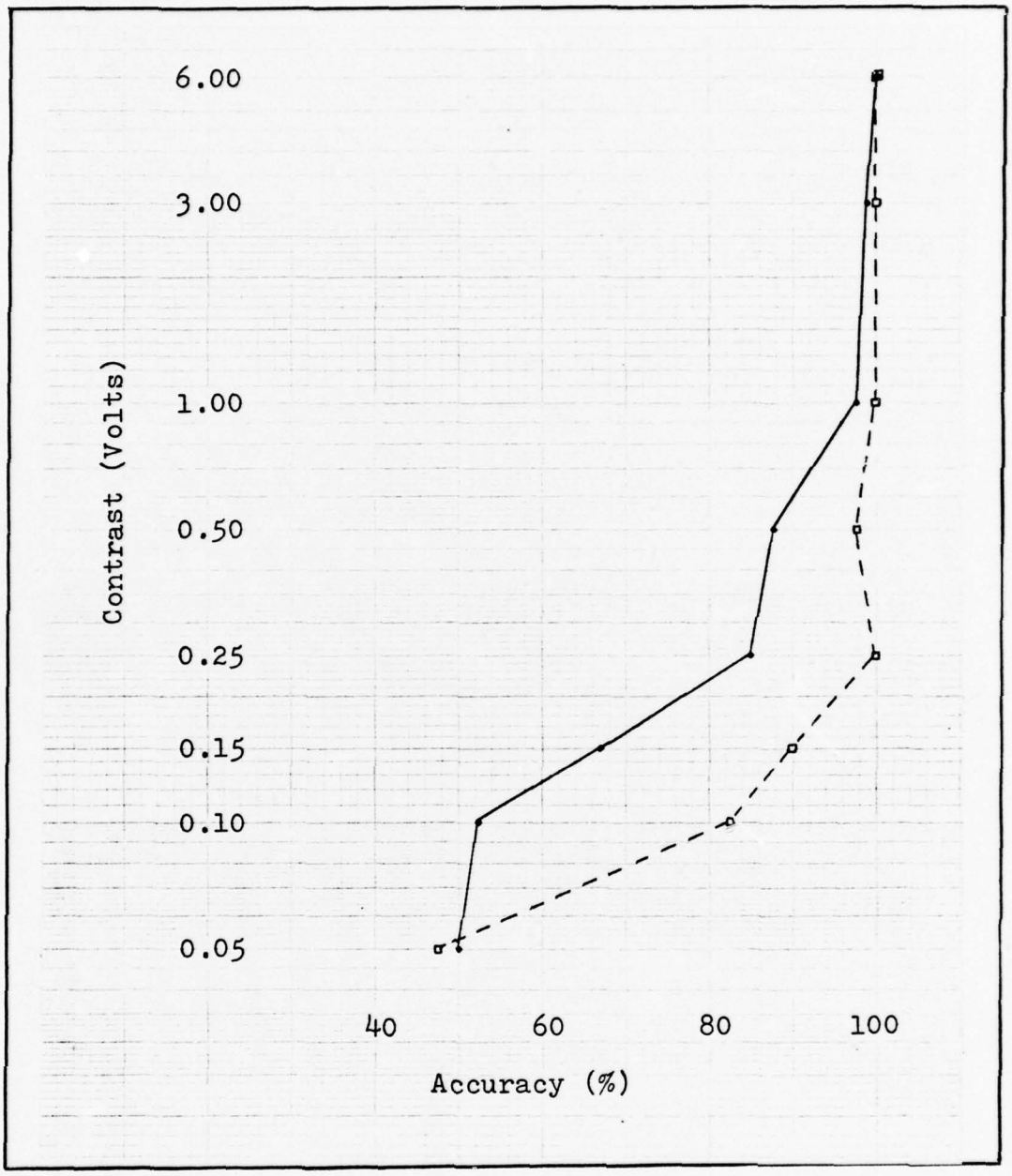

Fig. 67. Plot of Accuracy: CH, 50 msec, Positions 3 (——) and 4 (- -).

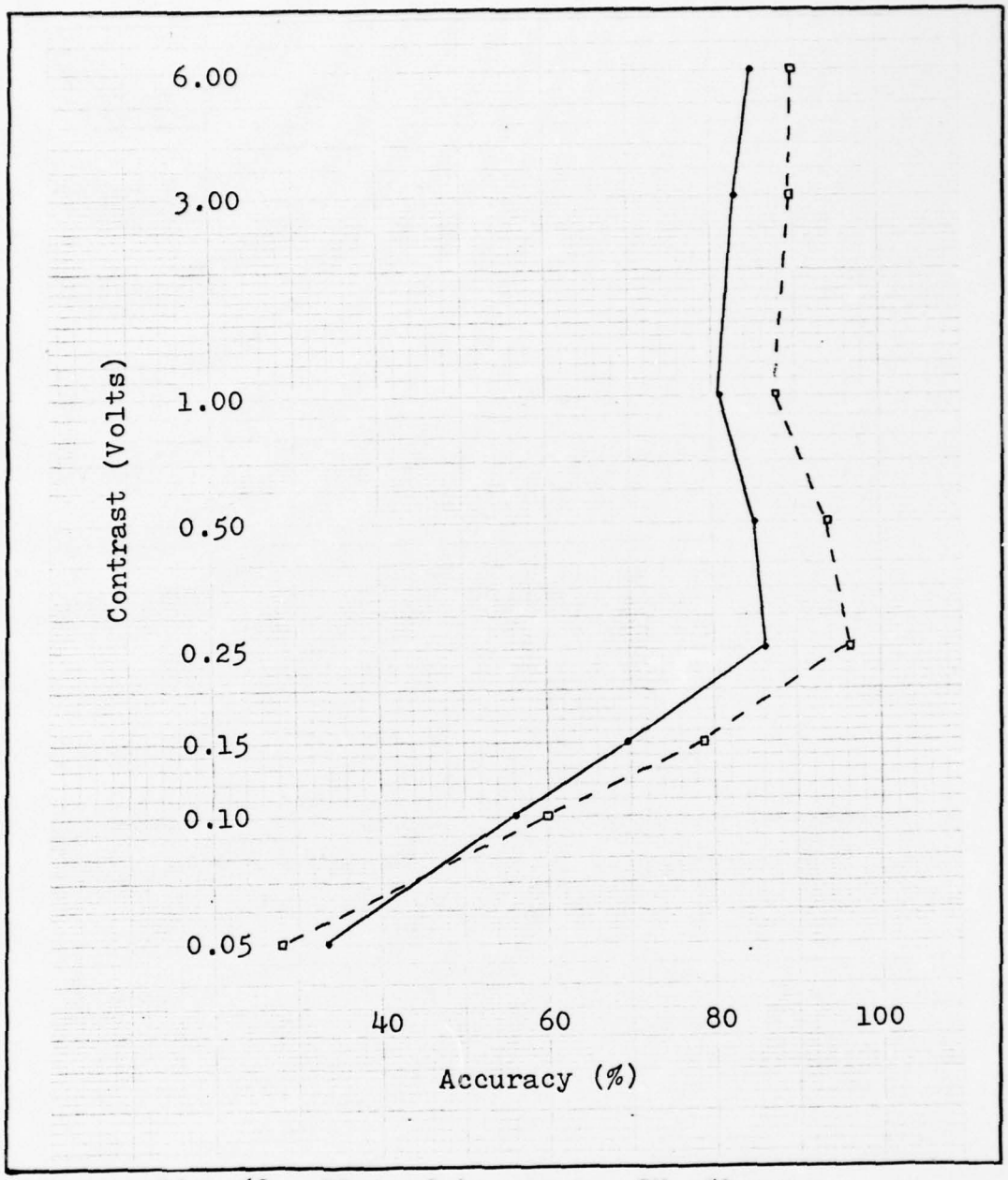

Fig. 68. Plot of Accuracy: CH, 50 msec, Positions 5 (——) and 6 (- -).

Appendix Q

Accuracy Values (%): CH, 20 MSEC

Table XVIII
Accuracy: CH, 20 msec

Contrast (Volts)	Peripheral Scope Position 1	2	3
6.00	100.0	100.0	100.0
3.00	(100.0)	(100.0)	100.0
1.00	100.0	100.0	82.5
0.50	(100.0)	97.5	57.5
0.25	100.0	92.5	50.0
0.15	(76.3)	(73.0)	(50.0)
0.10	57.5	57.5	(50.0)
0.05	(50.0)	(50.0)	(50.0)

	4	5	6
6.00	100.0	81.3	88.8
3.00	(99.0)	73.5	90.0
1.00	97.5	81.3	83.8
0.50	95.0	66.3	92.5
0.25	75.0	50.0	62.5
0.15	(62.3)	(37.8)	57.0
0.10	52.5	(28.0)	(52.8)
0.05	(50.0)	(25.0)	(45.5)

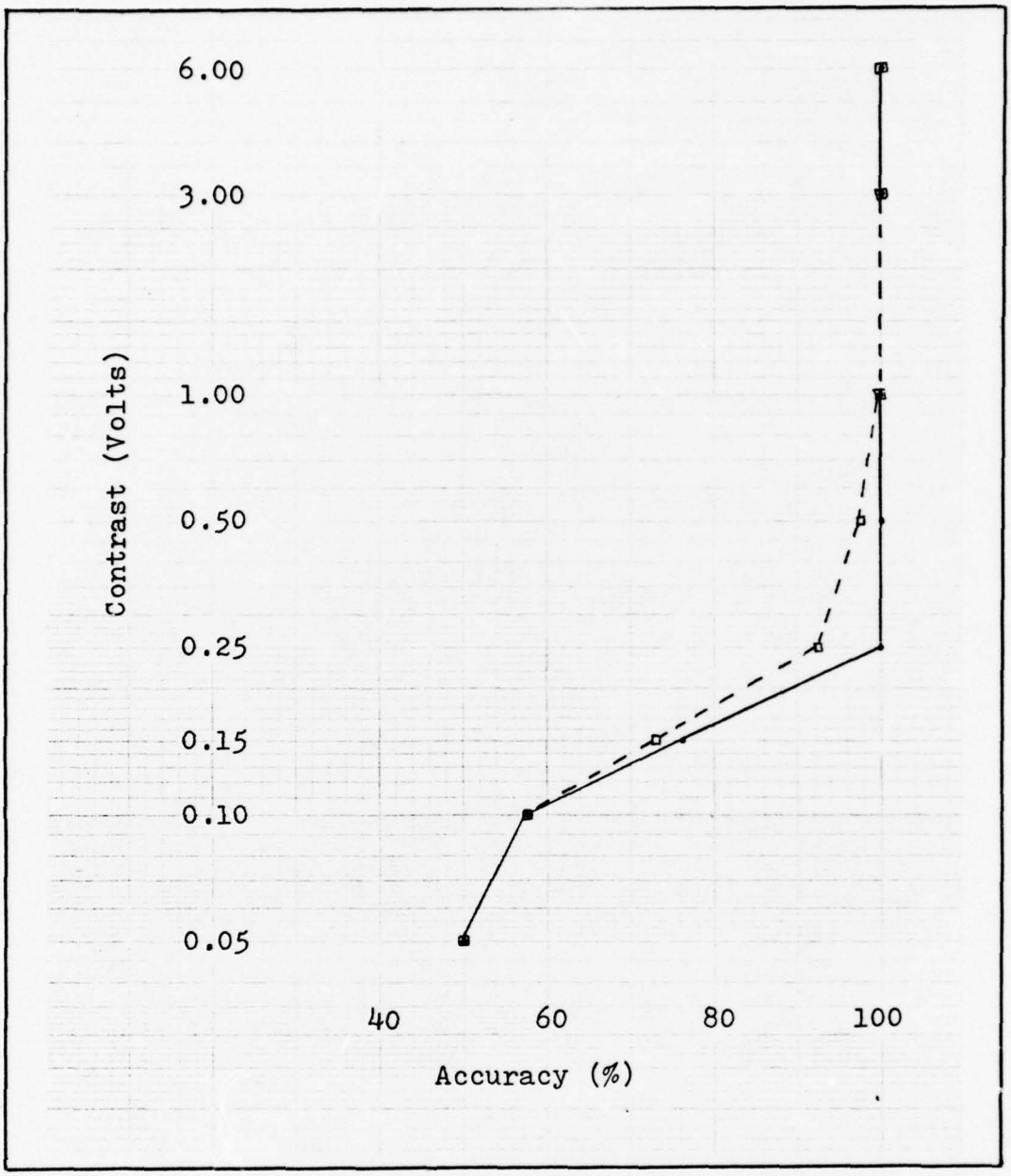

Fig. 69. Plot of Accuracy: CH, 20 msec, Positions 1 (——) and 2 (- -).

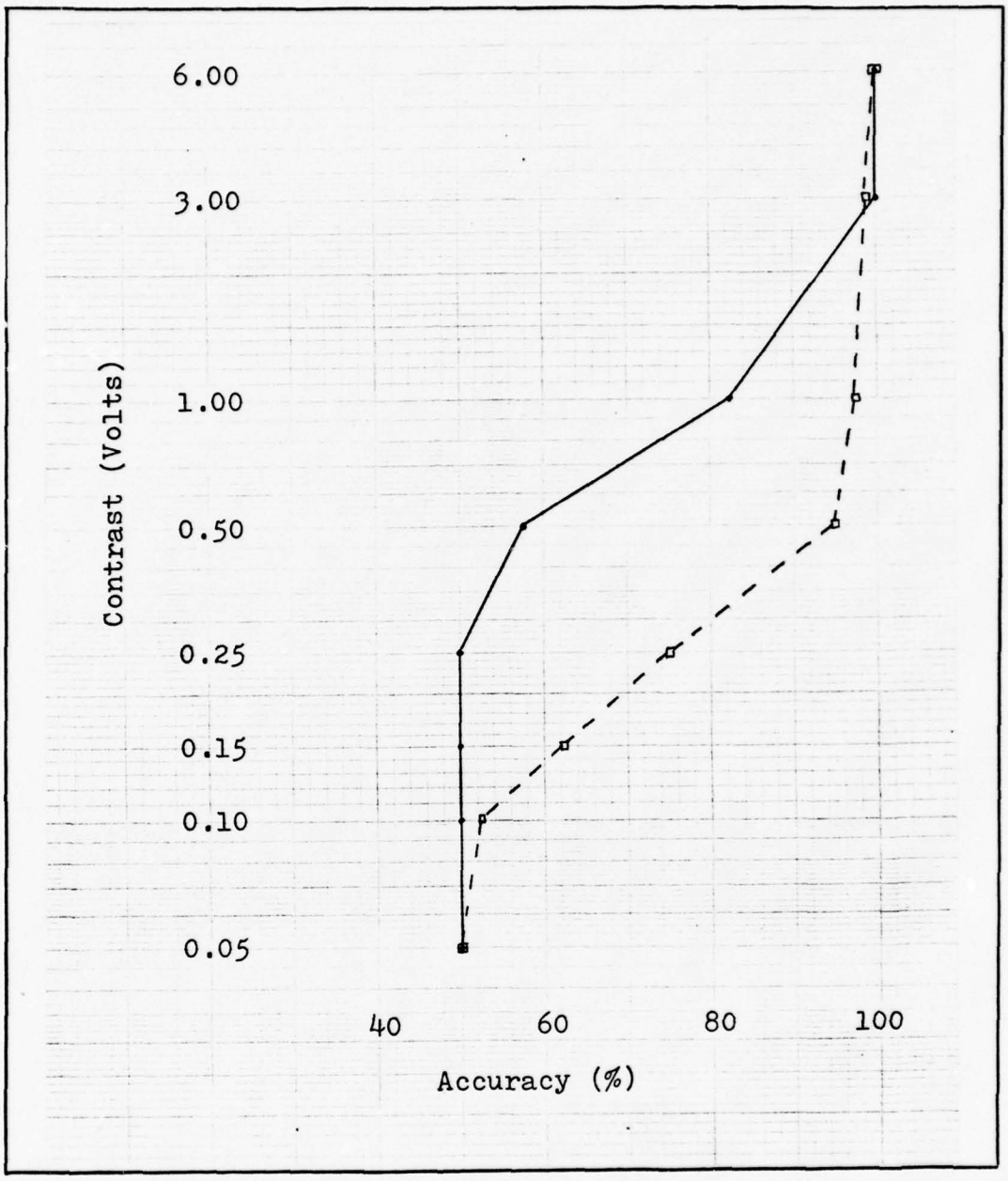

Fig. 70. Plot of Accuracy: CH, 20 msec, Positions 3 (——) and 4 (- -).

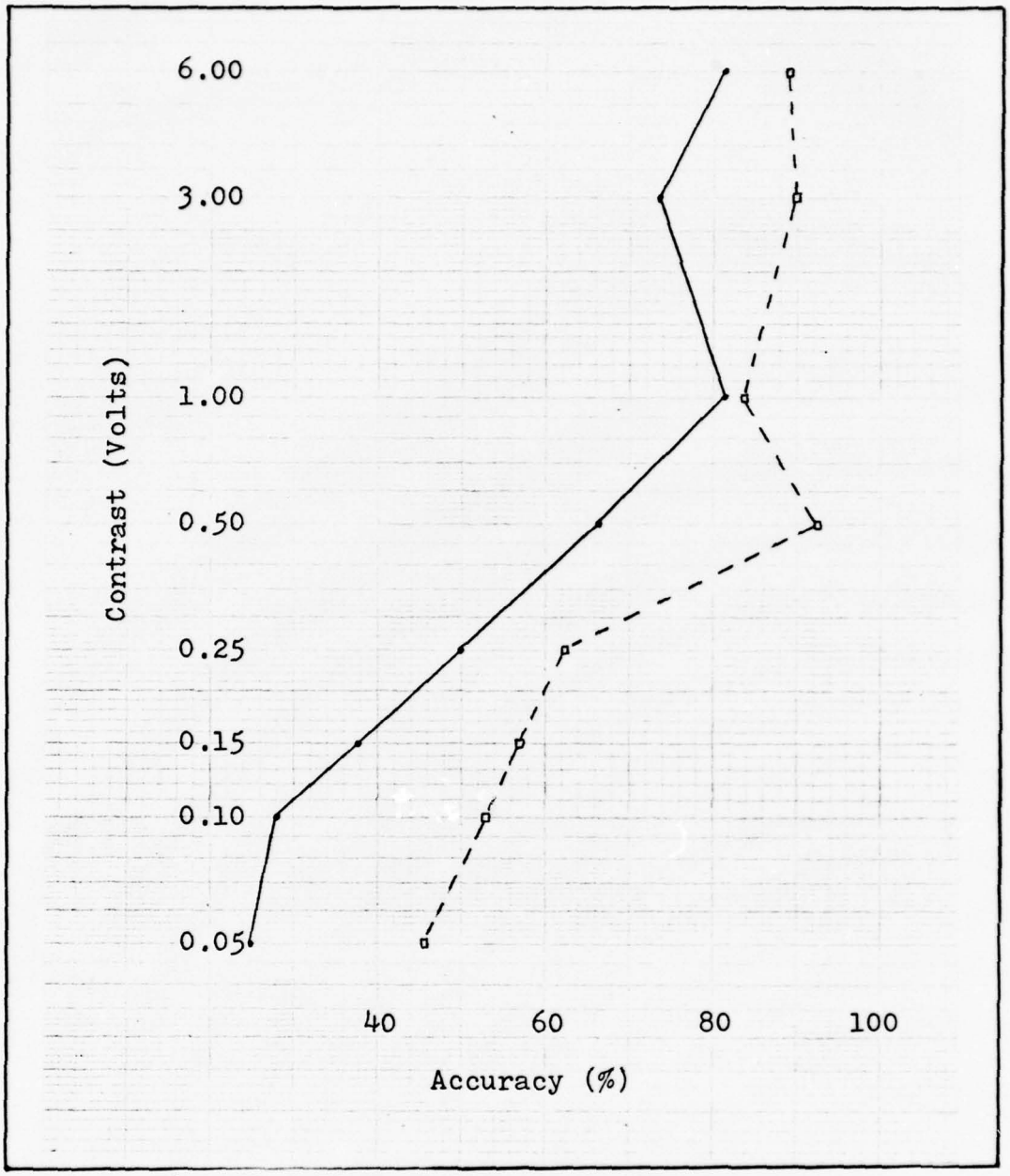

Fig. 71. Plot of Accuracy: CH, 20 msec, Positions 5 (——) and 6 (- -).

Appendix R

Accuracy Values (%): RS, 500 MSEC

Table XIX
Accuracy: RS, 500 msec

Contrast (Volts)	Peripheral Scope Position 5	6
6.00	---	---
3.00	---	---
1.00	83.3	80.0
0.50	90.0	83.3
0.25	70.0	91.7
0.15	(68.0)	(85.0)
0.10	66.7	80.0
0.05	---	---

	7	8
6.00	---	---
3.00	83.3	83.3
1.00	93.3	100.0
0.50	95.0	100.0
0.25	93.3	95.0
0.15	(82.3)	(91.2)
0.10	73.3	88.3
0.05	---	---

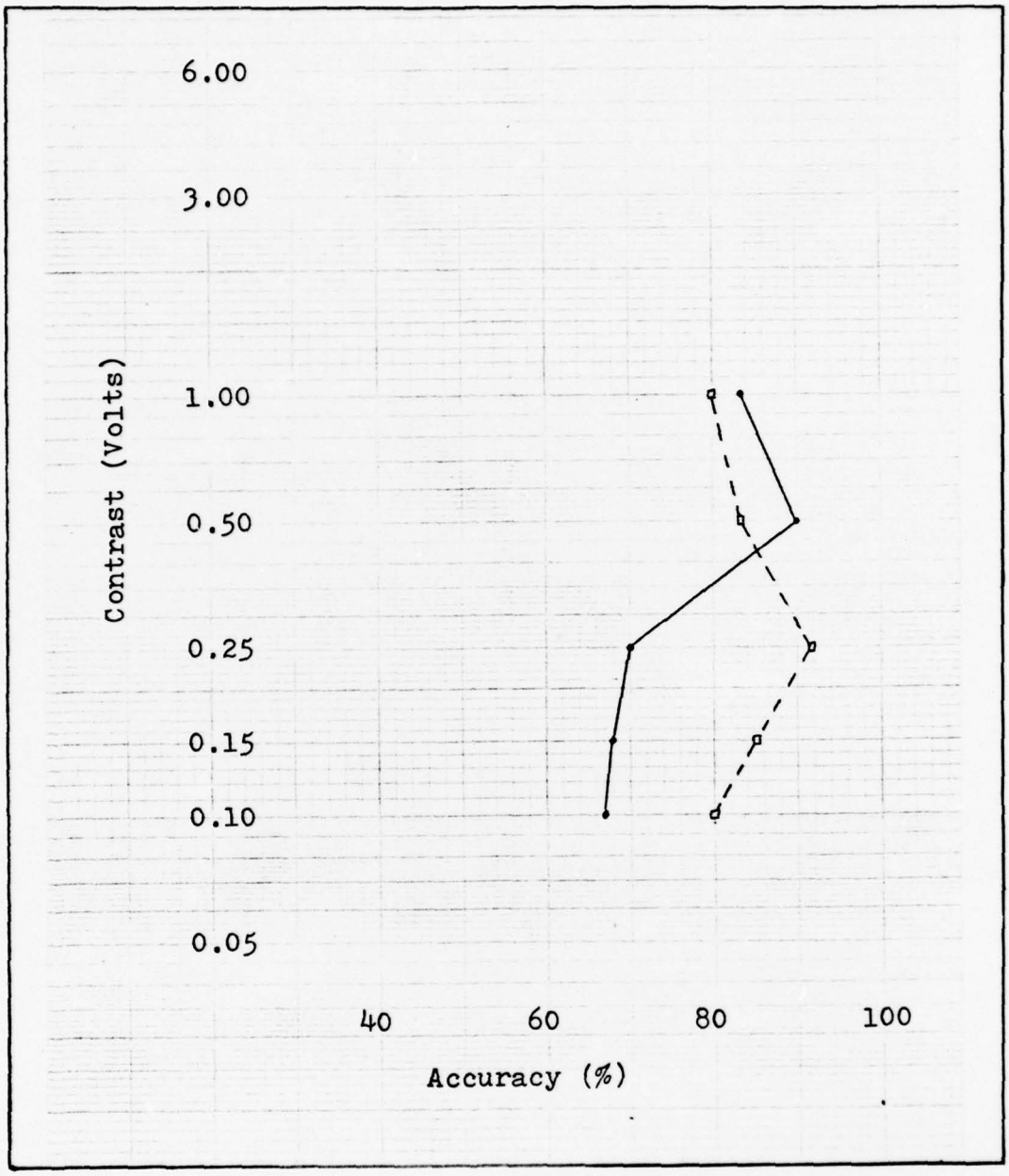

Fig. 72. Plot of Accuracy: RS, 500 msec, Positions 5 (——) and 6 (- -).

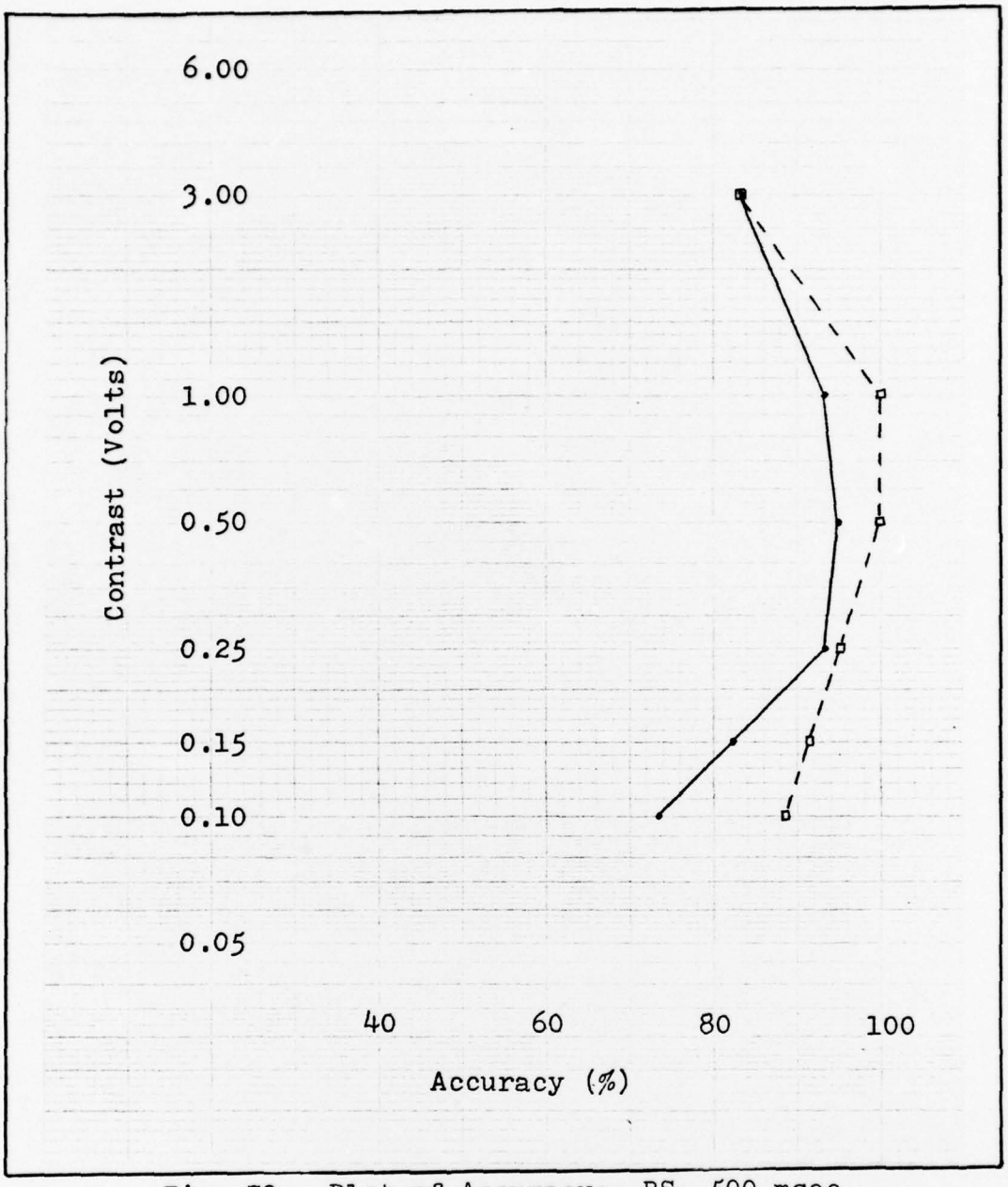

Fig. 73. Plot of Accuracy: RS, 500 msec, Positions 7 (——) and 8 (- -).

Appendix S

Accuracy Values (%): RS, 100 MSEC

Table XX
Accuracy: RS, 100 msec

Contrast (Volts)	Peripheral Scope Position 5	6
6.00	---	---
3.00	---	---
1.00	66.7	80.0
0.50	71.7	83.3
0.25	50.0	91.7
0.15	(49.0)	(84.2)
0.10	48.3	80.0
0.05	---	---

	7	8
6.00	---	---
3.00	---	---
1.00	93.3	100.0
0.50	95.0	100.0
0.25	93.3	95.0
0.15	(82.0)	(91.3)
0.10	73.3	88.3
0.05	---	---

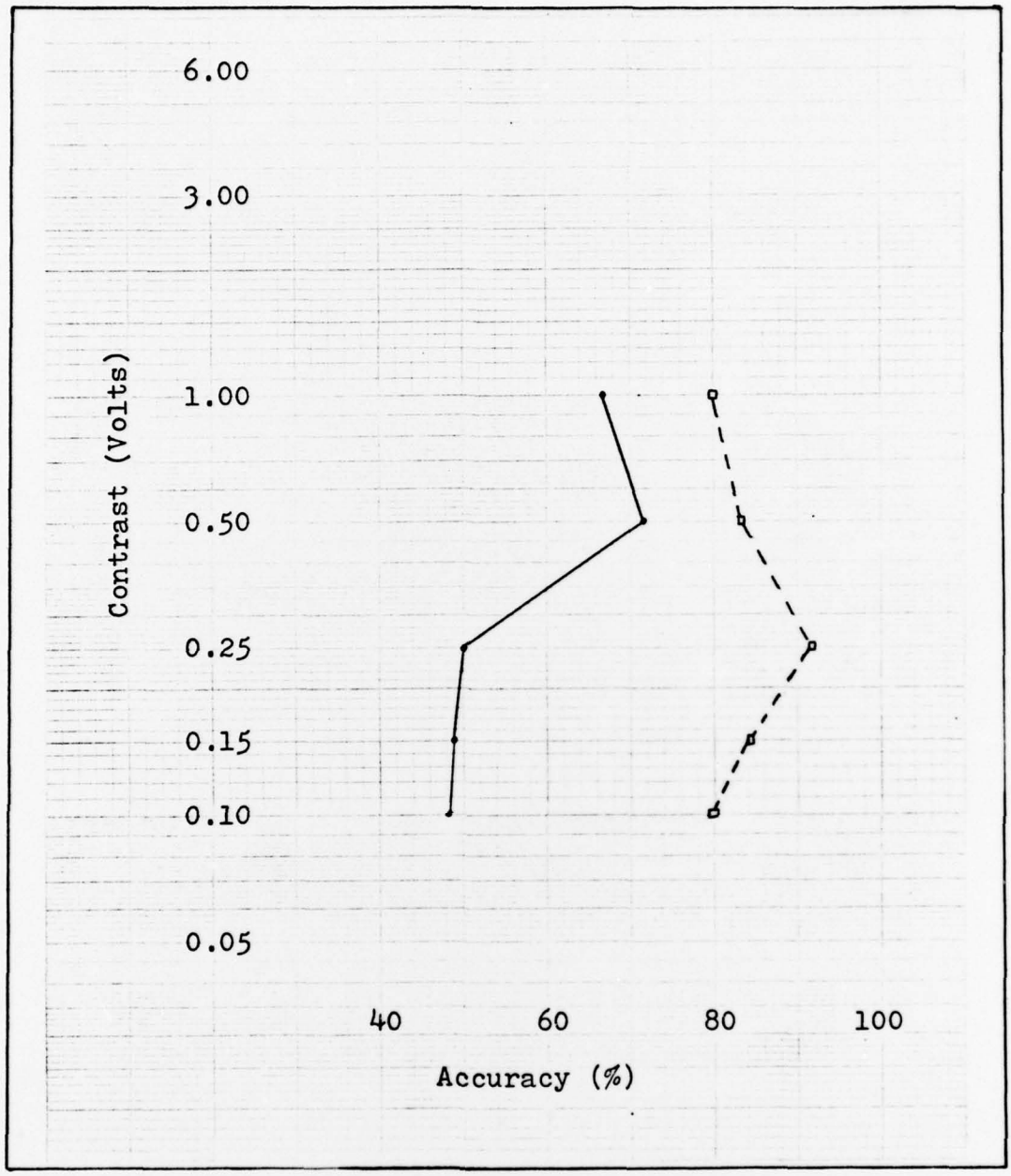

Fig. 74. Plot of Accuracy: RS, 100 msec, Positions 5 (——) and 6 (- -).

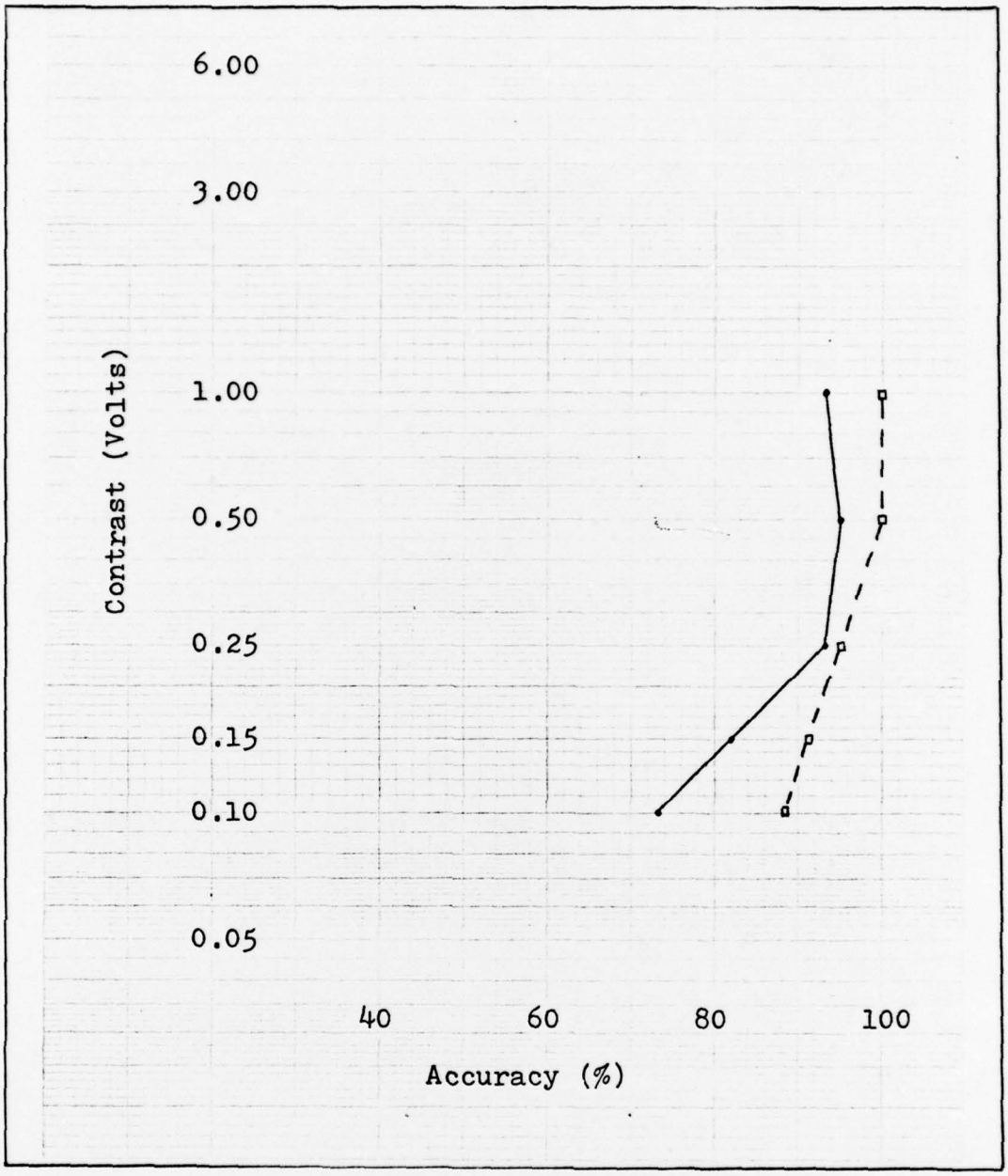

Fig. 75. Plot of Accuracy: RS, 100 msec, Positions 7 (——) and 8 (- -).

Appendix T

Summary of Test Data

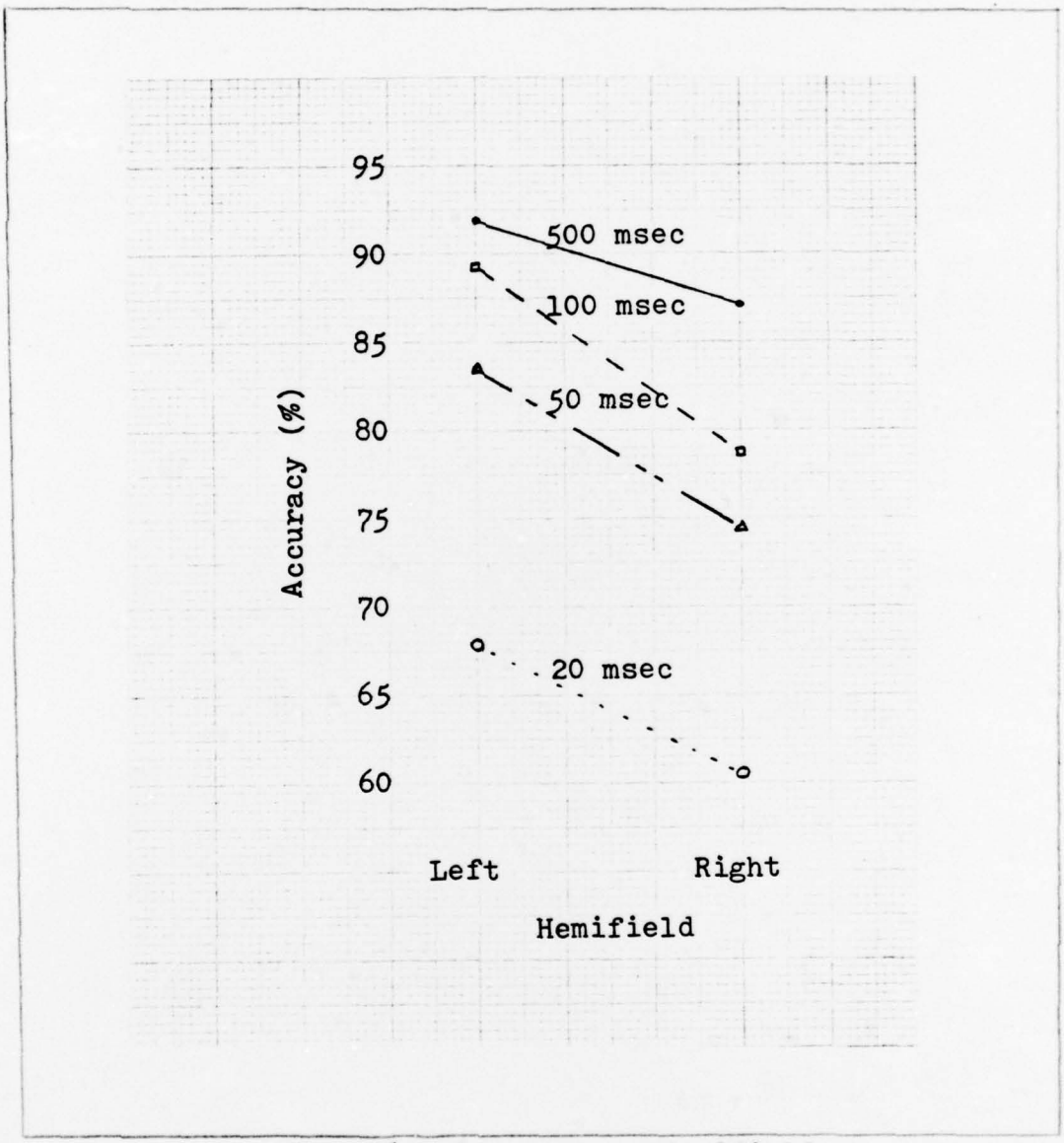

Fig. 76. Accuracy vs Hemifield.

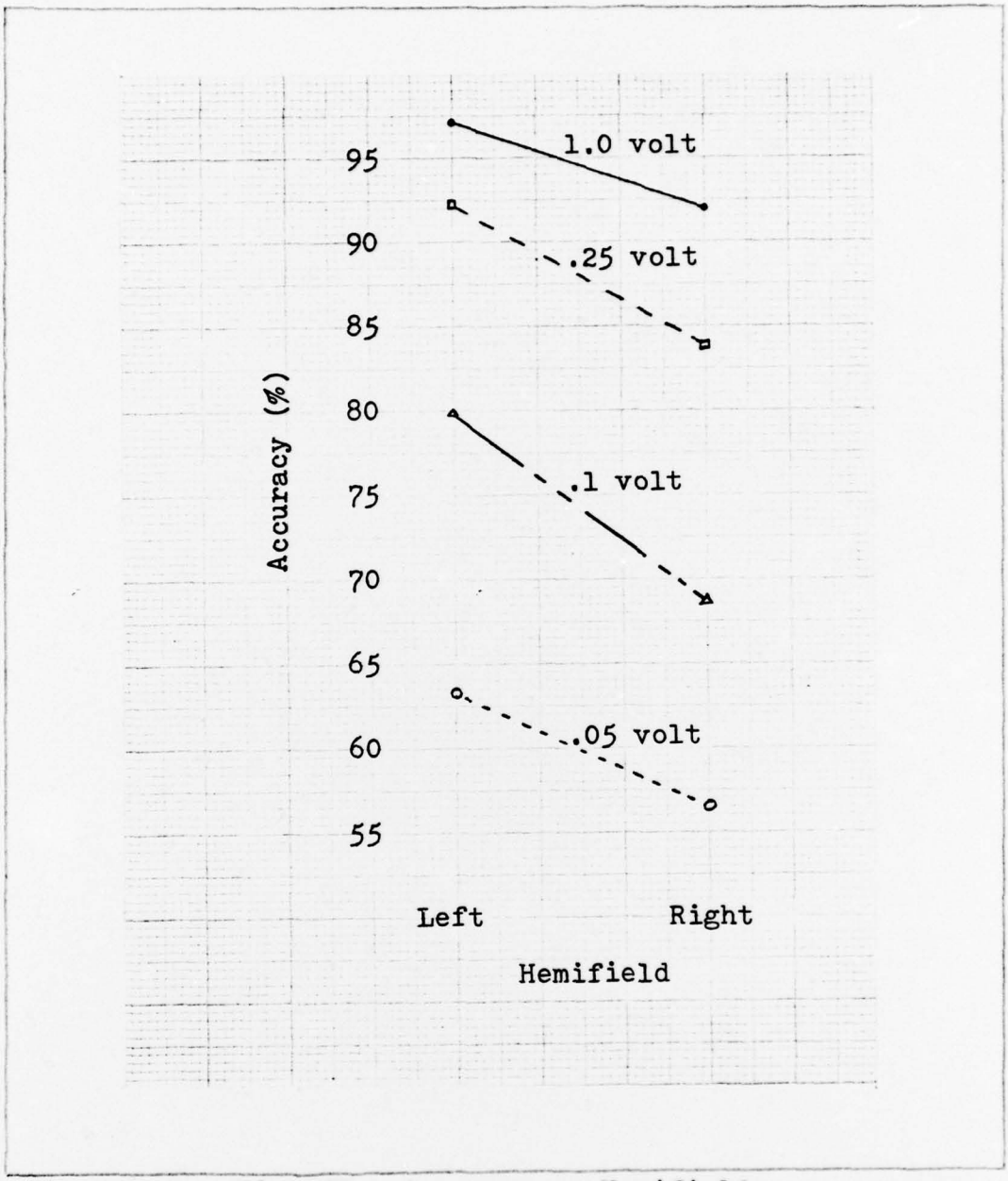

Fig. 77. Accuracy vs Hemifield.

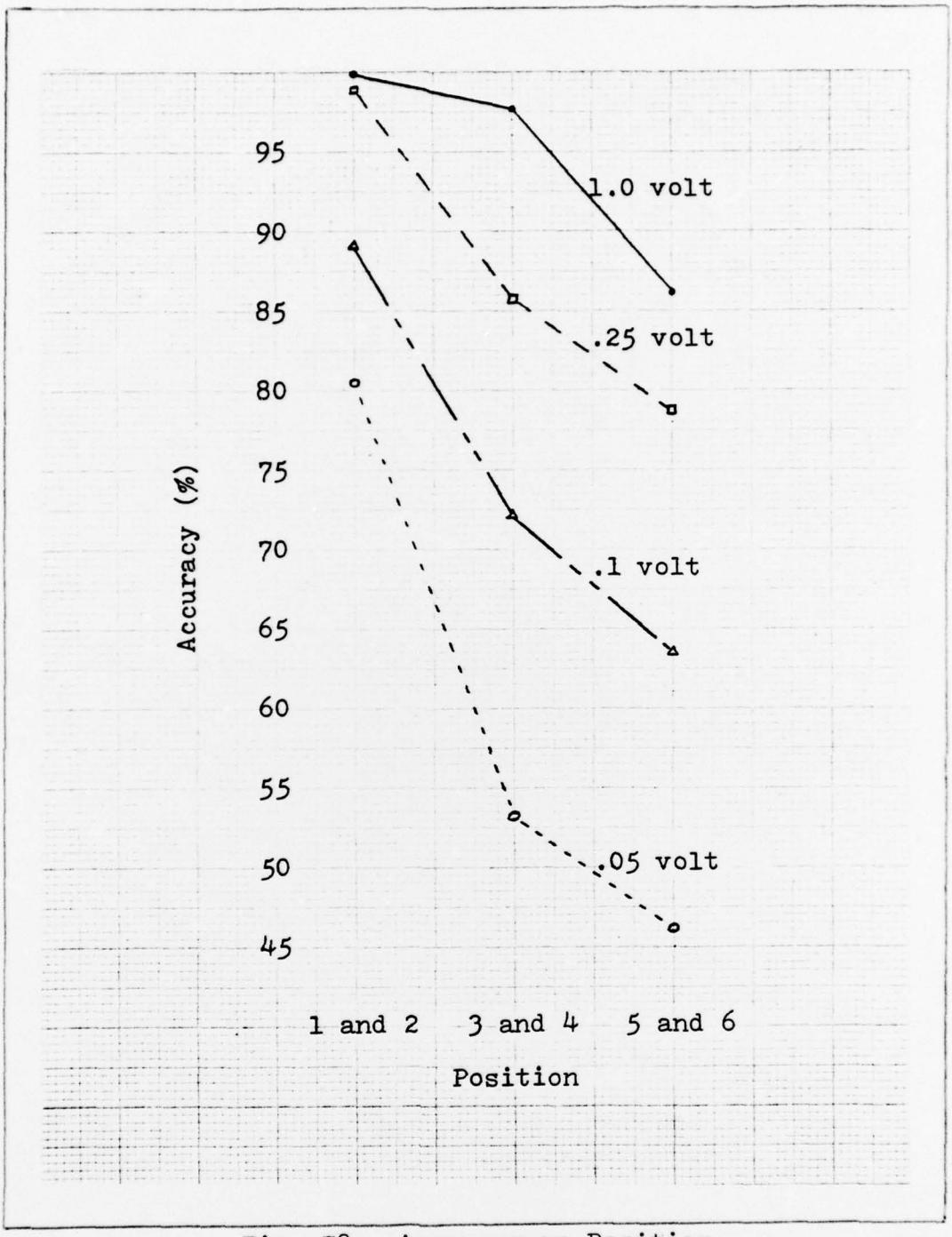

Fig. 78. Accuracy vs Position.

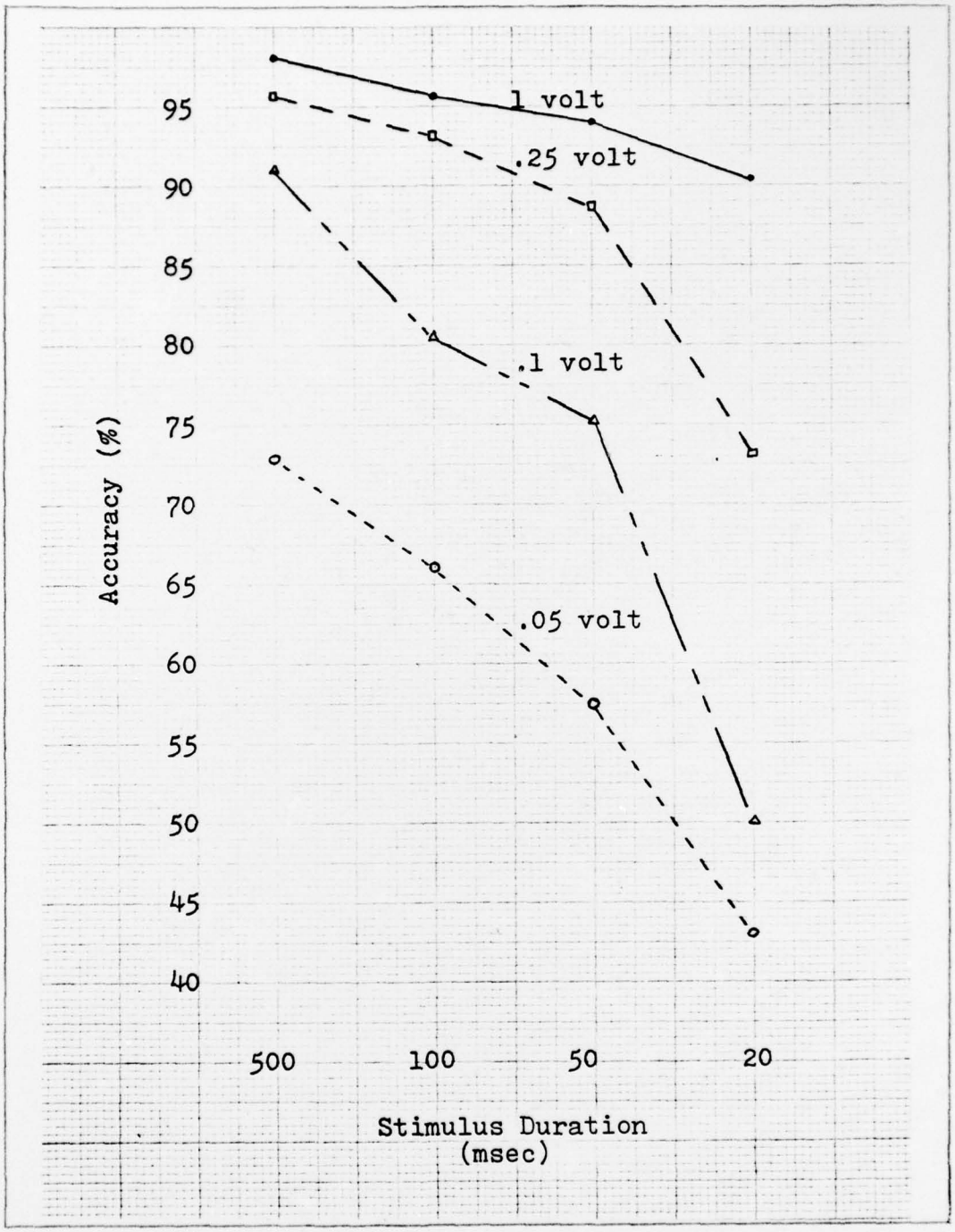

Fig. 79. Accuracy vs Display Duration.

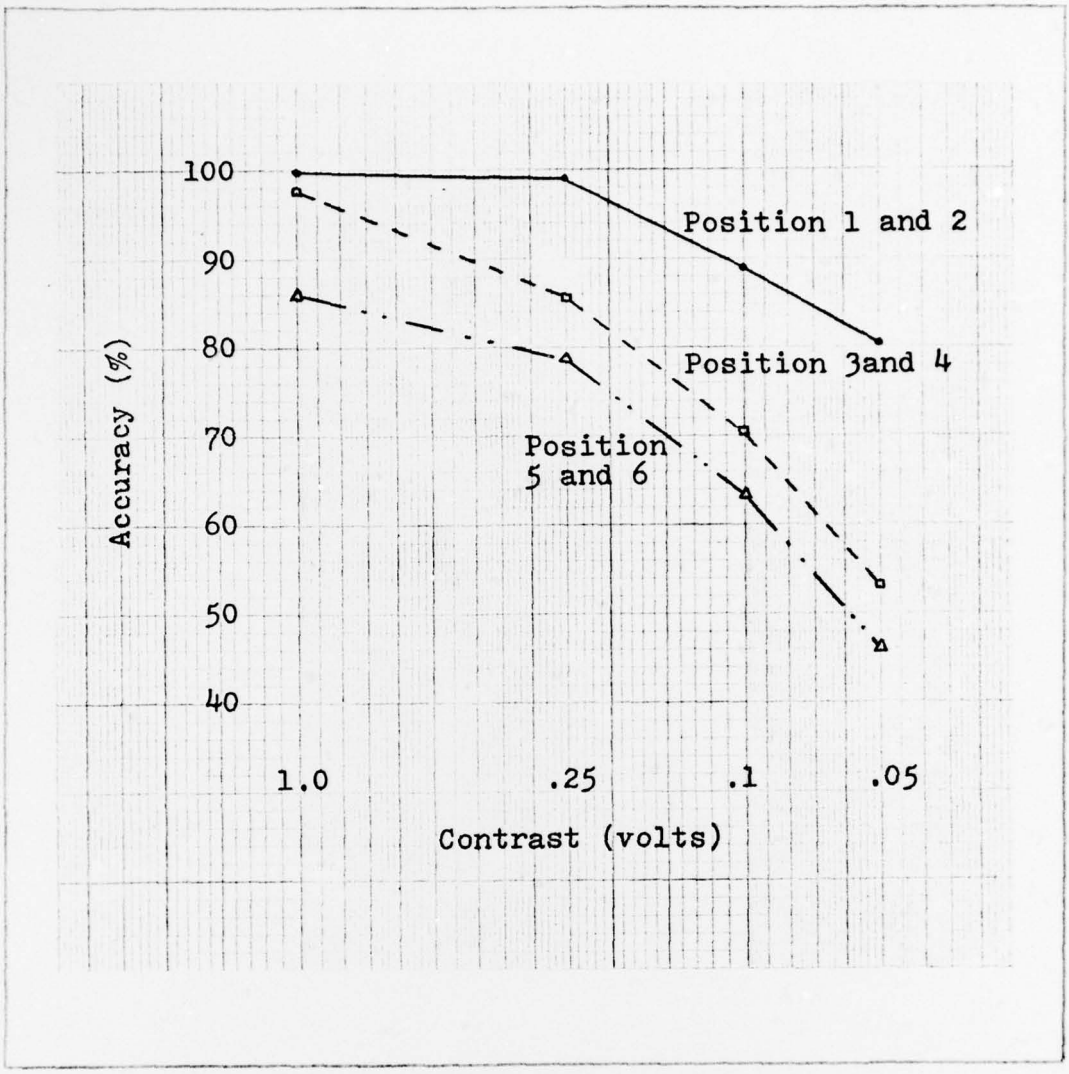

Fig. 80. Accuracy vs Contrast.

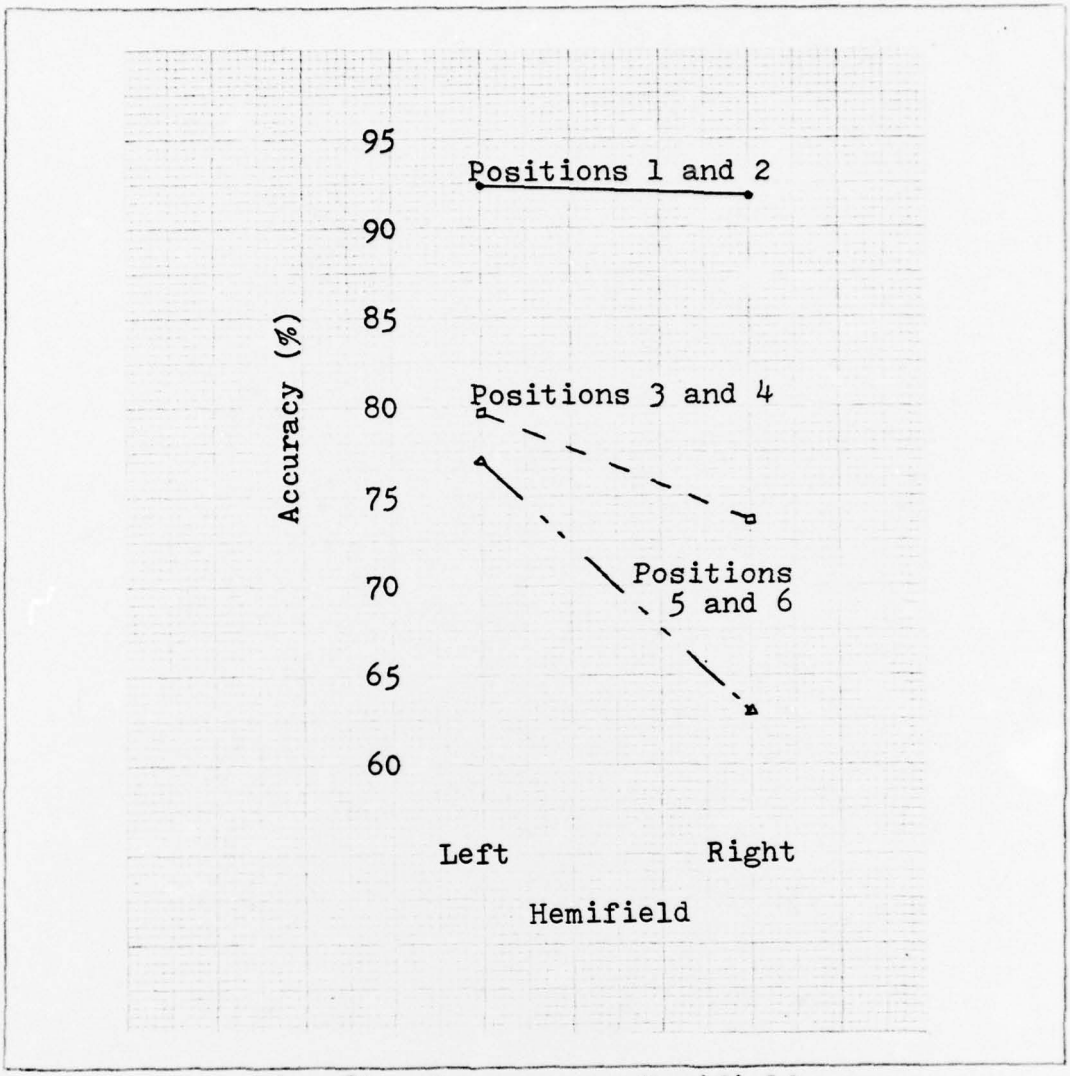

Fig. 81. Accuracy vs Hemifield.

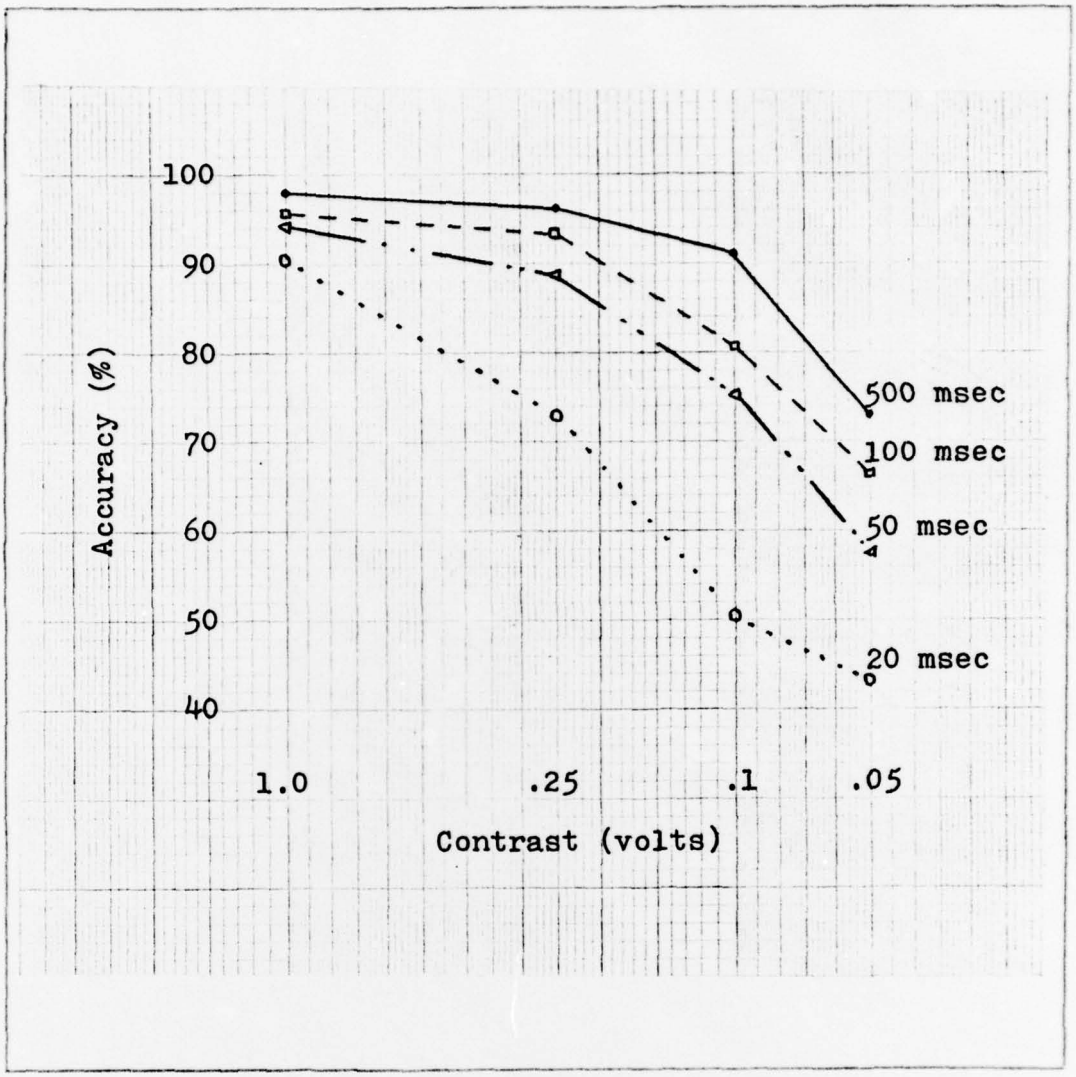

Fig. 82. Accuracy vs Contrast.

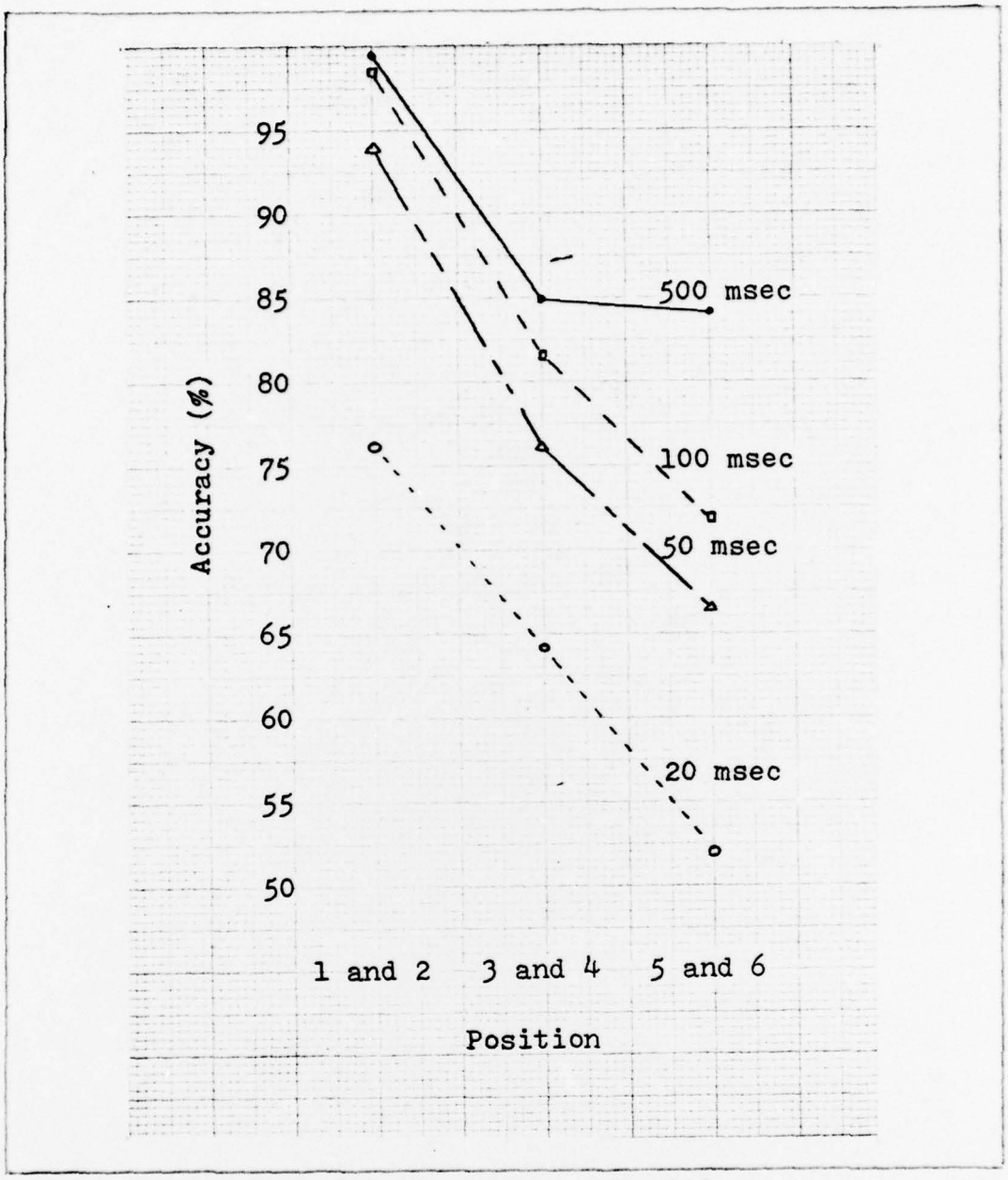

Fig. 83. Accuracy vs Position.

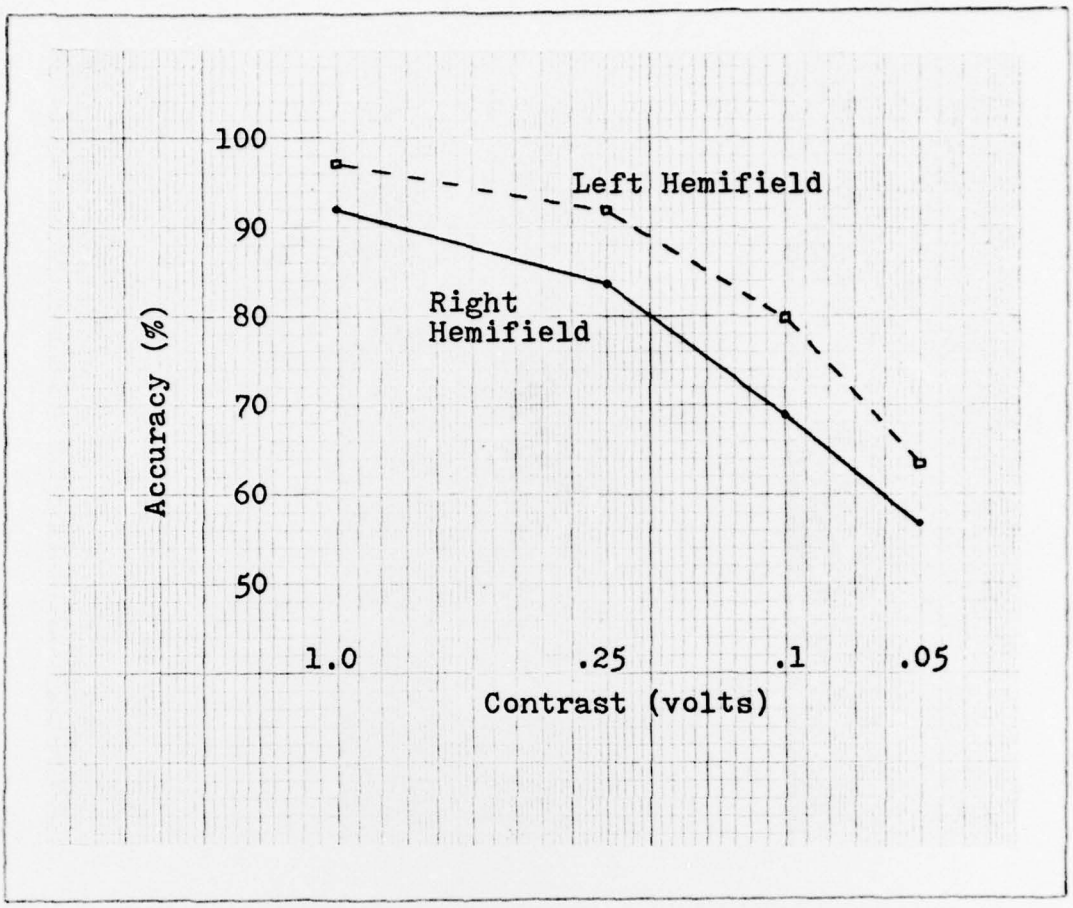

Fig. 84. Accuracy vs Contrast.

VITA

Daniel R. Burchfield [redacted] After graduating from high school in Anderson, Indiana in 1961, he attended Evansville College. There, he earned a Bachelor of Arts in Secondary Education and a commission in the US Air Force in April 1965. He entered the Air Force in August 1965 and graduated from pilot training in September 1966. Since that time, he has flown various fighter-type aircraft in Aerospace Defense, Tactical, and Air Training Commands. He served in Southeast Asia as a Forward Air Controller. In 1974, he entered the USAF Institute of Technology where he earned a Master of Science in Electrical Engineering in 1976.

[redacted]